

**Nutrient-dependent changes of tRNAome
explain metabolic-based strategies for
adaptive growth of *Bacillus licheniformis***

Dissertation
zur Erlangung des akademischen Grades
Doctor rerum naturalium
(*Dr. rer. nat.*)

eingereicht an der
Mathematisch-Naturwissenschaftlichen Fakultät
der Universität Hamburg

vorgelegt von

Iolanda Ferro, M. Sc.

Hamburg, 2016

Die vorgelegte Arbeit wurde von Januar 2013 bis Mai 2015 am Institut für Biochemie und Biologie der mathematisch-naturwissenschaftlichen Fakultät der Universität Potsdam und von Juni 2015 bis Mai 2016 am Institut für Biochemie und Molekularbiologie am Fachbereich Chemie der Fakultät für Mathematik, Informatik und Naturwissenschaften an der Universität Hamburg unter Anleitung von Frau Prof. Dr. Zoya Ignatova angefertigt.

Gutachter:

Frau Prof. Dr. Zoya Ignatova

Herr Prof. Dr. Ulrich Hahn

Tag der Disputation: 22 Juli 2016

*“In nature nothing is created,
nothing is lost,
everything changes.”*

Antoine Lavoisier, *Traité élémentaire de chimie*

A part of this work was published in the following scientific article:

“Quantifying the 'escapers' among RNA species.”

Ferro Iolanda, Ignatova Zoya, *Biochemical Society Transactions*, 2015

TABLE OF CONTENTS

1. Introduction	1
1.1. Transfer RNA	1
1.1.1. tRNA biogenesis.....	2
1.1.2. tRNA modifications.....	4
1.1.3. Aminoacylation of tRNA and editing strategies	5
1.1.4. tRNA as regulatory molecules of the T-box riboswitch system.....	7
1.2. Translation: protein synthesis and the role of tRNAs.....	8
1.2.1. Translation cycles in bacteria	9
1.2.2. The kinetic of translation is shaped by tRNA abundance	10
1.2.3. tRNA pool varies in response to environmental changes.....	11
1.3. Aim of the thesis	13
2. Results	14
2.1. Different approaches for tRNA identification and quantification	14
2.1.1. Narrow physiological constraints shape tRNA structure	14
2.1.2. Detection of single tRNA species.....	15
2.1.3. Modifications – another obstacle for tRNA quantification	16
2.1.4. Global attempts to quantify the tRNA concentration and aminoacylation level	17
2.2. Regulation of the aminoacylation level and adjustment of the total tRNA pool in <i>B. licheniformis</i> depending on nutrient availability	21
2.2.1. The level of aminoacyl-tRNAs is maintained constant independent of the changes in the nutrient availability	21
2.2.2. The tRNA pool changes in a nutrient-dependent manner	28
2.2.3. Nutrient availability fine-tune tRNA expression by GTP-dependent transcription initiation	31
2.2.4. Uniform charging of the tRNA isoacceptor families is regulated via T-box-dependent activation of the cognate aaRS expression: the evolutionary strategy to escape toxicity effect.....	34
2.3. Genome-wide characterization of transcriptional and translational changes in different media	39
2.3.1. Ribo-Seq and RNA-Seq libraries	39
2.3.2. Comparative Analysis of Ribo-Seq and RNA-Seq libraries	39
2.3.3. Translational speed mirrors tRNA abundance	43

2.3.4.	Transcriptional and Translational Response induced by nutritional changes	46
2.3.5.	Transcriptional and translational response induced in the stationary phase	49
2.3.6.	Keeping under control the concentration of toxic amino acid in the cell	52
3.	Discussion and conclusion.....	58
	T-box riboswitch regulates the charged fraction of tRNA in <i>Bacillus</i>	59
	T-boxes monitor the amino acid levels in cells	60
	Regulation of the amino acid catabolic pathways	60
	GTP-dependent expression of tRNAs	63
	Metabolic changes induced by different nutrient availability	65
	Conclusions	66
4.	Materials and Methods	68
4.1.	Materials	68
4.1.1.	Chemicals and reagents	68
4.1.2.	Enzymes	68
4.1.3.	Oligonucleotides	69
4.1.4.	Buffers and reagents.....	72
4.1.5.	Kits	73
4.1.6.	Media	74
4.2.	Methods	76
4.2.1.	Bacterial strains and growth conditions	76
4.2.2.	RNA isolation, labelling and microarray detection	76
4.2.3.	Northern blot and qRT-PCR analysis	77
4.2.4.	Ribosome profiling, RPF isolation.....	78
4.2.5.	Random mRNA fragmentation and size selection	79
4.2.6.	Library preparation	79
4.2.7.	Mapping of the sequencing reads.....	80
5.	References.....	82
6.	Appendix.....	97
6.1.	Hazard statements (H statements)	97
6.2.	Precautionary statements (P statements)	98
6.3.	List of hazardous substances used in the study.....	99
7.	Acknowledgments	101
9.	Declaration on oath.....	103

LIST OF FIGURES

Figure 1. The ‘clover leaf’ structure and identity elements of tRNA.....	2
Figure 2. tRNA biogenesis	3
Figure 3. T-box riboswitch senses and regulates intracellular amino acid availability.....	8
Figure 4 Labeling of tRNAs.	16
Figure 5. Growth curve and tRNA charging level in various media.....	22
Figure 6 Chemostat-controlled growth or temperature do not affect the level of aminoacylated tRNAs.	24
Figure 7. Changes in the total and charged tRNA in stationary phase.....	27
Figure 8. tRNA abundance varies with the nutrient composition of the growth medium.	28
Figure 9. The tRNA concentration between different Bacillus strains is similar.....	29
Figure 10. Strain optimization boosts tRNA expression.	30
Figure 11. The expression of 5S and 16S ribosomal RNAs.....	33
Figure 12. The expression of T-box regulated genes depends on growth rate.....	36
Figure 13. Growth curve of bacteria culture.....	38
Figure 14. Correlation of mRNA and RPF sequencing reads.	40
Figure 15. Correlation of sequencing reads of mRNA (A, C) and RPF (B, D) of LB, MM and MS samples.	42
Figure 16. Reproducibility of randomly fragmented mRNAs (A-C) and RPF (B-D) of two biological replicates.....	42
Figure 17. Reads calibration to determine the nucleotide sitting at the A site.....	43
Figure 18. Comparative analysis of the eCU of LB and MM growing cells.....	44
Figure 19. Ribosome dwells longer at codons read by lowly abundant tRNAs.....	46
Figure 20. Fold change analysis on transcriptional and translational level in <i>B.licheniformis</i> under LB or MM growth.	49
Figure 21. Fold change analysis on transcriptional and translational level in <i>B.licheniformis</i> exponentially or stationary growing in MM.....	51
Figure 22. Catabolic pathway of T-box related amino acids.....	53
Figure 23. Fold-change analysis of genes from amino acid metabolic pathways.	53
Figure 24. Expression levels of catabolic enzymes for T-box related amino acids.	54
Figure 25. Catabolic pathway of non T-box related amino acids.....	55
Figure 26. Expression levels of catabolic enzymes for non T-box related amino acid.....	56

LIST OF TABLES

Table 1. Absolute quantification of <i>B. licheniformis</i> tRNA. <i>B. subtilis</i> tRNA (Kanaya et al. 1999) was used as a baseline for the quantification from the microarrays.	26
Table 2. tRNA genes distribution along the genome	32
Table 3. Effective codon usage of <i>B. licheniformis</i> and codon usage of <i>B.subtilis</i>	45
Table 4. Sequences of the tDNA probes used in the microarrays.....	69
Table 5. Oligonucleotides used for qRT-PCR and library preparation.....	71
Table 6. Amino acid concentration for MMaa.....	75

ABBREVIATIONS

μ	growth rate
aa-AMP	aminoacyl-adenylate
aaRSs	aminoacyl-tRNA synthetases
AC	anticodon
ATP	adenosine triphosphate
D	dihydrouridine
DE	differentially expressed
eCU	effective codon usage
EF-Tu	elongation factor
IF	initiation factor
iNTP	initiating nucleotide
LB	Luria Bertani
MM	Minimal Medium
MMaa	Minimal Medium supplemented with amino acids
Mrna	messenger RNA
nt	nucleotides
OD	Optical Density
RF	release factors
Ribo-Seq	ribosome profiling
RPF	ribosome protected fragments
RRF	ribosome recycling factor
rRNA	ribosomal RNA
SD	Standard Deviation
SD	Shine-Dalgarno sequence
TC	ternary complex
tRNA	transfer RNA
Ψ	pseudouridine

Zusammenfassung

Änderungen in der Genexpression und Anpassungen des Proteoms beeinflussen die Wachstumsrate von Bakterien als Reaktion auf Umweltveränderungen. Das Wachstum wird entscheidend von der Proteinsynthese und Verfügbarkeit von translationellen Komponenten beeinflusst. Dazu gehören tRNAs, genauer Aminoacyl-tRNAs, welche eine zentrale Rolle in der Biosynthese spielen und die Kinetik der translationellen Elongation prägen und die Proteinproduktion beeinflussen. In der vorliegenden Arbeit wird der Einfluss der verfügbaren Nährstoffe auf die tRNA-Häufigkeit sowie auf die Beladung der tRNAs in *Bacillus licheniformis* näher charakterisiert. Dazu wird die Technologie von tRNA-Microarrays genutzt, die es erlaubt sowohl tRNA-Häufigkeit als auch -Beladung zu bestimmen. Wir zeigen, dass der Anteil an Aminoacyl-tRNAs konstant bleibt und nicht von den verfügbaren Nährstoffen abhängt, während sich die absolute Abundanz der tRNAs verändert. Die nähere Analyse des Aufbaus von Operons und Initiatorsequenzen lässt den Schluss zu, dass die Transkription von tRNAs durch GTP-abhängige Mechanismen, welche die Nährstoffkonzentrationen wahrnehmen, streng kontrolliert wird. T-Box Riboswitches kontrollieren das Verhältnis von geladenen und ungeladenen tRNAs und helfen somit einen konstanten Anteil an aminoacylierten tRNAs, trotz Änderungen an totalen tRNA-Leveln, aufrechtzuerhalten. Einige Aminosäuren inhibieren das Wachstum von *B. licheniformis*, wenn diese dem Nährstoffmedium hinzugegeben werden und wir schlussfolgern, dass das T-Box System evolutionär ausgewählt wurde, um die Level an freien toxischen Aminosäuren zu regulieren und zu reduzieren, indem sie zur Beladung von tRNAs verwendet werden. Mithilfe von RNA-Seq und Ribo-Seq, zwei Techniken des „Next Generation Sequencing“, wurde die ribosomale Verweildauer auf jeden Codon und die Korrelation zwischen Translationsgeschwindigkeit und tRNA-Häufigkeit bestimmt. Zusätzlich wurden Änderungen in der globalen Genexpression sowohl auf transkriptioneller als auch translationeller Ebene in komplexem LB-Medium und Minimalmedium während der exponentiellen und stationären Wachstumsphase ermittelt. Diese Analyse zeigt metabolische Strategien auf, welche die bakterielle Anpassung ermöglichen.

Abstract

Changes in gene expression and proteome adaptation modulate bacterial growth rate in response to environmental changes. Growth crucially depends on protein synthesis and abundance of translational components among them tRNAs and more specifically, the aminoacyl-tRNAs, play a crucial role in biosynthesis and shape the kinetics of translational elongation and influence protein production. Here, we characterize the impact of nutrient availability on tRNA abundance and charging pattern of *Bacillus licheniformis* taking advantage of the power of tRNA microarray technology which allows determining both total tRNA abundance and aminoacylated fraction. We demonstrate that of aminoacyl-tRNA fraction is kept constant and does not depend on the nutrient availability, while the total tRNA abundance changes. Analysis of the operon architecture and initiator sequence suggests that tRNA transcription is tightly controlled by GTP-dependent mechanism by sensing nutrient concentration. T-box riboswitch controls the ratio between charged and uncharged tRNAs, thus maintaining constant the aminoacylated fraction despite variations in the total tRNA levels. Some amino acids inhibit *B. licheniformis* growth when added to the nutrient medium and we conclude that T-box system has been evolutionarily selected to tightly regulate the free amino acid level of toxic amino acids by sequestering them for tRNA charging. Using the power of two next-generation sequencing techniques, RNA-Seq and Ribo-Seq, we determine the ribosomal dwelling occupancy on each codon and extract the correlation between translational speed and tRNA abundance. Additionally, we determine global gene expression changes at both transcriptional and translational level in complex LB medium, minimal medium in exponential and stationary phase. This analysis reveals the metabolic strategies which enable bacterial adaptation.

1. Introduction

1.1. Transfer RNA

“It is therefore a natural hypothesis that the amino acid is carried to the template by an ‘adaptor’ molecule, and that the adaptor is the part which actually fits on to the RNA. In its simplest form one would require twenty adaptors, one for each amino acid. . . If the adaptors were small molecules one would imagine that a separate enzyme would be required to join each adaptor to its own amino acid... “

F. H. C. Crick, 1958

How can the amino acid sequence in proteins be assembled on the basis of an RNA sequence? Francis Crick in 1955 proposed that amino acids might be first attached to short single strands of RNA molecules thereby making the amino acids recognizable to a complementary sequence of nucleotides on the template. Paul Zamecnik, in 1958, discovered for the first time these adaptor species and called them “soluble RNA” (Hoagland et al. 1958). The later renamed “transfer RNAs” are ubiquitous nucleic acid entities, ~70 to 100 nt long, with the ability to fold into a tightly folded “clover leaf” secondary structure (Figure 1) and an L-shaped tertiary structure (Kim et al. 1973) which allows tRNAs to perform their specific adapter role during protein synthesis. tRNAs can also participate in a plethora of non-translational activities including cell wall biosynthesis (Dare and Ibba 2012), antibiotic biosynthesis (Shepherd and Ibba 2013), protein turnover (Francklyn and Minajigi 2010), virus-specific functions (Albers and Czech 2016), precursor of small regulatory RNA (Fu et al. 2015). Their major function is to read the genetic code by coupling an mRNA codon, the coding nucleotide triplets, with an amino acid. Each tRNA is charged with a corresponding amino acid and one by one brought to the ribosome. The essential elements of a tRNA are its *anticodon*, which decodes the mRNA triplet code, and its *acceptor* (or CCA) terminus, which is esterified with its cognate amino acid.

Analysis of the tRNA content of organisms in all domains of life showed that they never contain a full set of tRNAs complementary to the 61 different codons since tRNAs, using different deciphering strategies, may read more than one synonymous codon (Grosjean et al. 2010). Translation of multiple synonymous codons by a single tRNA has been demonstrated to occur by wobble base pairing: standard Watson-Crick base pairing (A-U, G-C) is required at the first and second positions of a codon, and “wobbling”, a pairing between two

nucleotides in RNA molecules that does not follow Watson-Crick base pair rules (e.g., G-U), is allowed at the third position of a codon (first base of the anticodon on a tRNA) (Crick 1966; Soll et al. 1966). Modified nucleotides present in tRNAs further extend the range of recognized synonymous codons by forming wobble base pairs (Murphy et al. 2004; Agris et al. 2007)

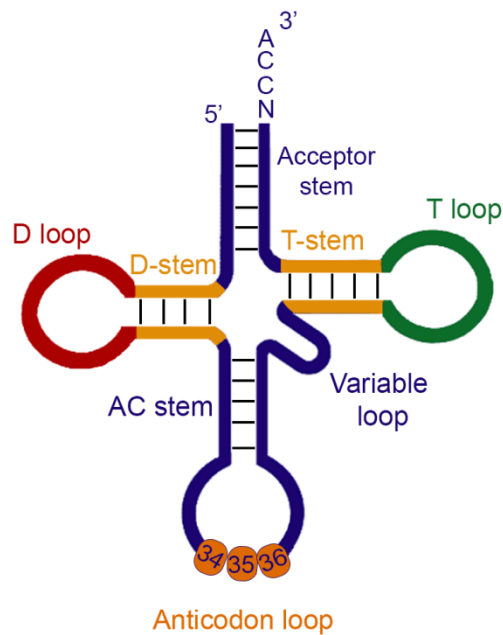


Figure 1. The ‘clover leaf’ structure and identity elements of tRNA.

The acceptor stem is usually 7 base pairs (bp) long, the D-stem is 3-4 bp, and the anticodon (AC) stem is 5 bp. The variable (V) region (4-23 nt long) and the D-loop (4-12 nt long) introduce some diversity in the tRNA length, nevertheless the anticodon in the anticodon loop is always numbered 34-36 and the CCA tail at the 3' terminus is numbered 74-76. The 3' CCA is encoded in the prokaryotic tRNA genes, while in eukaryotes the triplet is added post-transcriptionally by a CCA-adding enzyme.

1.1.1. tRNA biogenesis

In bacteria, tRNA genes are frequently found to clusters on the chromosome. Furthermore, they are present in multiple gene copies. tRNA molecules are synthesized as precursors and processed by a sequence of maturation events (Figure 2). During tRNA maturation, a series of individual processing steps occurs, which can include the processing of polycistronic transcripts, the removal of 5' leaders and 3' trailers by specific endo and/or exonucleases, splicing of possible introns, and addition of the 3'-terminal CCA sequence (if not present) to

generate a functional full-length tRNA. Moreover, tRNA processing may also include numerous specific base modification and editing events.

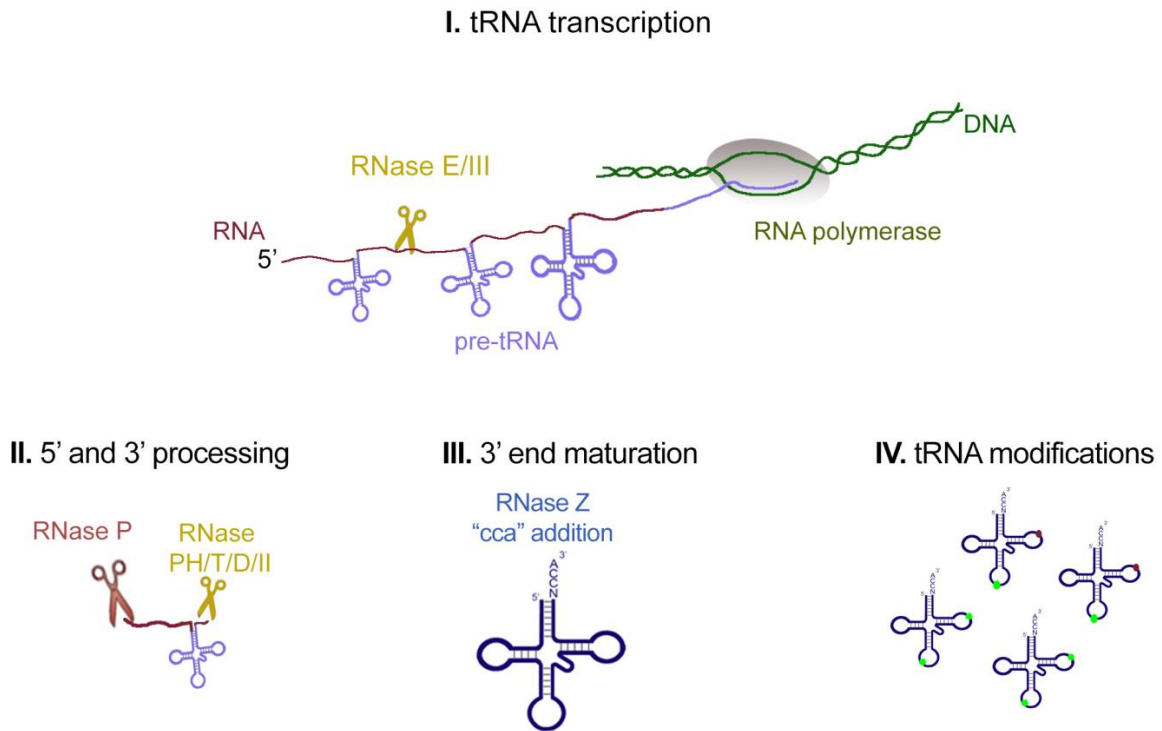


Figure 2. tRNA biogenesis

tRNA molecules are transcribed (I) as precursors and processed by a sequence of maturation events which include 5' and 3' processing (II), trimming which is mediated by RNase P and PH/T/D/II respectively, addition of the CCA tail by RNase Z at the 3' end of tRNA lacking this sequence (III) and post-transcriptional modifications (IV).

The processing pathway of tRNAs is initiated by an endonucleolytic cleavage downstream of the CCA terminus, usually carried out by a combination of two enzymes termed RNase E (Ray and Apirion 1981) and RNase III (Apirion and Miczak 1993). RNase III recognizes double-stranded RNA structures as substrates (Deutscher 2006) while RNase E cleave single-stranded AU-rich sequences (Morl and Marchfelder 2001). After this first cleavage the 5' leader is trimmed. In case of clustered tRNA precursors other endoribonucleases, such as RNase E and RNase III, might be required to generate smaller precursor molecules before RNase P activity. Across all domains of life, the 5' tRNA leader is processed by a ribonucleoprotein called RNase P which generates a precursor molecule with a monophosphate at the 5' end and a terminal 2'-3'-cis glycol (Altman 2011). Accurate recognition by the RNase P is mediated via three specific features of the tRNA: the TΨC

loop, the acceptor stem, and the CCA end (Reiter et al. 2010). After removal of the 5' extension a second exonucleolytic trimming reaction generates the mature tRNA 3' end. Unlike the activities of RNase P which results in complete 5' end maturation, the 3' end endonucleolytic cleavage usually leaves a stretch of extra nucleotides that must be removed by exoribonucleases.

Two main 3' end processing pathways exist in bacteria. The pathway used for a particular tRNA precursor depends on whether or not the 3' CCA end is encoded in its gene. In *E. coli*, where all tRNAs are encoded with their CCA motif, an exonucleolytic reaction is sufficient, catalysed by one of redundant 3' to 5' exonucleases, including RNase PH, RNase T, RNase D and RNase II, with the first two playing key roles. In contrast, maturation of the 3' end of tRNAs in *B. subtilis*, which lacks the CCA motif for about one third of the tRNA genes, can be either endonucleolytic or exonucleolytic (Wen et al. 2005). In the presence of the 3' CCA end, processing is initiated either through an endonucleolytic cleavage at or downstream of the 3' CCA sequence followed by exonucleolytic digestion until the mature 3' CCA end has formed, or direct exonucleolytic digestion of 3' trailer of the primary transcript (Condon 2007; Hartmann et al. 2009). In *B. subtilis* tRNAs lacking the CCA end are first processed by an essential endonuclease called RNase Z, which cleaves downstream of the discriminator base (Redko et al. 2007). Subsequently, the edited tRNA is completed by the addition of the 3'-CCA motif by the tRNA nucleotidyl transferase or NTase (Tomita and Yamashita 2014). The mature tRNAs (Figure 1) are characterized by cloverleaf structure formed from the 5' to the 3' by an acceptor stem, a D-stem loop, an anticodon (AC) stem-loop connected to a T-stem loop via a variable (V) region. The acceptor stem is usually 7 base pairs (bp) long, the D-stem is 3-4 bp, and the anticodon (AC) stem is 5 bp. The variable (V) region (4-23 nt long) and the D-loop (4-12 nt long) introduce some diversity in the tRNA length, nevertheless the anticodon in the anticodon loop is always numbered 34-36 and the CCA tail at the 3' terminus is numbered 74-76 (Giege 2008).

1.1.2. tRNA modifications

tRNAs are the most extensively modified RNA molecules with more than 100 different post-transcriptional modifications described (Czerwoniec et al. 2009). The modified nucleosides are mainly located in single-stranded regions of the tRNA. The exact functions of many of these modifications are unknown, the ones in and around the anticodon triplet are often related to translation efficiency and fidelity; they influence charging efficiency, cognate

codon reading, and prevent missense and frameshift errors, whereas those in the tRNA body seem to be critical for tRNA folding and stability (El Yacoubi et al. 2012) (Novoa et al. 2012). Some modified bases are uniformly present in almost all tRNAs, such as dihydrouridine (D), ribothymine and pseudouridine (Ψ) giving the specific name to the corresponding D-loop and the T-loop (or T Ψ C-loop). Nucleosides present in the anticodon loop at positions 34 and 37 are not only frequently modified (45% in position 34 and 78% in position 37), but they exhibit a large variety of chemistry (Sprinzl and Vassilenko 2005; Bjork and Hagervall 2014). The modifications at position 37 increase the stability of the codon-anticodon interaction, especially A:U and U:A pairs, preventing frame-shifting (Grosjean et al. 1977) and intra-loop base interactions (Agris 2008). On the other hand, modifications of position 34 are involved in maintaining the fidelity of translation by influencing codon choice and discrimination which is considerably important when two amino acids are defined by codons that differ by only one nucleotide in the triplet, such as AUG encoding for methionine and AUA, AUU and AUC encoding for isoleucine (Soma et al. 2003). Indeed, a key tRNA modification present mainly in eukaryotes but to some extent also in bacteria is the modification of adenosine 34 to inosine 34 which allows non-Watson-Crick pairing with A, C, and U. A second one, mainly found in bacteria, is represented by the uridine-34 to hydroxyuridine and derivatives that allows wobble pairing with A, G, and U. Many of the differences observable in the tRNA sets of archaea, bacteria, and eukaryotes can be explained by these modifications (Novoa et al. 2012).

Environmental factors e.g. nutrient availability or growth rate may induce additional modification, as previously shown in case of DNA damage response in yeast (Begley et al. 2007), temperature adaptation in thermophilic bacteria (Noon et al. 2003) or may depend on the growth rate of *E. coli* (Emilsson et al. 1992).

1.1.3. Aminoacylation of tRNA and editing strategies

The tRNA molecules are translationally functional only when aminoacylated with an amino acid. Aminoacyl-tRNA synthetases (aaRSs) are a family of enzymes, divided into two structurally distinct classes (class I and class II) accordingly with the architecture of their active site, that catalyse the aminoacylation process (Giege and Springer 2012). Aminoacylation of tRNA is achieved in two-step reactions in which aaRSs firstly activate the appropriate amino acid with adenosine triphosphate (ATP) in the presence of Mg^{2+} , forming an aminoacyl-adenylate (aa-AMP), and then transfer the activated amino acid to either the 2'

or the 3' hydroxyl group of the terminal adenine (A76) located at the ubiquitous CCA terminus of the tRNA molecule (Ibba and Soll 2004). The fidelity of tRNA charging by amino acids ensures correct translation of the genetic code into proteins, thus accurate discrimination of amino acids and cognate tRNA recognition by the aaRSs are the first two critical steps of protein synthesis. To discriminate between different amino acids, aaRSs use several chemical features such as charge, hydrophobicity, size and shape which are guided through specific contacts between residues in or close to their active site and the side chain of the amino acid (Ibba and Soll 1999). However, the large similarity in size and/or chemical characteristics between amino acids sometimes does not provide a sufficient recognition motif for aaRSs. Therefore, some aaRSs have evolved amino acid editing mechanisms, indispensable checkpoint for correct aa-tRNA synthesis. Several editing strategies such as pre-transfer editing or post-transfer editing can be employed (Zhou and Wang 2013). In the first case, the editing refers to the hydrolysis of mis-activated aa-AMP prior to transfer on the tRNA. Three different pre-transfer mechanistic models have been suggested so far: 1) the *translocation model*, in which cognate aa-AMP is synthesized at the active site but hydrolyzed at the editing site of the aaRS; 2) the *selective release*, occurring when a non-cognate amino acid is released from the active site into solution and subjected to spontaneous hydrolysis due to its intrinsic instability; 3) the *active site hydrolysis*, where the non-cognate aa-AMP is hydrolyzed at the active site before release (Ling et al. 2009). On the other hand, the post-transfer editing takes place after the activated amino acid has been attached to the designated tRNA isoacceptor during which aaRS hydrolyses mischarged tRNA to yield free tRNA and non-cognate amino acid. The cleavage of the amino acid from tRNA occurs in the separate hydrolytic editing domain therefore mischarged 3' end of the tRNA is transferred from the aminoacylation to the editing active site (Pang et al. 2014b). The second critical step during the aminoacylation process is represented by the tRNA recognition. Accurate selection of the cognate tRNA from the cellular pool requires 'identity elements', plus additional signals that prevent recognition of the tRNA by non-cognate aaRSs, which tend to cluster in the anticodon and in the acceptor stem regions of the tRNA where there is typically direct interaction with the aaRS (Giege et al. 1998). For some tRNAs, having multiple isoacceptors with too many different anticodon nucleotide combinations to provide a unique anticodon-aaRS match, there is a need of additional critical identity elements, e.g. the unique base pairs such as G3:U70 in the acceptor stem of tRNA^{Ala} (Hou and Schimmel 1988) or the extra-long variable loop of the tRNA^{Ser} (Achsel and Gross 1993). Despite the editing activity of aaRSs, some mischarged tRNA species have been found to be essential for counteracting specific

cellular stresses (Zhou and Wang 2013). Although the mRNA abundance of the different aaRS is quite similar, their protein levels oscillate (Frenkel-Morgenstern et al. 2012) and the activity among the individual aaRS differs in vivo (Jakubowski and Goldman 1984) challenging the assumption of uniform charging levels of all tRNAs. Moreover, various bacterial species differently regulate the expression of the aaRS implying various modes of regulation of the aminoacyl-tRNA level.

1.1.4. tRNA as regulatory molecules of the T-box riboswitch system

Bacteria regulate gene expression by using specific mRNA structures, called riboswitches, which are able to sense the intracellular concentration of metabolites or second messengers (Mandal et al. 2003; Winkler and Breaker 2005; Caron et al. 2012). Riboswitches represent one of the most efficient mechanisms to regulate expression at the transcriptional and translational level. This class of regulatory RNAs is composed of two structural elements: the aptamer, where the sensor molecule binds, and a second structured stem which can be stabilized as terminator or anti-terminator hairpin. Riboswitches are versatile devices for synthetic biology applications often used to design complex gene regulation circuits (Suess and Weigand 2008; Kang et al. 2014; Wachsmuth et al. 2015). The T-box family is one of the most abundant riboswitches present in *Firmicutes* regulating several genes of the amino acid metabolism, such as synthetases, transporters or biosynthetic genes. T-boxes sense and respond to amino acid starvation directly surveying the charging levels of cognate tRNAs, which are therefore their signal molecules (Gutierrez-Preciado et al. 2009). The structure of the T-box elements is characterized by a highly structured untranslated leader region upstream of the translation initiation site possessing conserved features that allow recognition of a specific cognate tRNA (Grundy and Henkin 1994). To regulate transcription of the downstream gene, depending on the presence of an uncharged tRNA, the regulatory hairpin can fold into alternative secondary structures forming the anti-terminator or terminator element facilitating, in the first case, the read-through and thus increasing the expression of the downstream encoding gene (Henkin and Grundy 2006). Only a cognate tRNA can interact and positively regulate T-boxes transcription anti-termination (Grundy and Henkin 1993). Indeed, only specific interaction through the anticodon and the ‘specifier’ trinucleotide, located in a loop near the base of the stem I domain, and through the single-stranded 3’ terminus NCCA of tRNA and the ‘anti-terminator bulge’ in the T-box anti-terminator domain is able to stabilize the anti-terminator structure (Figure 3) (Vitreschak et al. 2008; Gutierrez-

Preciado et al. 2009). Recently, crystal structures demonstrate that the T-box riboswitches can achieve high selectivity recognizing their cognate tRNAs by exploiting post-transcriptional tRNA modifications, indispensable for interaction such as the anticodon and the elbow. The T-box structure and its specific interaction with the tRNA has been extensively reviewed (Zhang and Ferre-D'Amare 2015). The use of this system allows bacteria to monitor the availability of individual aminoacylated tRNAs. Although the presence of the T-box RNA seems to be the result of evolutionary selection to respond to a specific uncharged tRNA, not all tRNAs are signal for T-box regulated genes.

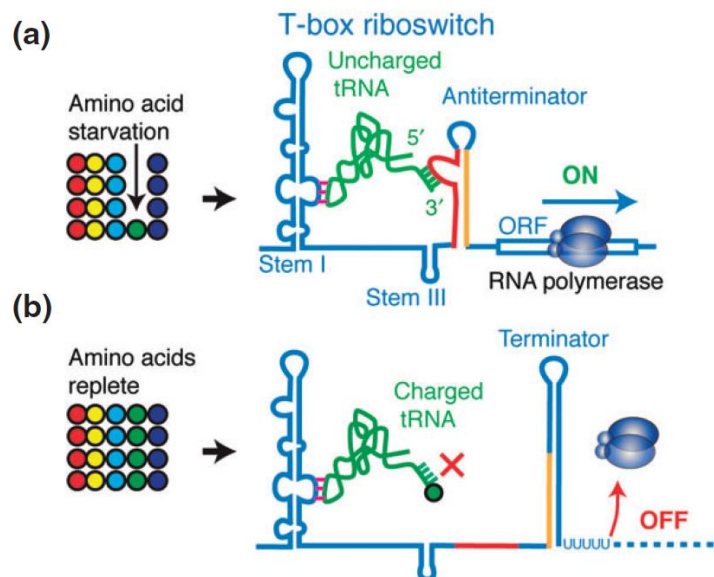


Figure 3. T-box riboswitch senses and regulates intracellular amino acid availability.

(a) Starvation for a particular amino acid (green circle) leads to reduced charging of its cognate tRNA (green). A cognate uncharged tRNA binds the T-box and stabilizes the antiterminator structure allowing transcription of the downstream genes. (b) when the tRNA charging is sufficient, the terminator structure is stabilized since charged tRNAs are rejected sterically and are unable to stabilize the antiterminator. (adopted from (Zhang and Ferre-D'Amare 2015))

1.2. Translation: protein synthesis and the role of tRNAs

After aminoacylation the translationally functional tRNAs can be bound by the elongation factor EF-Tu in bacteria (eEF1A in eukaryotes) to form a ternary complex with GTP (TC, aa-tRNA:EF-Tu:GTP) and reach the ribosome. Translation is a key step in gene expression, converting the genetic information encoded in messenger RNAs (mRNAs) into contiguous

chains of amino acids. During an iterative process, the ribosome, the translating machine which moves along the mRNA, scans mRNAs codon by codon and incorporates amino acids into the growing polypeptide chain (Rodnina et al. 1999). The amino acids are carried to the ribosome by the ternary complex.

The ribosome is a ribonucleoprotein molecule consisting of two major parts that carry out different roles in translation. In bacteria, these are the small 30S subunit, with decoding function, and the large 50S subunit, which catalyses the formation of peptide bonds, forming together the 70S ribosome. Both subunits are composed of ribosomal RNA (rRNA) and proteins. There are three binding sites for tRNAs on the ribosome: A-, P- and E-site (Melnikov et al. 2012). The A site serves to bind the incoming aminoacyl-tRNA, the P site is occupied by the peptidyl-tRNA attached to the nascent polypeptide chain, and the E (exit) site where the deacylated tRNA dissociate from the ribosome. During protein synthesis, tRNAs translocate from the A to the P site and from the P to the E site.

1.2.1. Translation cycles in bacteria

Translation can be divided into four main steps: *initiation*, *elongation*, *termination* and *recycling*. During *initiation*, firstly the 30S subunit forms an initiation complex (30SIC) with the initiator tRNA (fMet-tRNA, which promote its recognition by initiation factor IF2) and the mRNA with the help of the initiation factor 2 (IF2) and two additional factors (IF1 and IF3) (Gualerzi and Pon 2015). The interaction between the 16S rRNA and a specific sequence upstream of the start codon on the mRNA, called Shine-Dalgarno sequence (SD), mediates the positioning of the start codon together with its decoding fMet-tRNA in the ribosomal P-site (Shine and Dalgarno 1975). Subsequently, the 50S ribosomal subunit joins, inducing the formation of the 70S initiation complex (Antoun et al. 2006) and the entry in the *elongation* phase. The repetitive cycle of elongation rounds requires the ability of tRNAs, to interact in a codon-anticodon manner with the mRNA in the A-site. Firstly, the appropriate aa-tRNA, complexed with EF-Tu-GTP, accommodate in the empty A-site of the ribosome stimulating GTP hydrolysis by EF-Tu which allows release of the EF-Tu-GDP complex and enables peptide-bond formation between the two amino acids, bound by their tRNAs to the A and P sites. This results in a deacylated tRNA in the P site and peptidyl-tRNA in the A site (Rodnina et al. 1999). In the final step of the elongation cycle, called translocation, the ribosome moves (Rodnina and Wintermeyer 2011) one codon in 3' direction of the mRNA so that the peptidyl-tRNA from the A site translocates to the P site, while the uncharged tRNA shifts from the P

site to the E site where it is released (Rodnina and Wintermeyer 2011). A new codon of the mRNA is now in the A site waiting for the cognate aa-tRNA. Repetitive cycles of elongation take place until the ribosome encounters one of the three stop codons (UAG, UAA, UGA) signaling *termination* of translation (Korkmaz et al. 2014). Unlike sense codons, none of the stop codons are recognized by a tRNA, but by proteins called class I release factors (RF1 and RF2, in prokaryote). RF1 recognizes UAG, whereas RF2 is specific for UGA and both factors recognize UAA. The class I RFs catalyzes hydrolysis of the ester bond between the nascent polypeptide chain and P-site tRNA inducing peptide release. Subsequently, RF3, belonging to class II RFs, mediate the release of RF class I from the ribosome which will be then ready to be disassembled in two subunits by the ribosome recycling factor (RRF) together with elongation factor G (EF-G) and *recycled* for new translational round (Petry et al. 2008).

1.2.2. The kinetic of translation is shaped by tRNA abundance

Proteins are synthesized with an average rate of about 10-25 amino acids/second, in *E. coli* (Bremer H 1996; Proshkin et al. 2010). Various determinants can influence translational speed acting on the initiation, such as tRNA^{fMet} concentration, the translation initiation region of the mRNA and three initiation factors (IFs) (Bentele et al. 2013; Del Campo et al. 2015; Gualerzi and Pon 2015), and on the elongation for which the key determinant is the tRNA abundance, in particular its charged fractions, but also codon bias, mRNA secondary structures (Varenne et al. 1984; Sorensen et al. 1989; Zhang et al. 2009; Del Campo et al. 2015; Gorochowski et al. 2015; Quax et al. 2015).

The distribution of synonymous codons in genes is not random, each organism prefers a different set of codons over others and this phenomenon is called codon bias (Sharp and Li 1986). Codon bias is thought to result from selection for efficient and accurate translation of highly expressed genes (Kanaya et al. 2001). The use of specific subsets of codons is a strategy to optimize not only protein synthesis efficiency but also to mediate a response to changes in the environment surrounding the cell. Functionally related genes, which need to be expressed at similar levels, tend to have similar patterns of codon usage (Fraser et al. 2004). It has been shown that subsets of preferentially expressed genes form distinct groups in terms of codon usage, and that these codon composition preferences change in response to external stimuli (Frenkel-Morgenstern et al. 2012). Thus, cells may need to dynamically alter their intracellular tRNA composition in order to adapt to their new environment or physiological role. For bacteria, a positive correlation between codon frequency and tRNA concentration

has been previously demonstrated (Ikemura 1985). tRNAs reach ribosome driven solely by molecular diffusion (Fluitt et al. 2007), the only limiting step for its interaction with the ribosome may be its aminocylated concentration. It has been estimated that during exponential growth, the charged fractions of all tRNAs are about 80% such that it is sufficient to maintain the rate of translation (Sorensen 2001). The speed of translation fine-tunes the expression level and it also guarantees a correct protein folding (Zhang and Ignatova 2011). The synthesis rate of each single codon of the messenger-RNA is highly affected by the cognate tRNA concentration (Varenne et al. 1984; Dong et al. 1996; Zhang et al. 2009) which also influences translational attenuation (Lavner and Kotlar 2005), co-translational folding and specific localization like protein translocation across membranes (Woolhead et al. 2006; Zhang and Ignatova 2011; Pechmann et al. 2014). The nascent polypeptides can follow diverse folding pathways. About one third of the polypeptides fold co-translationally (Ciryam et al. 2013). To coordinate the co-translational folding clusters of rare codons are selected to decrease the translational rate (Zhang et al. 2009). Rare codons have been found to be located in specific regions, such as turns or links between secondary structured regions (Makhoul and Trifonov 2002), links between consecutive domains (Zhang et al. 2009) or encoding signal peptides in proteins to be secreted (Fluman et al. 2014). Substitution of rare codons by synonymous frequent codons can cause improper protein folding inducing either degradation or aggregation (Murphy et al. 2004; Fedyunin et al. 2012; Yu et al. 2015). Hence, the tRNA abundance can shape the kinetic of translation safeguarding translation efficiency and fidelity of protein biogenesis.

1.2.3. tRNA pool varies in response to environmental changes

Protein biosynthesis is a highly accurate but energetically expensive process (Akashi and Gojobori 2002). Bacteria maximize its efficiency modulating the abundance of translational components as described in the optimization theory by Ehrenberg and Kurland in 1984 (Ehrenberg and Kurland 1984). In particular, by adjusting ribosome concentration and the average rate of protein synthesis per ribosome, it is possible to fine tune translational activity and to adapt to different nutritional environments for optimal growth (Picard et al. 2012; Ehrenberg et al. 2013). Fast adaptation to dynamically changing environments is the major strategy of unicellular organisms for evolutionary success. In order to maximize the efficiency of translation, the codon frequencies and tRNA copy numbers co-evolve. Studies on *E. coli*, *B. subtilis*, *S. cerevisiae* and *C. elegans* show a correlation between accumulation of tRNA

species and the copy numbers of their corresponding genes demonstrating that tRNA composition is influenced by a gene dosage effect (Ikemura 1981, Dong, Nilsson et al. 1996, Percudani, Pavesi et al. 1997, Kanaya, Yamada et al. 1999, Duret 2000). Different environmental conditions induce fluctuation of the tRNA pool, with changes in the expression of specific tRNA genes, influencing the abundance of total tRNAs, or acting on the expression of genes responsible for their aminoacylation, altering the fraction of charged tRNAs. The amounts of translationally-active tRNAs are regulated by several factors, including the tRNA gene copy number, transcriptional activity, post-transcriptional modifications and RNA degradation. It has been demonstrated, for *E. coli*, that at high growth rates tRNAs specific for optimal codons become more abundant in comparison to those for minor codons (Dong et al. 1996; Berg and Kurland 1997). Moreover, depending on the cellular status, the pool of active tRNAs of eukaryotic cells is rapidly changed, enabling distinct translational programs to be expressed, such as cell cycle, differentiation and stresses (Wilusz 2015). Another layer of regulation induces changes of the aminoacylated fraction. One classical example is represented by the amino acid starvation response. During amino acid starvation the charged level of cognate tRNA decreases while some tRNAs cognate to rare codons remains high (Elf et al. 2003; Dittmar et al. 2005). Thus, under these conditions, the high charging level of the rare cognate tRNA species is able to boost the amino acid biosynthetic pathway (Elf et al. 2003). Protein synthesis is delicately tuned in response to environmental changes and the ability to modulate the tRNA pool confers the cellular plasticity needed to respond to different stimuli. Thus, control of tRNA abundance is one of the fundamental mechanisms for cellular adaptation. But how bacteria can then respond to changes? Faster growing *E. coli* cells subjected to selective pressure regulate a small set of genes, especially rRNA, which constitute approximately 80% of total RNA, and tRNA genes (Varenne et al. 1984; Dong et al. 1996; Dittmar et al. 2004; Valgepea et al. 2013). The existence of a strong link between the growth rate and the concentration of rRNA and total tRNA has been proven, demonstrating that elevated rRNA and tRNA levels support faster growth (Jin et al. 2012).

1.3. Aim of the thesis

Regulation and variations in gene expression allow cells to specifically modulate protein synthesis. Translation can be influenced, in prokaryotes, by tRNA abundance and codon usage. Thus, tRNAs are not simply adaptor molecules that carry amino acids during protein synthesis but they can influence dynamics of translation, efficiency of protein folding and gene expression.

The aim of this thesis is to characterize the tRNAome of *Bacillus licheniformis* under different nutrient and growth conditions. Taking advantage of the potential of a tRNA microarray technology we set to determine variations in total abundance and in aminoacylated fraction of the different tRNA species in response to different growth conditions. Additionally, combining this analysis with two powerful high-throughput sequencing techniques, Ribo-Seq and RNA-Seq, we investigated the dynamics of transcription and translation dependent on the nutrient availability.

2. Results

2.1. Different approaches for tRNA identification and quantification

2.1.1. Narrow physiological constraints shape tRNA structure

tRNAs are synthesized as precursors and processed in a sequence of maturation events which differ for eukaryotes and prokaryotes (Phizicky and Alfonzo 2010; El Yacoubi et al. 2012). Mature tRNAs are prepared for their classic function in translation by attachment of an amino acid by the cognate aminoacyl-tRNA synthetases (aaRSs) to their common 3' CCA ends (Figure 1), which by prokaryotes are encoded in the tRNA gene and in eukaryotes are enzymatically added post-transcriptionally. Among all RNA entities, tRNAs undergo by far the greatest number of post-transcriptional modifications (Czerwoniec et al. 2009; Phizicky and Alfonzo 2010). Modifications in the stem loops are crucial for structural integrity and stability of the tRNA or as recognition for the aaRSs, whereas those in the anticodon loop maintain accuracy of decoding (Gustilo et al. 2008; El Yacoubi et al. 2012; Torres et al. 2014). Modifications of the anticodon nucleosides (particularly at position 34, Figure 1) are also associated with increasing the diversity of the codon recognition through non-Watson-Crick base pairing between the third base in the codon and the first in the anticodon loop (i.e. wobbling), so that one tRNA can decode more than one codon (El Yacoubi et al. 2012; Novoa et al. 2012). Consequently, the number of tRNA isoacceptors (that are different tRNA species with distinct anticodon sequence but carrying the same amino acid) to decode all 61 sense codons are usually much fewer than 61 (Chan and Lowe 2009).

The actual number of nuclear-encoded tRNA genes, particularly in the eukaryotes, is highly divergent; in humans, for example 513 nuclear-encoded tRNA genes encode 49 isoacceptors (Chan and Lowe 2009). Each tRNA isoacceptor is frequently encoded by an entire family of isodecoders, which bear the same amino acids and anticodon but differ in the sequence of the tRNA body (Goodenbour and Pan 2006). Although the role of the tRNA isodecoders remains unknown, they are not a result of neutral genome expansions of large genomes; different isodecoders are expressed in tissue-specific manner and shape the tissue-specific tRNA sets (Kutter et al. 2011; Ishimura et al. 2014).

The primary function of the majority of tRNAs is translation and interaction with the ribosome. Thus, in order to fit to the same ribosomal site, their length (e.g., tRNA length varies in a very narrow range of 71 to 89 nucleotides (nt) in humans) and 3D architecture are

constrained by common identity rules (Giege 2008). This high sequence, length and structural homology impede the identification and quantification of isodecoders.

2.1.2. Detection of single tRNA species

One of the pioneering techniques to identify tRNAs is Northern blot hybridization (Alwine et al. 1977), in which each tRNA can be separately detected with a radioactively or fluorescently labelled full-length tDNA probe. Since uncharged tRNAs have higher electrophoretic mobility than their aminoacylated counterparts, the method is suitable to determine both species (Sorensen 2001; Dittmar et al. 2005; Cruz Hernandez et al. 2013). Despite its common use, it is rather laborious approach; only one tRNA can be determined in one Northern blot. Furthermore, the method relies on hybridization and for each tRNA the optimal conditions for hybridization of the probe need to be established.

Quantitative RT-PCR (qRT-PCR) is a fast and specific method to detect nucleic acids. However, the reverse transcriptase is sensitive to the modifications in tRNA. The latter slow down or even completely arrest the reverse transcriptase and impede tRNA quantification. Thus, it might be a method of choice for tRNA identification. A new twist of the qRT-PCR technology, four-leaf clover qRT-PCR (FL-PCR) (Honda et al. 2015), increases the applicability of reverse transcription-based approaches to determine modified nucleic acid entities. The method consists of three steps: (i) tRNA deacylation, (ii) ligation of DNA/RNA hairpin adaptor which complements the 3' NCCA ends of the mature tRNAs (similar to the one used in the tRNA microarrays (Dittmar et al. 2006), see below, Figure 2A) to generate a “four-leaf clover” secondary structure, and (iii) reverse transcription of the DNA-RNA hairpin using forward and reverse primers derived from the T- or D-stems (Figure 1). The T4 RNA ligase 2 (Rnl2) ligates the DNA/RNA adaptor at a 3'-OH/5'-phosphate nick present only in mature tRNAs, which ensures the specificity towards mature and not to pre-tRNAs or tRNA fragments (Honda et al. 2015). Moreover, the reverse transcription in FL-PCR is quantitative, as it transcribes the least modified parts of each tRNA, i.e. the acceptor stem. A drawback of FL-PCR is the high number of cells needed to extract tRNA, since the efficiency of the organic solvent extraction of structured small RNAs decreases by using a small number of cells (Honda et al. 2015).

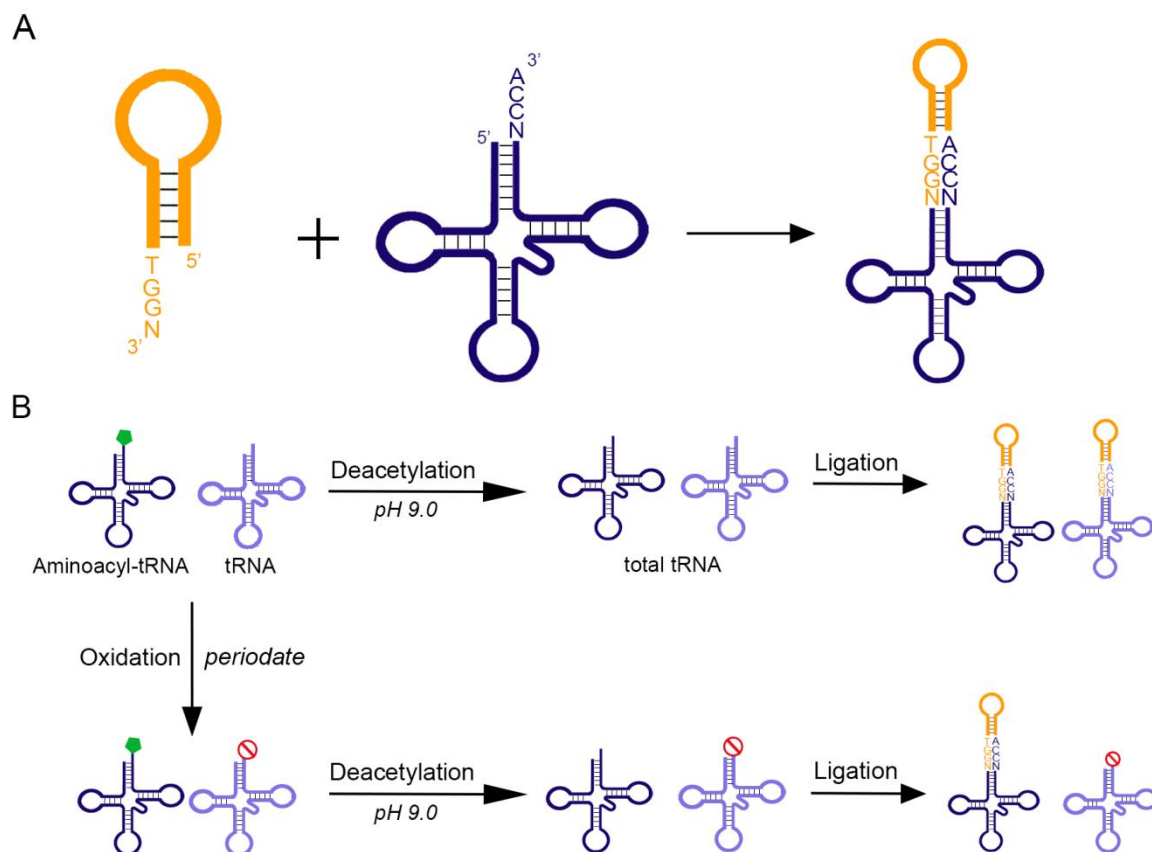


Figure 4. Labeling of tRNAs.

(A) Principle of tRNA labeling with hairpin oligonucleotide used in the FL-PCR and microarray approach. The hairpin oligonucleotide complements the unique common single-stranded CCA-ends. For fluorescent detection a fluorescently labelled nucleotide can be incorporated in its loop. (B) Schematic of the microarray-based approach to determine total tRNA (upper reaction) and aminoacyl-tRNAs (bottom reaction) concentration as developed in (Dittmar et al. 2005). For total tRNA determination, the amino acid moiety (green pentagon) is deacetylated prior to ligation of the hairpin oligonucleotide. Aminoacyl-tRNAs (dark blue) are insensitive to oxidation and upon deacetylation bind the hairpin oligonucleotide, unlike deacetylated tRNAs (light blue) whose 3'CCA ends are oxidised (no-entry sign) and cannot pair with the hairpin oligonucleotide.

2.1.3. Modifications – another obstacle for tRNA quantification

The complete set of modifications is known only for few organisms (Björk 1996; Johansson and Byström 2005; Puri et al. 2014). In eukaryotes, more than 100 modifications have been identified so far (Czerwoniec et al. 2009). Since modifications influence quantification, the tRNA quantification should be coupled to identification of the modification pattern. tRNA modifications can be identified *de novo* by coupling enzymatic digestion to liquid chromatography/mass spectrometry (LC-MS/MS) (Hossain and Limbach 2007; Wetzel and Limbach 2013) or electrospray ionization mass spectrometry (Emmrechts et al. 2007). With a cocktail of various nucleases, tRNAs are digested down to single nucleotides and modified bases are identified by the retention times in LC and confirmed by their unique mass-to-

charge (m/z) ratios with a tandem MS/MS. The majority of the modifications are visible by this method except pseudouridine (Puri et al. 2014). To obtain further site- and sequence-specific information on the modified nucleoside, tRNAs are partially digested with a nuclease cocktail (for example RNase T1, U2 and A) and the fragments identified by tandem MS/MS are mapped against the tRNA sequences (Hossain and Limbach 2007; Wetzel and Limbach 2013). Using this approach the modification patterns of *E. coli* (Hossain and Limbach 2007), *Lactobacillus lactis* (Puri et al. 2014) and yeast (Chan et al. 2010) have been identified. Some modifications may escape this detection due to inability to detect them in the positive ion mode of the MS/MS approach. For example in yeast, 2'-O-ribosyladenosine phosphate (Ar(p)) is invisible to this method most likely because of the negatively charged phosphate (Chan et al. 2010). This combined approach for detecting tRNA modifications requires knowledge on the tRNA sequences and is therefore only applicable for sequenced genomes.

2.1.4. Global attempts to quantify the tRNA concentration and aminoacylation level

2D-gel electrophoresis is a classical method to analyse the amounts of all cellular tRNAs. Upon complete denaturation (7M urea) tRNA isoacceptors are firstly separated according to their molecular weight, followed by separation based on the secondary structure upon a partial refolding (4M urea). This approach is suitable for quantifying small tRNA sets: for *E. coli* 44 out of 46 (Dong et al. 1996) and for *B. subtilis* 30 (out of 35) (Kanaya et al. 1999) isoacceptors were detected. tRNA of more complex organisms, e.g. multicellular eukaryotes, can be identified only partially.

Approaches using HPLC and MALDI-MS have been developed which are semi-quantitative with limited resolution for quantification. Using the HPLC methodology, differences in the tRNA pattern of proliferating versus quiescent rat liver cells have been detected (Kanduc 1997), although the method is restricted in detecting only isoacceptor families (that is, a family of all tRNAs carrying the same amino acid). Digestion of tRNAs with various RNases releases characteristic fingerprint products for each tRNA which then can be identified in MALDI-MS (Hossain and Limbach 2007). Although highly specific, the resolution of MALDI-MS is limited to approximately 30 tRNA species.

Exploiting the advantages of microarray technology, Tao Pan and co-workers detected differences in the expression of tRNA set in various human tissues (Dittmar et al. 2004; Dittmar et al. 2005). Each tRNA is detected with its own tDNA probe. A radioactive labelling of the tRNAs at their 5' or 3' termini is used for their absolute quantification, while labelling

with a fluorescent hairpin oligonucleotide at the common 3' CCA ends (Figure 2A) is informative on relative changes of single tRNA isoacceptors between two different conditions (thereby using hairpin oligonucleotides that bear two different fluorophores). The microarray approach does not provide a complete coverage of all tRNA isoacceptors; only tRNAs with difference of at least eight nucleotides can be reliably distinguished with this technology (in contrast, tRNAs that vary only by one or few nucleotide, i.e. proline isoacceptors with anticodons IGG, CGG, and UGG, hybridize to the same probe on the microarray) (Dittmar et al. 2004; Dittmar et al. 2005). Despite these limitations in resolution, divergent tRNA pools in proliferating and differentiating cells were detected with this approach (Gingold et al. 2014). Furthermore, modifying the probes on the microarray (i.e. using fragments of full-length tRNAs) allows detection of stress-inducible tRNA-derived fragments (Czech et al. 2013) with crucial roles in stress signalling (Ivanov et al. 2011; Anderson and Ivanov 2014).

A twist of the microarray technology allows for evaluating the aminoacylation level of individual tRNAs. For this, the total tRNA is isolated under conditions to preserve the aminoacyl-tRNA (i.e. acidic buffers with pH of 4.8) and oxidized with periodate (Figure 2B). The aminoacyl moiety maintains the 3'CCA ends intact, which upon deacylation ligate the fluorescently labelled hairpin oligonucleotide used for detection. Deacetylated tRNAs are sensitive to oxidation and cannot be detected (Figure 2A).

The power of the deep-sequencing technologies has been used to determine the whole tRNAome (Puri et al. 2014; Zhong et al. 2015). Because in its core it is based on reverse transcription of each tRNA to DNA, it bears the drawbacks of qRT-PCR. In particular, modifications that interfere with the quantitative PCR-based cDNA synthesis (such as N1-methyl-A and N1-methyl-G (Ebhardt et al. 2009)) and the extensive tRNA structure make tRNA-seq an inadequate approach for quantification but rather are suitable for identification (Puri et al. 2014). Often modifications are misread by the reverse transcriptase which appears as a mismatch by aligning the tRNA-derived reads. Allowing mismatches at the position of each modification when aligning the sequencing reads improves the quantification. This strategy allowed for quantification 47 out of 49 tRNA species (Zhong et al. 2015) and showed a reasonable overlap with earlier quantification of *E. coli* tRNAs by 2D-gel electrophoresis (Dong et al. 1996). The applicability of this mapping strategy in the tRNA-Seq is, at least currently, limited, despite its large depth, since it requires knowledge of the exact position of all modifications to be considered by mapping of the sequencing reads. Moreover, mismatches in the sequencing reads can be used to identify putative positions of nucleotide modifications, but since little information is available on the identity of the nucleotide

mismatch it is not possible to determine the type of modification using the identity of mismatch nucleotide (Chan et al. 2015).

Some reverse transcriptases have enhanced read through on modified ribonucleotides. Using a thermostable group II intron reverse transcriptase for the RNA-Seq library construction (Shen et al. 2015) have facilitated the generation of full-length cDNA copies of tRNA and enhanced the quantification potential of the tRNA-Seq technology. Moreover, the enzyme is insensitive to aminoacyl moiety at the 3' terminus (Mohr et al. 2013; Katibah et al. 2014) and thus the results are reproducible independent on the tRNA isolation protocol (i.e., by acidic or alkaline pH, to preserve or not the aminoacyl group).

A recent development of the tRNA-Seq using two-step approach minimizes the influence of modifications and improves the applicability of the deep sequencing approaches to quantify tRNA sets (Pang et al. 2014a). The crucial improvement of this approach is that it uses sequencing information of ~30 nt from the 3' end of tRNAs, which contain the fewest modified ribonucleosides in all tRNAs. Briefly, in the first step a pre-adenylated 20 nt long DNA linker (with a 3'-dideoxy end) is ligated to tRNA and the DNA linker is as a priming site for the reverse transcription (Pang et al. 2014a). This first reverse-transcription round minimizes the modification-induced fall-off or pausing of the reverse transcriptase to generate a quantitative ctDNA set that is then subjected to another round of linker ligation at the new 3'-end and subjected to deep sequencing (Pang et al. 2014a). Although only the mist 3' ends of the tRNAs are reverse transcribed and amplified, the unique signature of each tRNA is however preserved in these 3' end-derived fragments enabling quantification of all 76 uniquely expressed tRNAs in *S. cerevisiae*, including also some isodecoders (Pang et al. 2014a). Similar, however, to other deep-sequencing approaches, the concentration of single tRNA species varies between biological replicates which can be attributed to variations in the efficiency of the ligation and PCR amplification steps (van Dijk et al. 2014).

With advances in experimental technologies, we are beginning to understand the variety of cellular functions of tRNA and different programmes that operate to coordinate their expression in tissue-specific fashion, and the dynamics of tRNA as another regulatory layer to coordinate stress response. Mutation in tRNA genes and tRNA-biogenesis genes are linked to several human pathologies. Variations in tRNA abundance among different tissues may modulate the effect of tRNA-linked pathologies in a tissue-specific manner, underscoring the need for accurate quantification of tRNA expression and modification pattern for each specific cell type. This is a key area of study that will enable us to understand more clearly the genotype–phenotype relationship.

Furthermore, addressing differences in tRNA expression among various organisms will allow for improvement of the heterologous expression by tailoring the translation profile of the heterologous protein to the host-specific tRNAome.

2.2. Regulation of the aminoacylation level and adjustment of the total tRNA pool in *B. licheniformis* depending on nutrient availability

In this section we characterize the total abundance and the level of aminoacyl-tRNAs from the Gram-positive bacterium, *Bacillus licheniformis*, belonging to the subtilis group (Rey et al. 2004). We tested different growth conditions and media. We focused on one particular strain, *B.licheniformis* HD0583, selected for its high secretion potential (provided by K.Liebeton from B.R.A.I.N. AG, Zwingenberg, Germany), and we compared our results with the commercially available strain *B. licheniformis* DSM13.

From the variety of techniques available for tRNA quantifications (Ferro and Ignatova 2015), we chose tRNA-specific microarrays (Dittmar et al. 2004; Dittmar et al. 2005), which allow for measuring aminoacyl-tRNA level simultaneously for all tRNAs. This global analysis revealed strategies on how *B. licheniformis* maximizes growth at varying environments and nutrients.

2.2.1. The level of aminoacyl-tRNAs is maintained constant independent of the changes in the nutrient availability

B. licheniformis DSM13 genome bears 72 tRNA genes encoding 34 different tRNA isoacceptors (tRNA species differing in their anticodon but loaded with the same amino acid). To quantify the amount of aminoacylated tRNAs we used tRNA microarrays (Dittmar et al. 2005) with 34 complementary probes capturing all 34 tRNA isoacceptors (Table 4). We determined the amount of aminoacylated tRNAs, translationally competent, from the bacterium *B. licheniformis* HD0583, an highly protein secreting strain closely related to DSM13 strain. Bacteria were grown in complex, undefined medium (LB, Luria Bertani), minimal medium with only glucose as a carbon source (MM) and balanced defined medium, i.e. minimal medium to which all 20 proteinogenic amino acids (Table 6) were added (MMaa). The total RNA was isolated from exponentially growing bacteria ($OD_{600nm} \sim 1$) and from bacteria in stationary phase ($OD_{600nm} \sim 6$ in LB and $OD_{600nm} \sim 2$ in MM) (Figure 5 A). To preserve the aminoacyl moiety, tRNAs were isolated under acidic conditions and subjected to periodate oxidation (Dittmar et al. 2005). Only 3' ends of the deacylated tRNAs are susceptible to oxidation, while the aminoacyl group protects the 3' termini of the aminoacyl-tRNAs leaving them intact to ligate the fluorescently-labelled RNA/DNA stem-loop oligonucleotide used for detection on the microarrays. Simultaneous analysis (i.e. on one microarray) with the corresponding total tRNA isolated at pH 8 allows

determining fraction of the aminoacylated tRNAs. Interestingly, the tRNA isoacceptors were not uniformly charged and the level of aminoacylation in each condition largely varied (Figure 5 B-D). In some biological replicates few tRNA isoacceptors showed hyperfluorescence, i.e. charging levels over 100%, whose origin was unknown but can be observed in some microarray measurements (Dittmar et al. 2005). The hyperfluorescence effect was unstable among the biological replicates and yielded a large SD; thus for those tRNAs we consider the charging level as nearly as 100%.

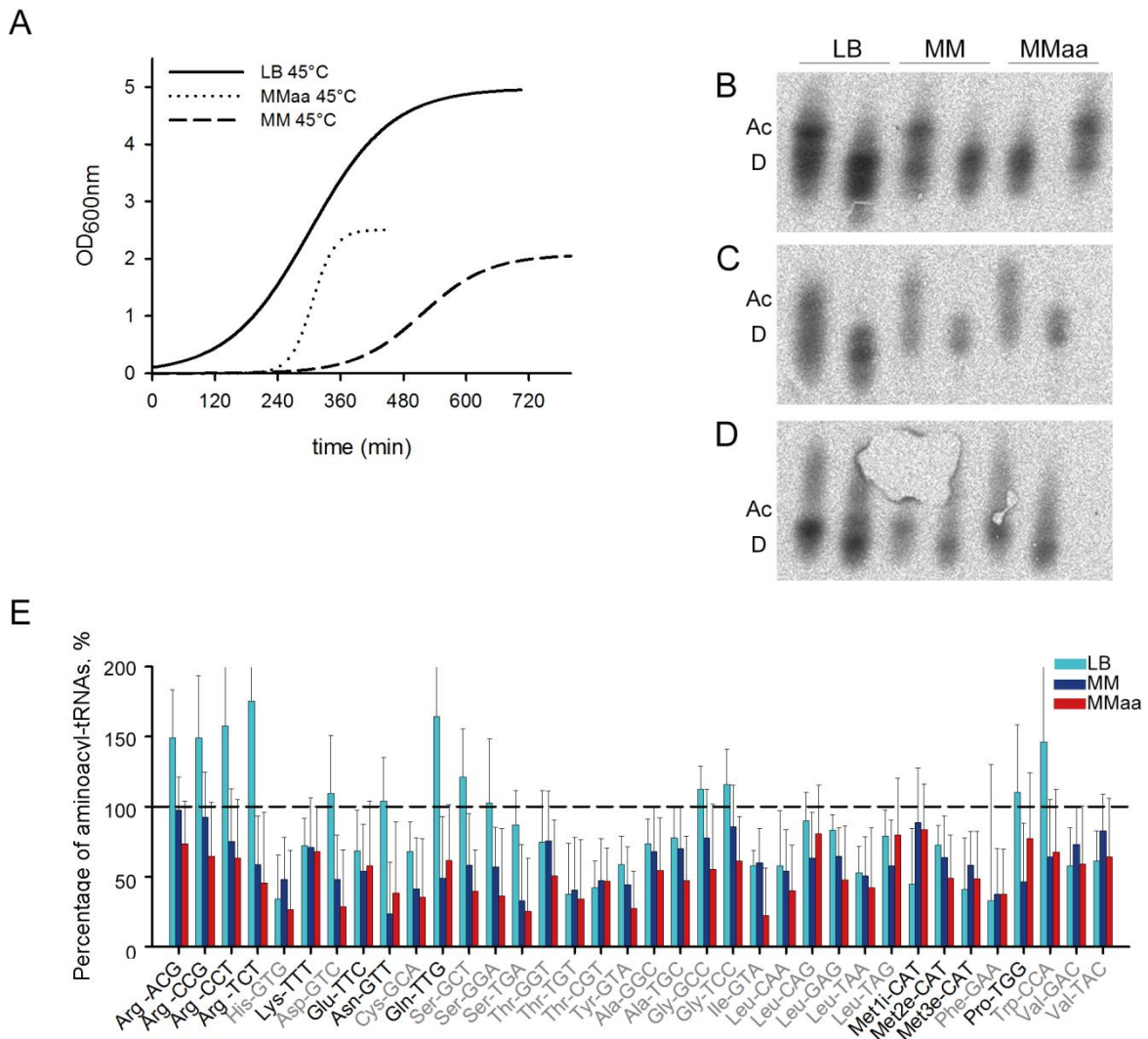


Figure 5. Growth curve and tRNA charging level in various media.

(A) Growth curves; Probing the aminoacylation level with Northern blot for: (B) tRNA^{Asn}, (C) tRNA^{His}, and (D) tRNA^{Ile} measured in three different media. Ac denotes sample isolated by acidic conditions preserving the aminoacyl-tRNA moiety; D represent total deacylated tRNA isolated by alkalic conditions. tDNAs covering the full-length tRNA were used as probes in the Northern blot analysis. (E) Charging level of the tRNA isoacceptors of exponentially growing *B. licheniformis* HD0583 (OD₆₀₀=1.0) in different media. LB medium (light blue), MM (dark blue) and MMaa (red). The fraction of the charged tRNAs is

normalized to the total amount of each isoacceptor which for each condition is independently set at 100% (horizontal dashed line). tRNA isoacceptors T-box regulator are written in grey, non t-box regulator are written in black.

The tRNA isoacceptors are non-uniformly aminoacylated within one growth condition and the charging level fluctuates from 100% down to approximately 40% for some tRNAs. The drop in aminoacylation of some tRNAs in MM compared to LB was expectable, since in MM amino acids, for proteins synthesis or tRNA charging, are exclusively supplied through intrinsic biosynthesis and the variations in the biosynthesis of each amino acid may explain the differences in charging within one isoacceptor family. Nevertheless, during growth in MMaa, in which every amino acid is provided extracellularly in a large excess, the lower fractions of aminoacyl-tRNAs, even lower than in LB, was rather unexpected. Also, subjecting bacteria to a chemostat-regulated growth that maintains steady growth rate with a continuous supply of nutrients did not improve the general tRNA charging pattern (Figure 6 A) implying that lower charging levels of the tRNAs are not caused by nutrient (i.e. amino acids) limited conditions. Furthermore, the charging pattern was also independent on the growth temperature (Figure 6 B and C). Surprisingly, those observations indicate that the tRNA aminoacylation level is independent and moreover non-controlled by amino acid availability. However, we realized one very interesting fact that despite variations in the growth rate (i.e. growth medium) the charging level of all tRNA isoacceptors within some tRNA isoacceptor families (e.g., tRNA^{His}, tRNA^{Lys}, tRNA^{Glu}, tRNA^{Gly}, tRNA^{Cys}, tRNA^{Thr}, tRNA^{Tyr}, tRNA^{Ala}, tRNA^{Leu}, tRNA^{Met}, tRNA^{Phe}, tRNA^{Pro}, tRNA^{Trp}, tRNA^{Val}) remained nearly constant for all three conditions suggesting the presence of a regulatory mechanism.

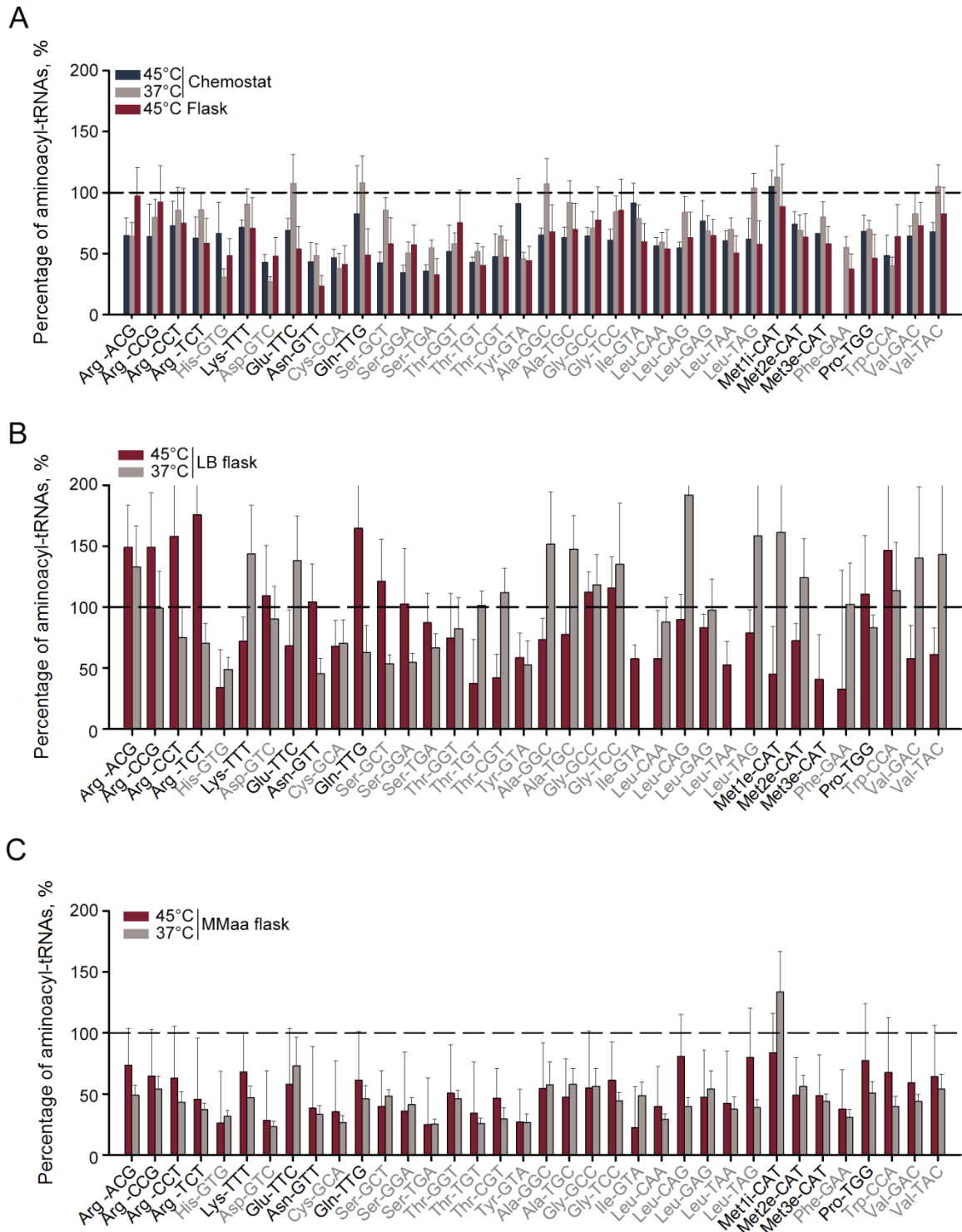


Figure 6. Chemostat-controlled growth or temperature do not affect the level of aminoacylated tRNAs.

(A) Proportion of aminoacyl-tRNAs in chemostat-controlled growth at 45 °C (blue) or 37 °C (grey) and in flasks at 45 °C (red wine). Only one replicate is shown for chemostat experiments. For the flask experiment data are means \pm SD (n=2); (B) Proportion of aminoacyl-tRNAs in of *B. licheniformis* HD0583 grown LB (B) or MMaa (C) at 45 °C (red wine) and at 37 °C (dark gray). The fraction of the charged tRNAs is normalized to the total

amount of each isoacceptor which for each condition is independently set at 100% (horizontal dashed line). Data are means \pm SD (n=2) Only one replicate is shown for 37°C experiments, for the experiment at 45°C data are means \pm SD (n=2). tRNA isoacceptors T-box regulator are written in grey, non t-box regulator are written in black.

When cells entered stationary phase the growth ceased and the level of some aminoacyl-tRNAs significantly dropped, while the concentration of each tRNA isoacceptor insignificantly changed (Figure 7 A and B). The amount of tRNAs charged with polar amino acids decreased the most. Notably, those tRNAs, especially tRNA^{Ser} and tRNA^{Thr} are generally low in their abundance compared to the other isoacceptors (Table 1). Moreover, we investigated whether altering tRNA demand, i.e. inducing protein overexpression, changes the observed charging pattern. Thus, we measured the tRNA aminoacylation level of *B.licheniformis* strain overexpressing *aprE*, a heterologous serine protease subtilisin. A clear decrease, in exponentially growing cells, of some aminoacyl-tRNAs is detected (Figure 7 C, light blue). In particular the charging level of the low abundant tRNA^{Ser} and tRNA^{Thr} was the most affected but also these isoacceptors were among the most requested, due to high frequency of their cognate codons for *aprE* synthesis. Further decrease in the level of charging is observed during stationary phase growth and the pattern resembled the one of the non-overexpressing strain (Figure 7 B and C). Taken together our results indicate that the tRNA charging level varies among the different isoacceptors and follows two distinct patterns: some tRNA isoacceptor families were nearly uniformly charged, while the charging of other fluctuated with different media.

In *Bacillus* the charging of tRNA appears to be nutrient independent suggesting that adaptation of translation and growth rate regulation, may take place by controlling the tRNA pool rather than regulating the aminoacylation level.

Table 1. Absolute quantification of *B. licheniformis* tRNA. *B. subtilis* tRNA (Kanaya et al. 1999) was used as a baseline for the quantification from the microarrays.

* For those five tRNA isoacceptors the absolute tRNA concentration was extrapolated using the tRNA dependence of the copy number

tRNA species	Concentration of <i>B. licheniformis</i> tRNA	Concentration of <i>B. subtilis</i> tRNA
tRNA ^{Ala} GGC	0.36	0.23
tRNA ^{Ala} TGC	1.42	1.24
tRNA ^{Arg} ACG	0.51	0.48
tRNA ^{Arg} CCG	0.35*	0.26*
tRNA ^{Arg} CCT	0.35*	0.26*
tRNA ^{Arg} TCT	0.11	0.13
tRNA ^{Asn} GTT	0.69	1.2
tRNA ^{Asp} GTC	1.03	1.31
tRNA ^{Cys} GCA	0.35*	0.25*
tRNA ^{Gln} TTG	1.09*	0.98*
tRNA ^{Glu} TTC	1.57	1.52
tRNA ^{Gly} GCC	1.11	0.85
tRNA ^{Gly} TCC	0.65	0.66
tRNA ^{His} GTG	0.60*	0.5*
tRNA ^{Ile} GAT	1.27	1.42
tRNA ^{Leu} GAG	0.19	0.22
tRNA ^{Leu} CAG	0.16	0.15
tRNA ^{Leu} TAG	0.23	0.2
tRNA ^{Leu} CAA	0.53	0.41
tRNA ^{Leu} TAA	0.26	0.2
tRNA ^{Lys} TTT	0.66	0.73
tRNA ^{Met 1} CAT	1.00	1
tRNA ^{Met 2-3} CAT	0.49	0.54
tRNA ^{Phe} GAA	0.87	0.75
tRNA ^{Pro} TGG	1.21	1.12
tRNA ^{Ser} GGA	0.23	0.2
tRNA ^{Ser} TGA	0.13	0.13
tRNA ^{Ser} GCT	0.25	0.2
tRNA ^{Thr} GGT	0.19	0.16
tRNA ^{Thr} CGT	-	-
tRNA ^{Thr} TGT	1.16	1.19
tRNA ^{Trp} CCA	0.14	0.15
tRNA ^{Tyr} GTA	0.63	0.38
tRNA ^{Val} GAC	0.50	0.42
tRNA ^{Val} TAC	0.92	0.9

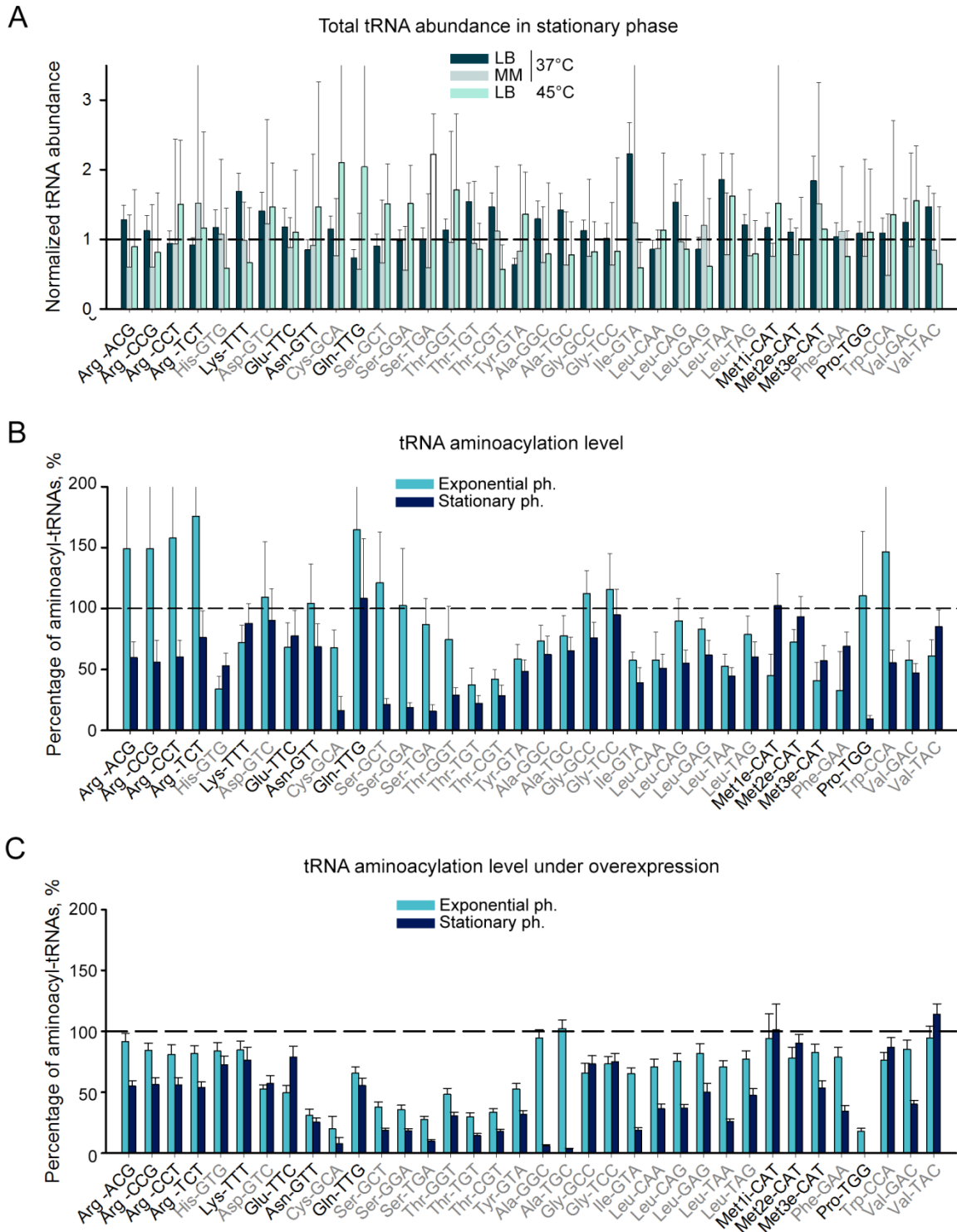


Figure 7. Changes in the total and charged tRNA in stationary phase.

(A) tRNA abundance changes between exponential and stationary phase *B.licheniformis* HD0583 grown at 37°C in LB medium (blue-green) and MM medium (grey), and cell grown at 45°C in LB medium (light green). The expression value of each *B.licheniformis* tRNA isoacceptor in exponential phase is set to 1 (horizontal dashed line). Data are means \pm SD (n=2) for MM, and single experiments for LB samples. Comparison of the proportion of aminoacyl-tRNAs of *B. licheniformis* HD0583 (B) and *B. licheniformis* HD0583_{apr2-}

pUBM72_aprE (C) grown in LB at 45 °C in exponential phase (light blue) and stationary phase (dark blue). The fraction of the charged tRNAs is normalized to the total amount of each isoacceptor which for each condition is independently set at 100% (horizontal dashed line). Data are means \pm SD (n=2). tRNA isoacceptors T-box regulator are written in grey, non t-box regulator are written in black.

2.2.2. The tRNA pool changes in a nutrient-dependent manner

Microarray analysis also allows comparing the relative tRNA amounts between two species or conditions. We determined the total tRNA concentration in the three different media previously described. In the medium with the highest growth rate ($\mu= 2 \text{ h}^{-1}$), LB medium, the concentration of almost all tRNA isoacceptors was the highest (Figure 8). The concentration of all tRNA isoacceptors decreased from LB to MMaa ($\mu= 1.45 \text{ h}^{-1}$) and MM ($\mu= 0.74 \text{ h}^{-1}$) which mirrored the growth rate reduction (Figure 5 A). tRNA^{Arg}CCT, tRNA^{Arg}TCT, tRNA^{Asn}GTT, tRNA^{Gln}TTG and tRNA^{Ser}GCT showed an increase in MM, which however was insignificant. tRNA^{Asn}GTT and tRNA^{Gln}TTG are encoded by four and six genes respectively which may contribute to their higher abundance.

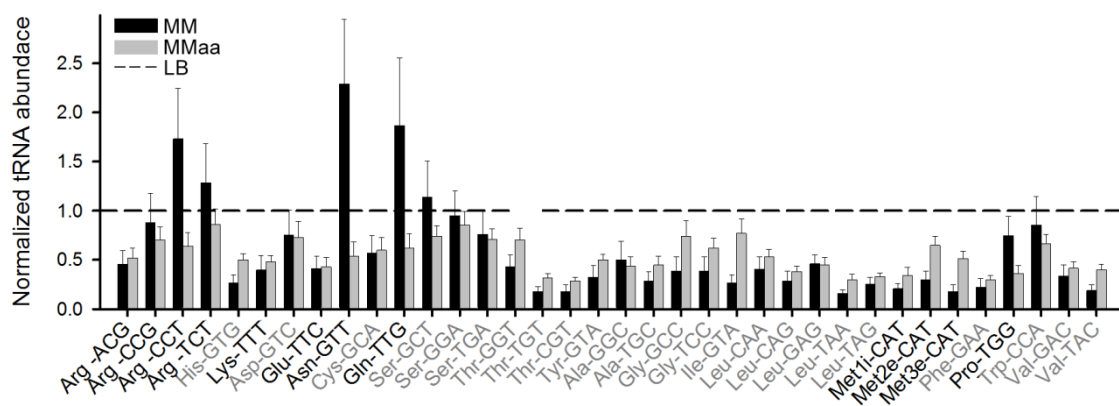


Figure 8. tRNA abundance varies with the nutrient composition of the growth medium.

Microarray analysis of the total tRNA isoacceptors of *B. licheniformis* HD0583 in MM (black) and MMaa (grey) at 45 °C. The expression value of each tRNA isoacceptor in LB is set to 1 (horizontal dashed line) and those in MM and MMaa are presented relative to LB. Data are means \pm SD(n=2). tRNA isoacceptors T-box regulator are written in grey, non t-box regulator are written in black.

Those results indicate changes of one tRNA isoacceptors in different conditions but comparison among tRNA species is only possible knowing the absolute abundance of each. Since the most (except for five, see Table 1) isoacceptors of *B. subtilis* were

quantified previously (Kanaya et al. 1999), we first compared the concentration of *B. licheniformis* DSM13 tRNA to that of *B. subtilis* 168 analysing them on the same microarray. The concentrations of the tRNA isoacceptors of *B. licheniformis* DSM 13 were very similar to that of *B. subtilis* (Figure 9 A). Furthermore, the tRNA concentration of the high secreting *B. licheniformis* strain HD0583 was also similar to *B. subtilis* (Figure 9 B), implying an evolutionary conservation of tRNA sets between related species.

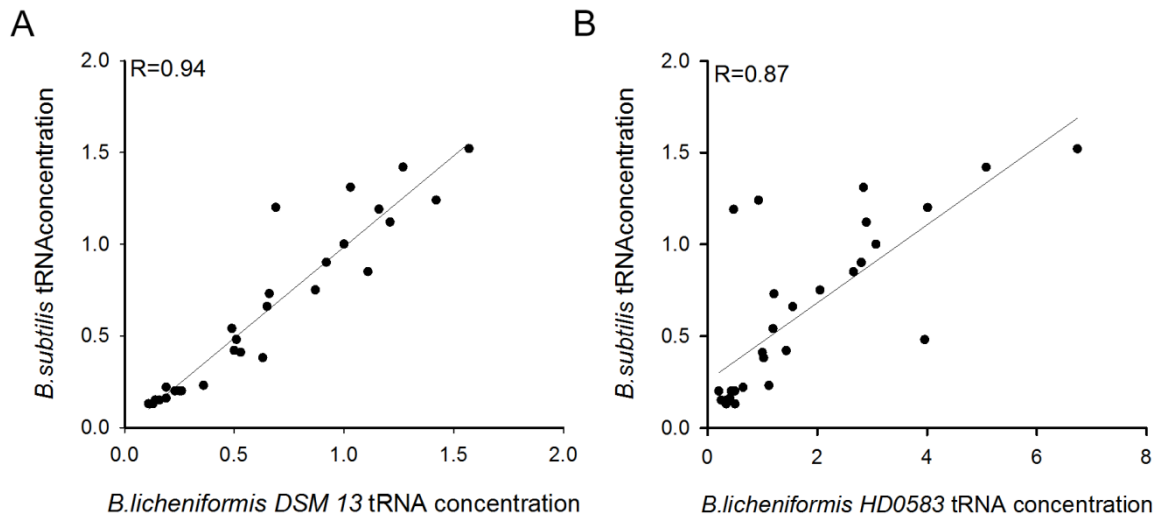


Figure 9. The tRNA concentration between different Bacillus strains is similar.

Comparison of the absolute concentration of *B. subtilis* with *B. licheniformis* DSM 13 (A) and *B. subtilis* with *B. licheniformis* HD (B) all grown at 37°C in LB. Each tRNA is presented as a fraction of the total tRNAs. The level of the initiator tRNA^{Met}CAT reading the AUG start codon was arbitrarily set to 1.0 as described in (Kanaya et al. 1999).

The three strains, *B. subtilis*, *B. licheniformis* DSM13 and *B. licheniformis* HD0583 exhibited very similar growth rates in LB at 37°C, 1.47 h⁻¹ (Durand et al. 2012), 1.38 h⁻¹ and 1.45 h⁻¹, respectively. However, strain optimization to enhance secretion capacity includes changes in the tRNA household: the tRNA concentration of *B. licheniformis* HD0583 results to differ, even more than fivefold, from the DSM strain (Figure 10A). Increasing the growth rate by growing the HD0583 strain at its optimal temperature of 45°C the expression of some tRNA was also altered (Figure 10 B).

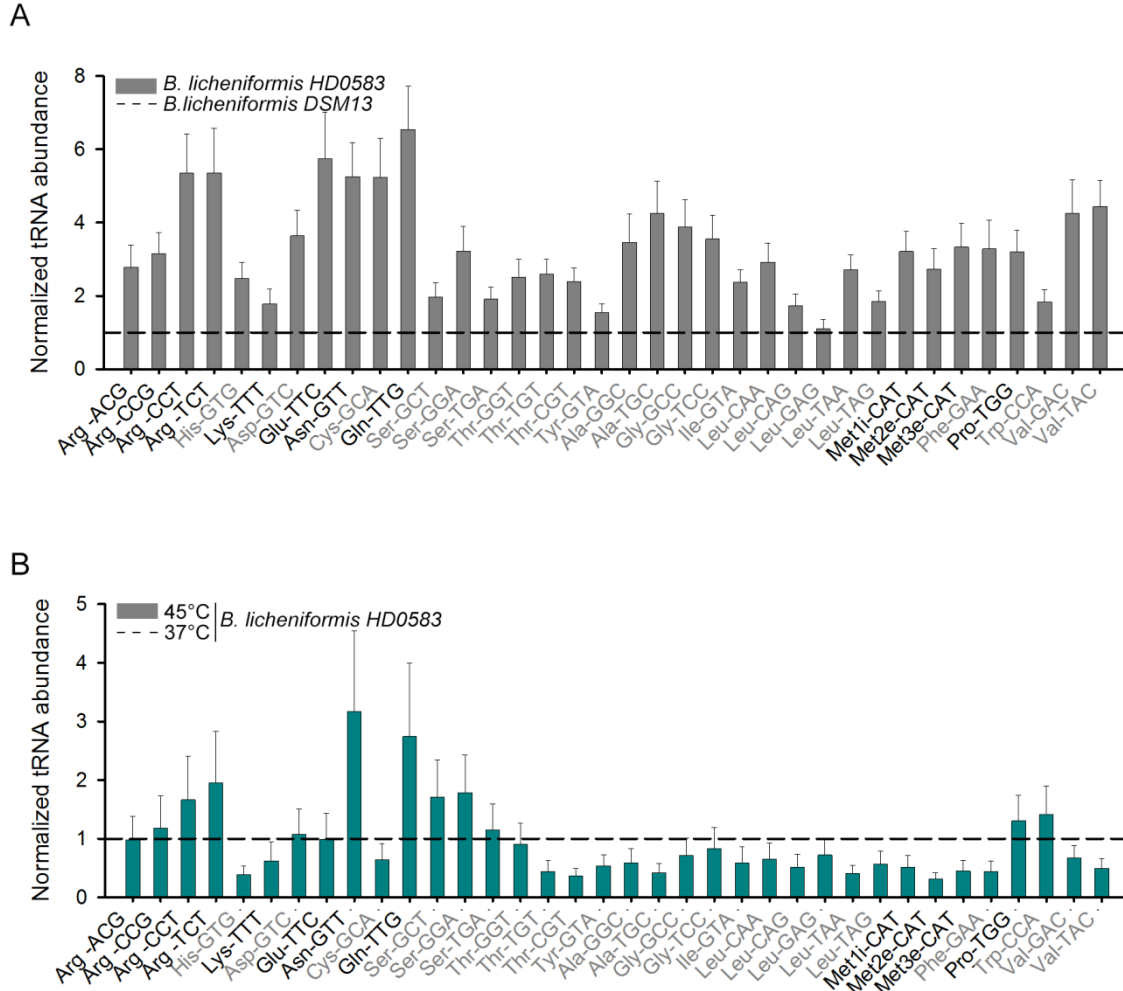


Figure 10. Strain optimization boosts tRNA expression.

(A) Microarray-based comparison of *B.licheniformis* HD0583 tRNA compared to *B.licheniformis* DSM13 tRNA, both grown in LB medium at 37°C. The expression value of each *B.licheniformis* DSM13 tRNA isoacceptor is set to 1 (horizontal dashed line). Data are means \pm SD(n=2). (B) Growth temperature shift from suboptimal (37 °C) to optimal (45 °C) resulted increased the amount of many tRNA isoacceptors. Microarray analysis of the tRNA abundance of *B.licheniformis* HD0583 grown at 37°C compared to cells grown at 45°C for which the concentration of each tRNA isoacceptor is set to 1 (horizontal dashed line). Data are means \pm SD(n=2). tRNA isoacceptors T-box regulator are written in grey, non t-box regulator are written in black.

In sum, the total tRNA concentration correlates with nutrient availability and growth rate, being elevated in fast growing cells. In particular, we noticed that with few exceptions all tRNAs underwent changes and not a fraction of them (Figure 9). Elevation of a set of specific tRNA isoacceptors is traditionally viewed as adjustment of the tRNA pool to

adequately mirror the codon usage of highly expressed genes at each condition (Novoa et al. 2012) but *Bacillus licheniformis* seems to follow a different adaptive strategy.

2.2.3. Nutrient availability fine-tune tRNA expression by GTP-dependent transcription initiation

Bacillus developed an evolutionary strategy to prevent overinvestment of energies by sensing and responding to purine nucleotides concentration. Transcription of many genes is proportional to the GTP level, being GTP the initiating nucleotide (iNTP) of many energetically costly products, like ribosomes (Dworkin and Losick 2001; Krasny and Gourse 2004; Krasny et al. 2008; Bittner et al. 2014). GTP concentrations changes with growth phase and nutritional conditions, being higher in rich medium, and lower under carbon, nitrogen, or phosphorus source limitation (Fujita and Losick 2005). We suggest that, since the processing and maturation mechanism is not tRNA specific, the mechanism acting on the tRNA expression may be the same G-dependent transcriptional regulation observed for rRNA genes. Gram-negative bacteria, like *E. coli*, usually transcribe their tRNA genes in small transcriptional unit or as single gene, and only one or two tRNA genes follow the rRNA genes (Ohnishi et al. 2000). Opposite, clustering of high numbers of tRNA genes adjacent to rRNA genes is common in many Gram-positive bacteria (de Vries et al. 2006). The 72 tRNA genes of *B. licheniformis* distribute in seven single genes and ten clusters, each containing from 2 to 20 tRNA genes. Five of the ten clustered genes are associated with the rrs operons (RNA operons) (**Table 2**).

Table 2. tRNA genes distribution along the genome

iNTP	rRNA operon																				
G	A	Ile GAT	Ala TGC																		
A		Ser TGA																			
G	B	Ile GAT	Ala TGC																		
		Met CAT 2e	Glu TTC																		
G	D	Met CAT 2e	Glu TCC																		
T		Glu TCC	Val TAC	Thr TGC	Tyr GTA	Gln TGG															
C		Asn GTT	Ser GTC	Glu TTC	Gln TTG	Lys TTT	Leu TAG	Leu GAG													
G	E	Arg ACG	Gly TCC	Met CAT li	Asp GTC																
G	F	Asn GTT	Ser GGA	Glu TCC	Val TAC	Met CAT li	Asp GTC	Phe GAA	Thr TGC	Tyr GTA	Trp CCA	His GTC	Gln TTG	Gly GCC	Cys GCA	Leu TAA	Leu CAA	Gly TCC			
G		Val GAC																			
C		Arg CCT																			
		Gln TTG																			
G		Arg TCT																			
		Val TAC	Thr CGT	Lys TTT	Leu CAG	Gly GCC	Arg ACG	Pro TGG	Ala TGC	Met CAT 2e	Met CAT 3e	Ser TGA	Met CAT li	Asp GTC	Phe GAA	His GTC	Gly TCC	Ile GAT	Asn GTT	Ser GTC	Glu TTC
		Ala GGC																			
		Arg CCG																			
G		Lys TTT	Glu TTC	Asp GTC	Phe GAA																

We firstly verified the GTP sensing regulation on rRNA synthesis in *B. licheniformis* observing that the transcriptional level of the 5S rRNAs is reduced by an average of 30% in MM growing cells compared to that in rich medium (Figure 11 A). Moreover, bacterial cultures subjected to upshift (from MM to MMaa) and downshift assay (from MMaa to MM) showed up- or down-regulation, respectively, for the 5S and 16S rRNA genes (Figure 11 B-C) indicating highly GTP dependence for rRNA expression. Under starvation the rRNAs, which represent the higher storehouse of nutrients in the cell, are immediately degraded. Opposite, when the nutrient availability increase, and consequently GTP level arises the transcriptional rate of GTP-dependent genes is enhanced.

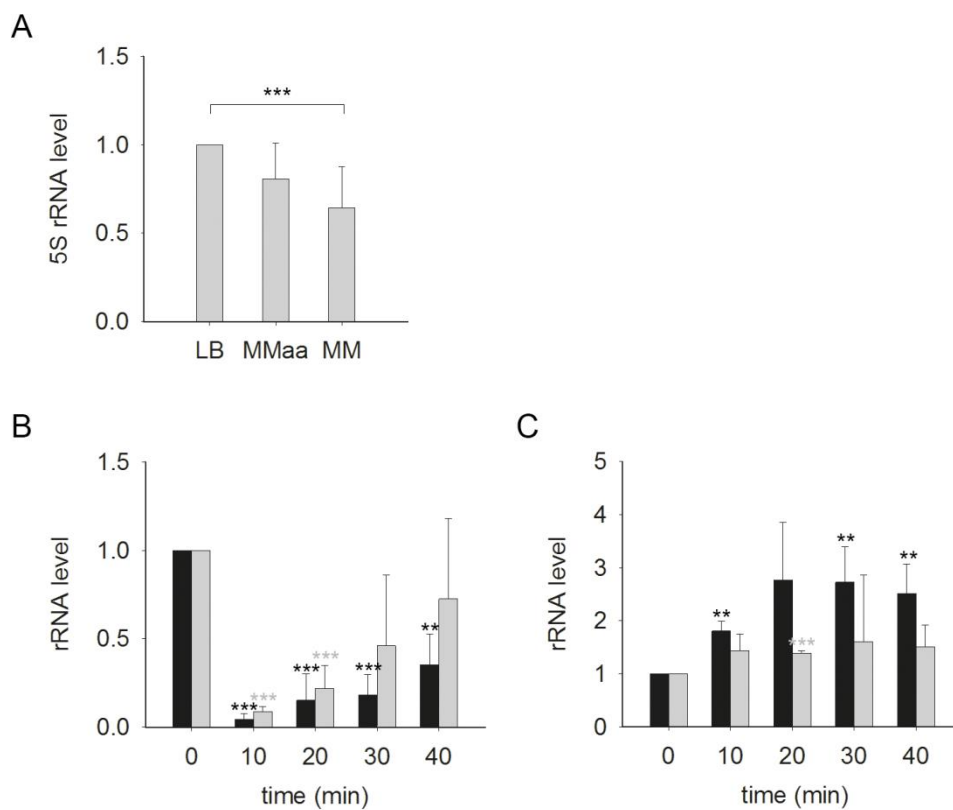


Figure 11. The expression of 5S and 16S ribosomal RNAs.

A) Expression level of 5SrRNA in different growth conditions; B) Expression level of 5S rRNA (grey) and 16S rRNA (black) during downshift growth from MMaa to MM; C) Expression level of 5S rRNA (grey) and 16S rRNA (black) during upshift growth from MM to MMaa. All data are referring to time 0. Data are means \pm s.d. (n = 3)**, p < 0.01, ***, p < 0.001.

The iNTP has been previously identified only for four tRNA transcriptional units so far (Wiegand et al. 2013a). Taking advantage of the RNA-Seq data (see next chapter) we predicted the iNTP for all seven rRNA operons and 3 tRNA operons. Notably, G is the iNTP of all rRNA, rRNA-tRNA operon and also for one tRNA operon and two single genes. Two single genes, encoding for tRNA^{Ser} TGA and tRNA^{Arg} CCT, are initiated by A and C, respectively. Notably, the tRNAs which remains unchanged among LB and MM are exactly the one starting with A or C (tRNA^{Ser} GCT, tRNA^{Ser} TGA and tRNA^{Arg} CCT) therefore not affected by GTP decrease.

Those observations confirm that tRNA expression is regulated by the presence of either guanine or adenine in the transcription initiation site thus dependent on nutrient availability.

2.2.4. Uniform charging of the tRNA isoacceptor families is regulated via T-box-dependent activation of the cognate aaRS expression: the evolutionary strategy to escape toxicity effect

Intrigued by our observation that all tRNA isoacceptors within one isoacceptor family, i.e. all loaded with the same amino acid, maintained a constant level, we hypothesized that the cognate aaRS may specifically monitor the level of the charged tRNAs within one family. Different strategies are used, among bacteria, to regulate the expression of the genes encoding AARSs. In contrast to what is found in *E. coli*, where different mechanisms, either at the transcriptional or translational level, are used to regulate the expression of various aaRS genes (Grunberg-Manago et al. 1985), in *B. subtilis* and other Gram-positive bacteria, many of these genes and many amino acid biosynthetic operons are regulated by a common mechanism known as T-box (Putzer et al. 1995). T box consists of highly conserved sequence located in the 5'-untranslated region of the mRNA which is recognized by a specific uncharged tRNAs. The binding with the uncharged tRNA prevents the formation of a terminator hairpin facilitating the read-through and thus increasing the expression of the downstream aaRS encoding gene (Henkin and Grundy 2006). Thirteen out of twenty-four (Novichkov et al. 2013) *aaRS* genes in *B. licheniformis* are under T-box regulatory mechanism and respond to cognate amino acid limitation (Putzer et al. 1995; Pelchat and Lapointe 1999; Henkin 2008; Vitreschak et al. 2008; Gutierrez-Preciado et al. 2009; Green et al. 2010). Among the 15 (tRNA^{His}, tRNA^{Ala}, tRNA^{Lys}, tRNA^{Glu}, tRNA^{Asn}, tRNA^{Cys}, tRNA^{Gln}, tRNA^{Thr}, tRNA^{Tyr}, tRNA^{Gly}, tRNA^{Leu}, tRNA^{Met}, tRNA^{Phe},

tRNA^{Pro}, tRNA^{Trp}, tRNA^{Val}) families of *B. licheniformis* HD0583 for which we detected uniform charging (Figure 5 E), 10 are loaded by T-box regulated AARSs (*HisS*, *AlaS*, *CysS*, *ThrS*, *TyrS*, *GlyS*, *LeuS*, *PheS*, *TrpS* and *ValS*). The total concentration of all these tRNA isoacceptors rises according to the growth rate (Figure 8). Thus, we hypothesized that since the cognate aaRSs sense and regulate the amount of aminoacyl-tRNAs to a steady level (i.e. uniform fraction of aminoacyl-tRNAs within each isoacceptor family) the aaRSs amount in different media should mirror the differences between the cognate tRNA isoacceptors. Quantitative mRNA expression analysis of the T-box regulated *thrS* and *valS* (Figure 12 A-B-C) reveal that aaRS expression follows the trend of the cognate tRNA isoacceptors (Figure 8) being the highest in LB and the lowest in MM. Another T-box regulated gene, *ProI*, which belongs to the proline biosynthetic pathway, resembled the behaviour of *thrS* and *valS* (Figure 12 A, D). Opposite, the mRNA expression level of the non T-box-regulated *ArgRS* showed uniform expression in MMAa and MM which was slightly lower than that in LB (Figure 12 A, E).

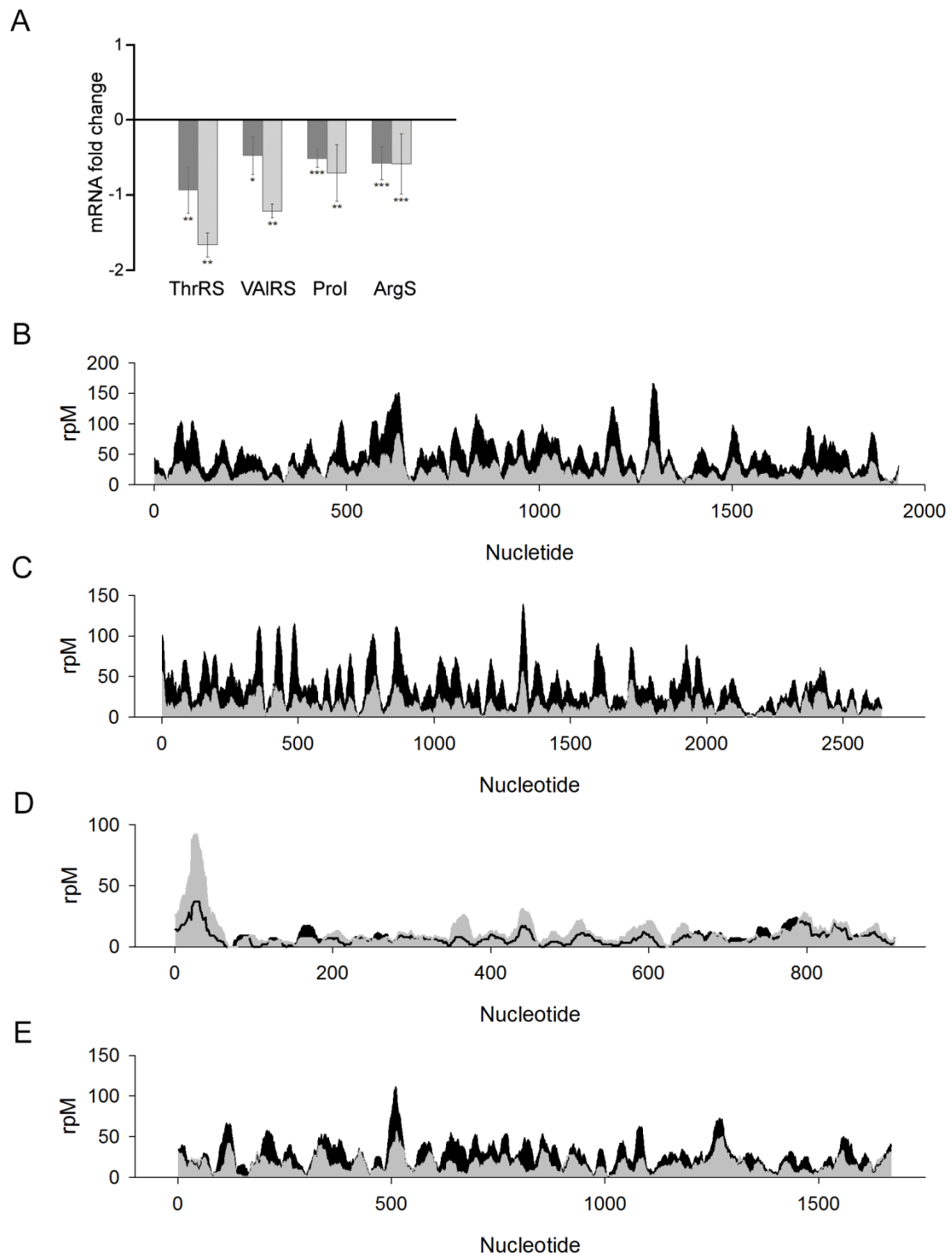


Figure 12. The expression of T-box regulated genes depends on growth rate.

(A) Real-time qRT-PCR analysis of T-box regulated *ThrRS*, *ValRS*, *ProI* and non-T-box regulated *ArgS* gene expression levels in MM (light grey) and MMaa (dark grey) normalized to the expression in LB. Data are means \pm s.d. ($n = 3$), **, $p < 0.01$, ***, $p < 0.001$. The mRNA expression profiles of T-box genes, *thrS* (B), *valS* (C), *proI* (D) and non T-box gene *argS* (E) in LB (black) and MM (grey) growing cells. The mRNA expression profiles were

obtained from RNA-Seq analysis and presented as rpM, reads per million, i.e. normalized to the sequencing depth.

In the other group of tRNAs (tRNA^{Arg}, tRNA^{Asp/Asn}, tRNA^{Lys}, tRNA^{Pro}, tRNA^{Met}, tRNA^{Glu/Gln}), which are charged by non-T-box-controlled aaRSs, we observed slight changes of the charging level, under different growth conditions, which however are not significant (Figure 5 E). This pattern is reminiscent of the charging pattern of tRNAs in *E. coli* which uses a variety of control mechanisms at both transcriptional or translational level to regulate the aaRSs in response to amino acid levels (Springer et al. 1985). The regulation of non-T-box regulated aaRSs in *B. licheniformis* is diverse though unknown for the majority of them; aspartyl-tRNA synthetase is under the control of σ^A promoter, methionyl-tRNA synthetase has a rho-independent transcription terminator structure, glutamyl-tRNA synthetase capable of charging tRNA^{Glu} as well as tRNA^{Gln} is constitutively expressed from a promoter 43 nts upstream of the structural gene (Condon et al. 1996). The reason why the T-box system has been evolved only for some amino acid families is still unclear. Supplementing bacteria culture with a mixture of all amino acids, varying in a range of 0.1-3.7mM each, was a strategy to enhance the growth suggesting that, for many amino acids, concentrations lower than 4mM may not inhibit the growth. Therefore, to evaluate possible toxic effects, we added them to different concentrations of (5mM, 10mM, 30mM, and 50mM) various amino acids into the medium to track any dose-dependent analysis of the amino acids. The cellular growth of *B.licheniformis* HD0583 in MM and MM supplemented with single amino acid (using seven of the thirteen T-box related amino acids and four of the seven) was compared. All T-box dependent amino acids (Figure 13 A-G) exhibited a negative effect on the growth rate. In particular serine and cysteine had the most dramatic inhibition while in presence of the others bacteria were still able to growth but not over OD_{600nm}~0.4. Opposite, non T-box regulated amino acids supported the growth (Figure 13 H-K) until the OD observed in the control medium. The obtained results support the hypothesis that T-box related amino acids maybe toxic on bacteria cells, thus, suggesting that the T-box system has been evolved to avoid toxicity keeping under control the level of free amino acid in the cells.

Remarkably, the T-box regulated gene expression in *B. licheniformis* is not only a powerful mechanism to keep the fraction of the aminoacylated tRNA constant in each medium but its main function is to prevent accumulation of the toxic free amino acid enabling the cell to stop the uptake of this compound when present in excess.

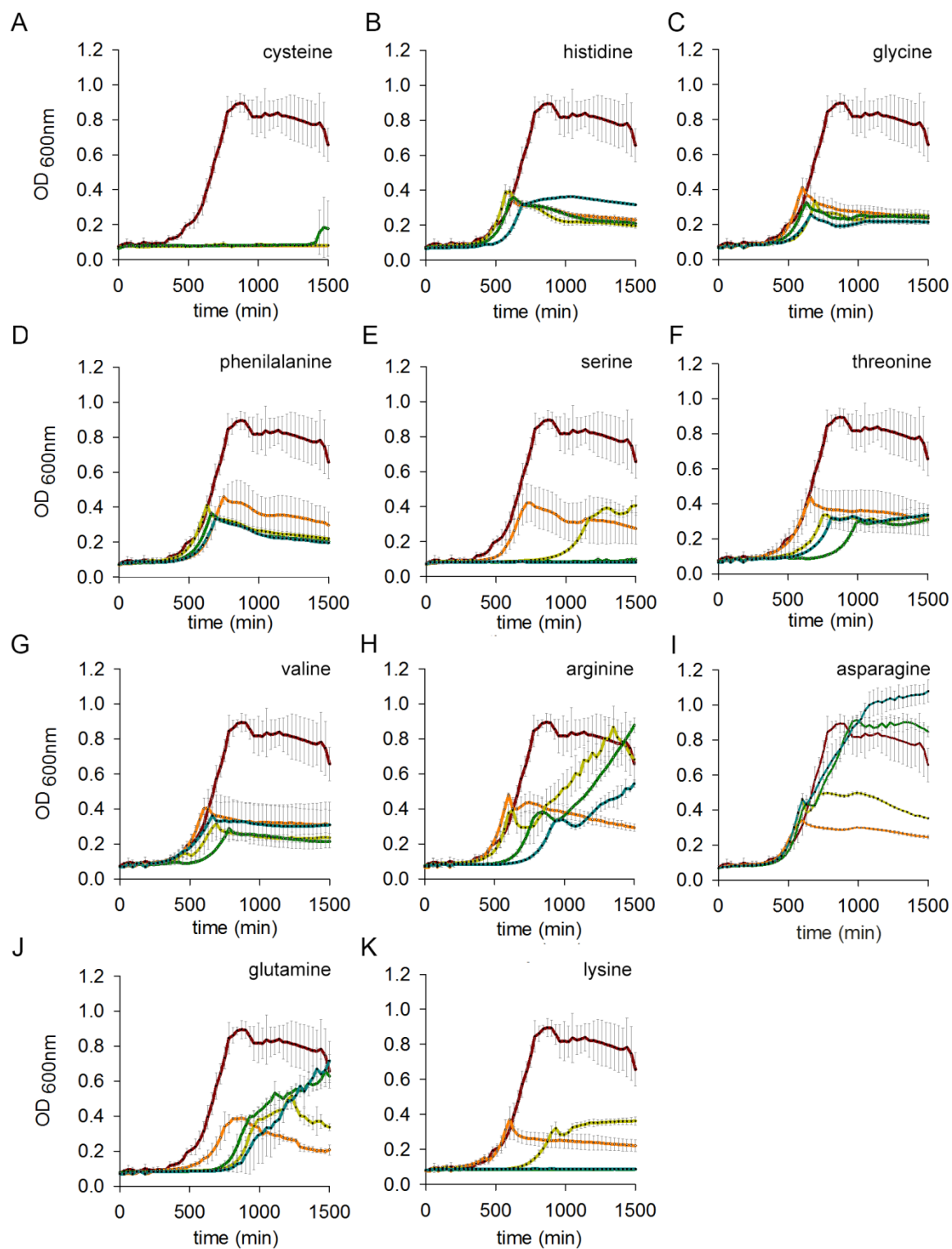


Figure 13. Growth curve of bacteria culture.

Cognate amino acids are added to MM culture with increasing concentration: 0mM red (control), 1mM orange, 10mM yellow, 30mM green, 50mM blue. For tRNA T-box regulating genes: (A) Cysteine. (B) Histidine. (C) Glycine. (D) Phenilalanine. (E) Serine. (F) Threonine. (G) Valine. For tRNA not T-box regulating genes: (H) Arginine. (I) Asparagine. (J) Glutamine. (K) Lysine. Data are means \pm s.d. (n = 3)

2.3. Genome-wide characterization of transcriptional and translational changes in different media

In order to investigate the relative transcriptional and translational expression level of different transcripts by different nutrient availability and growth rate we combined two powerful high-throughput sequencing techniques, Ribo-Seq and RNA-Seq. In this section we analyze, on a global transcriptome- and translome-wide scale, the effect of different nutrient conditions on *Bacillus licheniformis* growth.

2.3.1. Ribo-Seq and RNA-Seq libraries

Ribosome profiling (Ribo-Seq) is a powerful technology which allows addressing various aspects of translation regulation on a global, cell-wide scale. For sample preparation the most important and critical point is represented by the isolation of intact ribosome-mRNA complexes, named ribosome protected fragments (RPF) (Bartholomaeus et al. 2016). Therefore, exponentially growing, in LB and MM, and stationary growing, in MM, bacterial cultures were rapidly harvested by filtration and flash frozen to immediately stall translating ribosomes along their mRNAs, without any antibiotic pre-treatment that may induce bias (Hussmann et al. 2015). Subsequently, RPFs were generated via nucleic acid digestion of the non-protected mRNA fragments by MNase (Del Campo et al. 2015). In parallel, the total RNA was isolated from all cultures and, after depletion of rRNAs, was randomly fragmented by alkaline hydrolysis. Hence, RPFs and the total RNA fragments, with a range size of 20 to 30 nts, were selected for preparation of a high-throughput sequencing library sequenced using the Illumina HiSeq2000 sequencing machine.

2.3.2. Comparative Analysis of Ribo-Seq and RNA-Seq libraries

To evaluate the fidelity of our method we compared biological replicates and observed a good linear correlation coefficients, Pearson correlation coefficient of $R= 0.93$ and $R= 0.95$ for the RNA-Seq from LB and MM, respectively (Figure 14 A, C) while $R=0.94$ and $R= 0.97$ for the RPF replicates from MM and LB, respectively Figure 14(Figure 14 B, D), demonstrating high reproducibility of Ribo-Seq method.

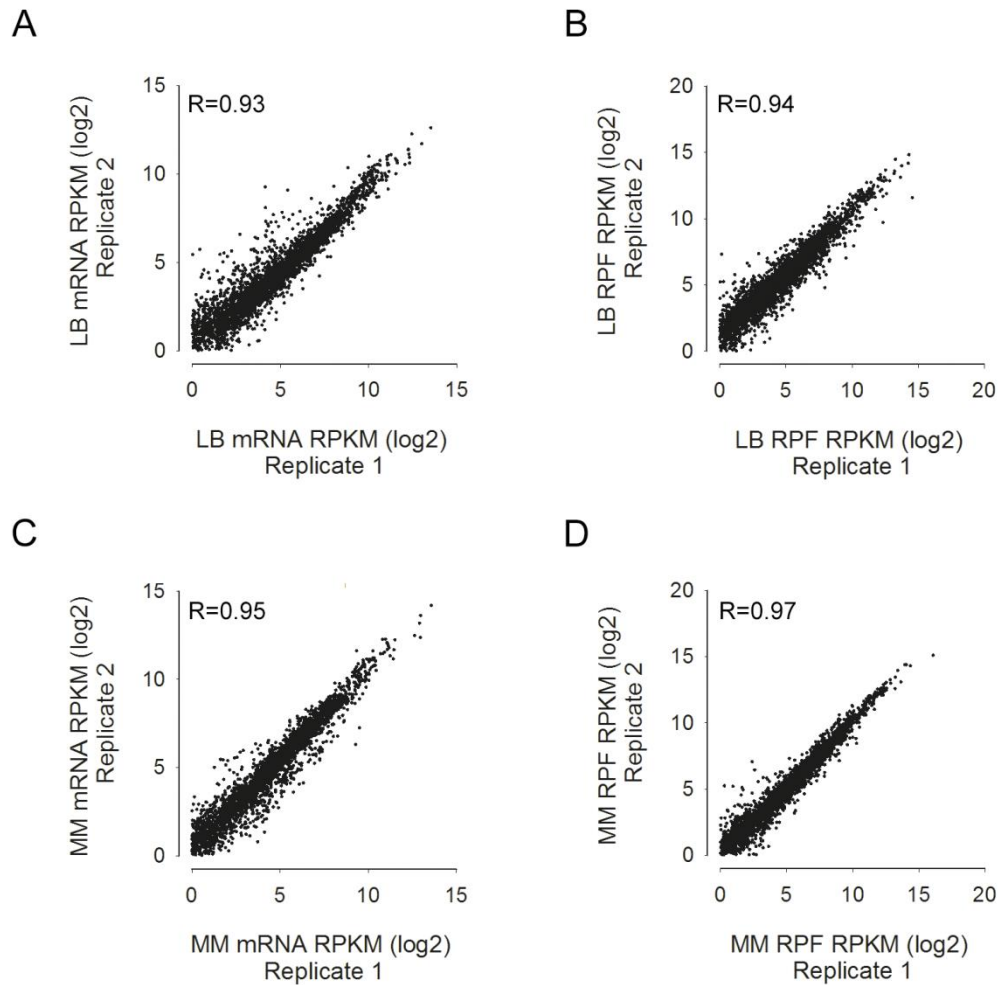


Figure 14. Correlation of mRNA and RPF sequencing reads.

Correlation of sequencing reads of mRNA (A, C) and RPF (B, D) between two biological replicates of LB (A, B) or MM (C, D). Reads are given in RPKM (reads per kilobase per million mapped reads). R indicates the Pearson correlation coefficient.

Within each dataset, a good linear relation between RPF and mRNA abundance was also observed (Figure 15). For further analysis the derived sequencing reads will be expressed as RPKM (See Materials and Methods section).

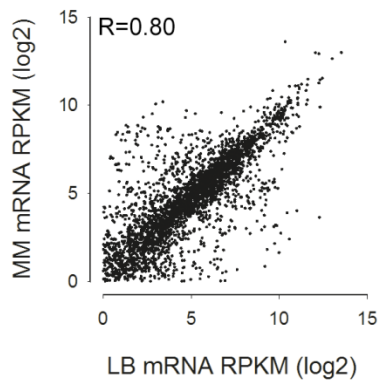
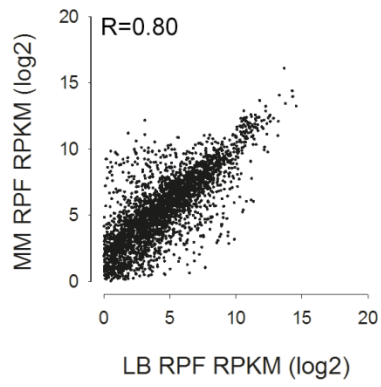
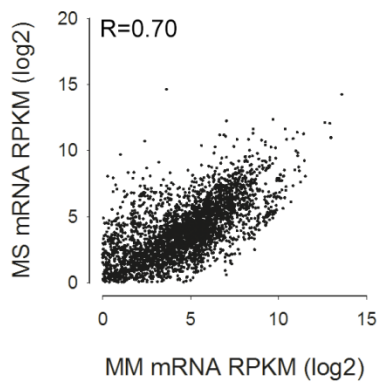
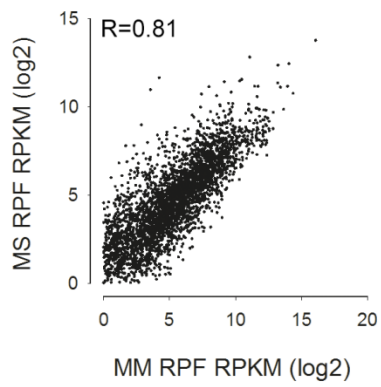
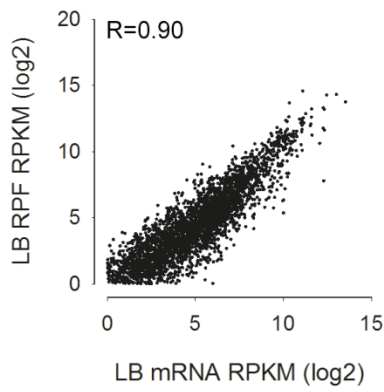
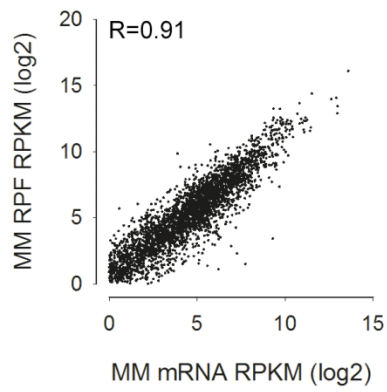
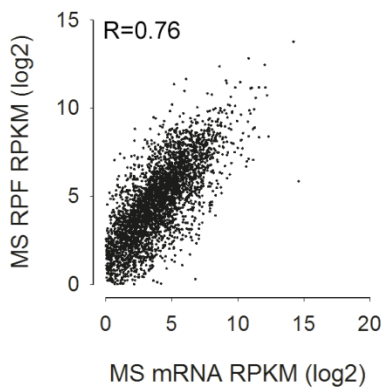
A**B****C****D****E****F****G**

Figure 15. Correlation of sequencing reads of mRNA (A, C) and RPF (B, D) of LB, MM and MS samples.

Correlation of sequencing reads of mRNA (A, C) and RPF (B, D) between LB and MM (A-B) and between MM and MS (C-D). (E-F-G) Correlation between the mRNA and RPF abundance (expressed as RPKM) from LB (E), MM (F) and MS (G) growing cells. For the correlation of LB and MM the first replicate was used for both. Reads are given in RPKM (reads per kilobase per million mapped reads). R indicates the Pearson correlation coefficient.

The \log_2 -change of each gene between the biological replicates of each condition is plotted as a histogram (Figure 16). The line delineates 95th percentile overlap between the \log_2 -distributions of the two biological replicates and it is used as a statistical threshold. At 95% for mRNA LB and MM, the \log_2 -fold change is equal to 1.5 and 1.6, respectively, and for RPF of both LB and MM is equal to 1.5.

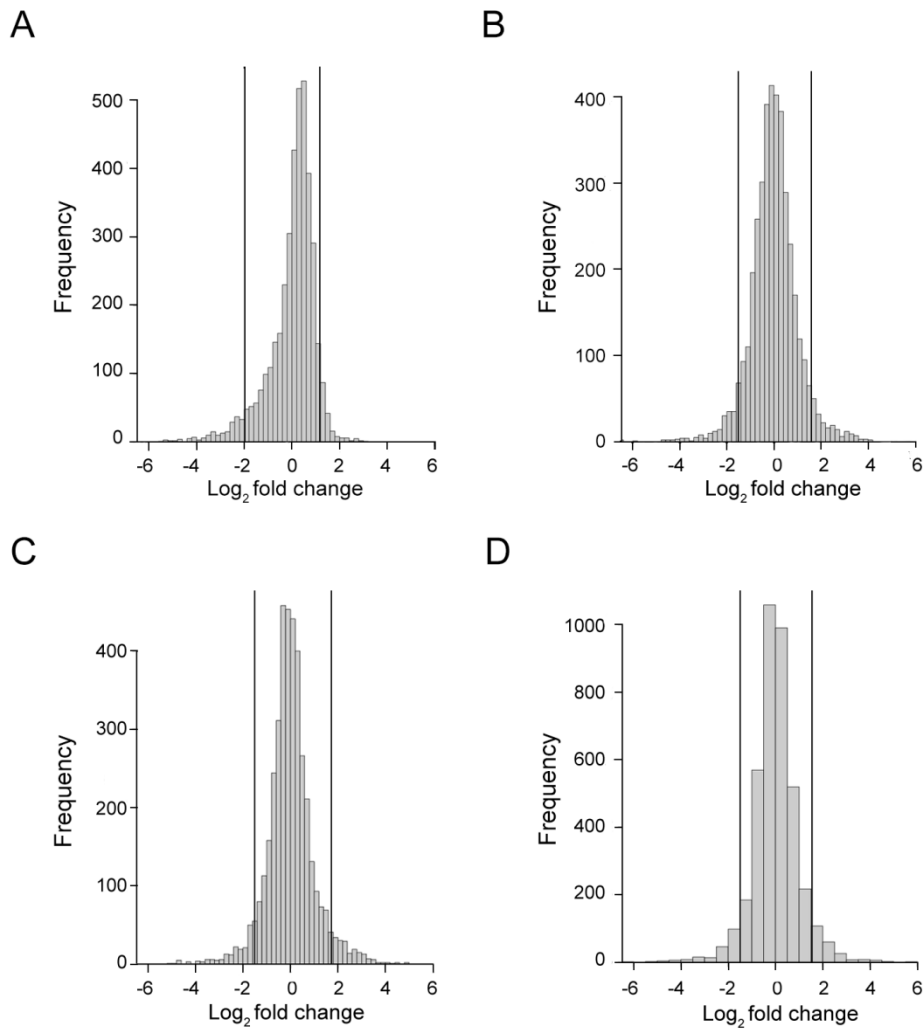


Figure 16. Reproducibility of randomly fragmented mRNAs (A-C) and RPF (B-D) of two biological replicates

The histogram of \log_2 -change of each gene between the two replicates, mRNA in LB (A) and MM (C) and RPF in LB (B) and MM (D), is plotted. The lines delineates 95th percentile overlap between the \log_2 -distributions of the two biological replicates. 95th percentile was used as a statistical threshold for the \log_2 -fold change analysis between different conditions.

2.3.3. Translational speed mirrors tRNA abundance

In our previous experiments we observed that with few exceptions the total abundance of all tRNAs underwent changes and not a fraction of them (Figure 8). We noticed also that some tRNAs are charged to low levels, under 50% (Figure 5 E). Since the rate of translation of a single codon depends on the concentration of the cognate tRNA (Zhang et al. 2009; Zhang et al. 2010), it raised the question as to whether those low charged amounts of some tRNAs may create some bottlenecks in translation. To address this, we determined the position of translating ribosomes from the Ribo-Seq data with codon precision. Our reads were calibrated assigning ribosome density to the 3' end which in prokaryotes contains precise and accurate information about the position of the ribosome (Woolstenhulme et al. 2015). We determined the nucleotides corresponding to the A-site and validated the calibration using a known ribosomal stalling site of *MifM* (Sohmen et al. 2015) (as shown in Figure 17 for reads of 24nt length).

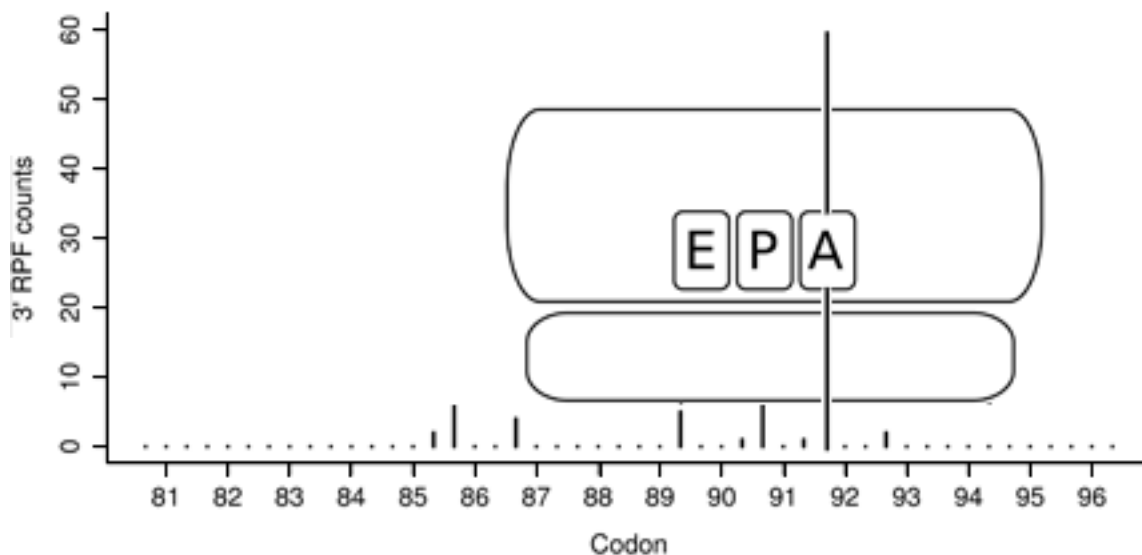


Figure 17. Reads calibration to determine the nucleotide sitting at the A site

All reads from our dataset are calibrated in order to determine the nucleotide corresponding to the A using a known ribosomal stalling site, corresponding to residues S92, of *MifM* (Sohmen et al. 2015) using the 3' end assignment method (Woolstenhulme et al. 2015).

For each ribosome we defined the identity of the A-site codon and the frequency of a codon in the ribosomal A site would represent the dwell time of the ribosome in expecting the cognate aminoacyl-tRNA if no secondary structure obstacles are met. Thus, the higher frequency of a codon in the ribosomal A site represents a longer dwell time (Ingolia 2014). To account for commonly used codons which will statistically occupy the ribosomal A site more often, the data were normalized for the effective codon usage (eCU) (**Table 3**), which is the genomic codon usage multiplied by the mRNA copies and is calculated from the RNA-Seq data. Comparison of the eCU from LB or MM growth emphasize that medium change does not change dramatically the eCU (Figure 18).

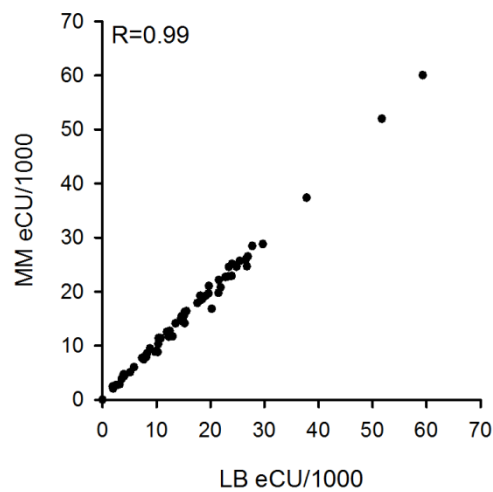


Figure 18. Comparative analysis of the eCU of LB and MM growing cells

Comparison of the Effective Codon Usage (eCU) calculated based on the transcriptome data of LB and MM growing cells.

Table 3. Effective codon usage of *B. licheniformis* and codon usage of *B.subtilis*.

Codon	eCU <i>B.licheniformis</i>	CU <i>B.subtilis</i>	Codon	eCU <i>B.licheniformis</i>	CU <i>B.subtilis</i>
aaa	53.4	43.0	gaa	58.8	46.9
aac	26.8	43.0	gac	25.8	46.9
aag	20.0	7.8	gag	22.5	15.6
aat	15.7	15.6	gat	28.9	35.2
aca	19.4	39.1	gca	22.2	7.8
acc	8.0	7.8	gcc	17.4	3.9
acg	18.0	19.5	gcg	24.1	23.4
act	10.1	7.8	gct	21.0	3.9
aga	8.7	19.5	gga	23.7	46.9
agc	14.4	19.5	ggc	26.8	11.7
agg	4.0	0	ggg	8.6	7.8
agt	2.6	0	ggt	15.0	11.7
ata	3.9	0	gta	13.1	15.6
atc	36.9	19.5	gtc	22.4	7.8
atg	26.8	31.2	gtg	14.7	23.4
att	26.1	39.1	gtt	22.5	15.6
caa	20.4	23.4	taa	2.8	3.9
cac	8.7	15.6	tac	13.1	7.8
cag	17.9	15.6	tag	0.5	0
cat	10.4	0	tat	15.2	27.3
cca	5.2	11.7	tca	12.5	23.4
ccc	2.4	0	tcc	8.0	0.0
ccg	17.8	23.4	tcg	7.5	0
cct	10.5	15.6	tct	12.8	11.7
cga	2.1	3.9	tga	0.5	0
cgc	14.9	11.7	tgc	3.9	3.9
cgg	5.8	0	tgg	7.3	0
cgt	10.3	15.6	tgt	2.0	3.9
cta	3.5	3.9	tta	11.3	7.8
ctc	11.5	11.7	ttc	16.9	31.2
ctg	21.1	19.5	ttg	14.8	7.8
ctt	26.0	15.6	ttt	20.1	46.9

Plotting the frequency of each codon in the ribosomal A-site as a function of genomic codon usage showed that TGG (Trp), TGC (Cys) and CCA (Pro) were among the codons with the longest dwell time in both LB and MM (Figure 19 A and B), highlighting that these particular tRNAs pairing to TGG and TGC triplets might be a bottleneck (Figure 19 A-B). However, their cognate tRNAs, tRNA^{Trp}CCA and tRNA^{Cys}GCA, exhibited high charging level (Figure 5 E), but are among the ones with the lowest abundance (**Table 1**).

These tRNAs are obviously a bottleneck point in translation independent of the growth conditions indicating that translational speed correlates with tRNA availability. Interestingly, Pro (CCA) is read by tRNA^{Pro} which exhibits high charging level and it is relatively abundant. A possible explanation for the long dwelling time at this proline codon is attributable to the poor reactivity of the cognate peptidyl-tRNA, being a poor peptidyl donor at the end of the nascent chain and a poor peptidyl acceptor on the incoming aminoacyl- tRNA.

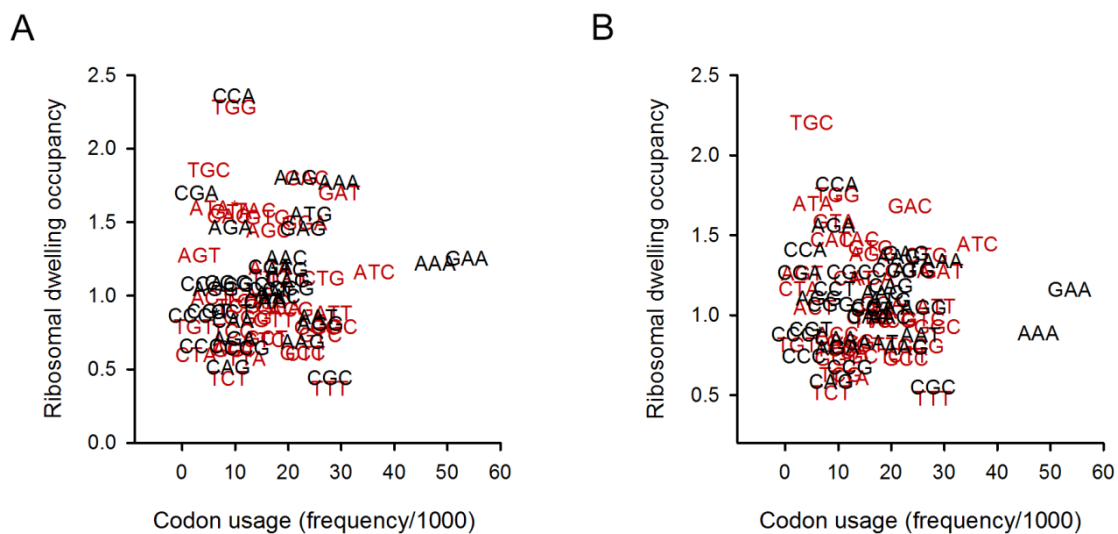


Figure 19. Ribosome dwells longer at codons read by lowly abundant tRNAs.

Frequency of each codon in the ribosomal A site when culturing cells in LB (A) and MM (B) medium as a function of the genomic codon usage. Codons read by T-box regulated tRNAs are color-coded red while the ones encoded by non T-box regulated tRNAs are in black.

2.3.4. Transcriptional and Translational Response induced by nutritional changes

To characterize the differentially expressed genes between the different conditions, we compared changes at both the level of transcription and translation by assessing the fold changes of the mRNA and RPF values.

Fold change analysis (Figure 20 A) identified significant up-regulation, in LB compared to MM, of 216 and 234 genes transcriptionally (mRNA) and translationally (RPF) changed, respectively. Similarly, in MM we observed up-regulation of 227 (mRNAs) and 210 (RPFs) genes. To characterize the biological functions affected by different conditions we used the DAVID functional annotation clustering tool (Huang da et al. 2009a; Huang da et

al. 2009b) which provides the typical gene-term enrichment analysis and clusters of redundant and heterogeneous terms into groups belonging to the same pathway. For the sake of simplicity only one term from each of the significant enriched clusters is showed (Figure 20).

In LB there are 158 genes which are co-regulated and induced at both transcriptional and translational level. The most enriched clusters of this group contain genes involved in cell motility (*motA*, *motB*), including flagellar assembly (*fli* and *flg* genes) and chemotaxis (*che* genes) (Figure 20 D). Two other gene clusters belong to catabolic pathways for precursor metabolites, carbohydrate (*iol* operon), and nitrogen (*nar* genes) metabolism. 11% of the genes only transcriptionally changed (Figure 20 B) showed enrichment for the energy production pathway like oxidoreductase (*bkd* family) involving in the BCAA degradation. The group of genes up-regulated only at translational level (Figure 20 C) contains genes of the *fli* family involved in the flagellar assembly.

In contrast, cells grown in MM reveal enrichment for biosynthetic processes (Figure 20 E-F). Uniquely transcriptionally up-regulated genes (Figure 20 E) are belonging to the *pur* and *pyr* family responsible of nucleotide biosynthesis while no significant enrichment is observable for the uniquely translationally changed genes. The 62% of the genes (Figure 20 F), transcriptionally and translationally modulated, are involved into nitrogen compound metabolism like amino acids (*leuC*, *metE*, *ilvA*) and nucleotides biosynthesis (*pur* family).

Taken together those observation indicate a clear metabolic differentiation between energy yielding bacteria, LB growing, and energy consuming bacteria, MM growing.

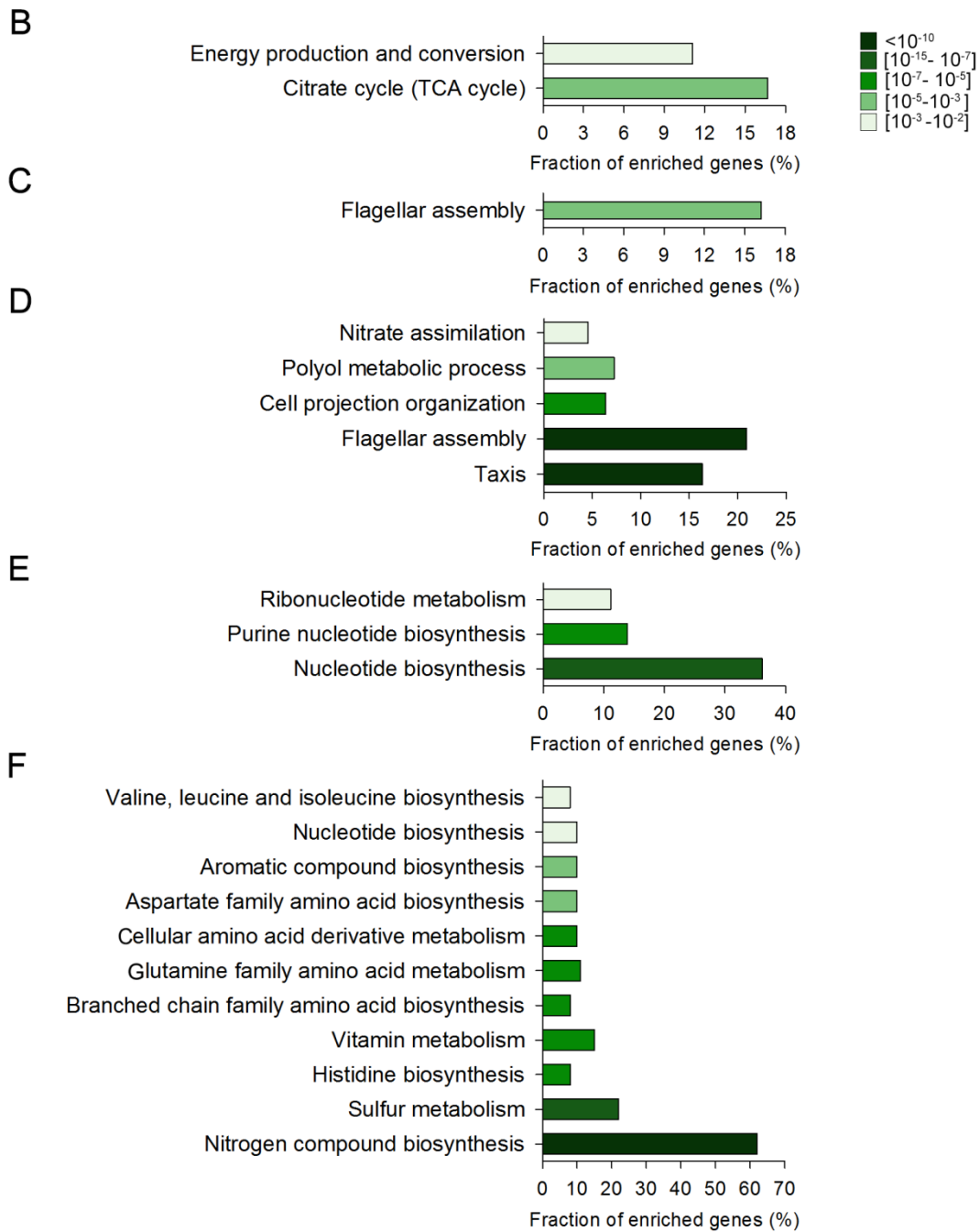
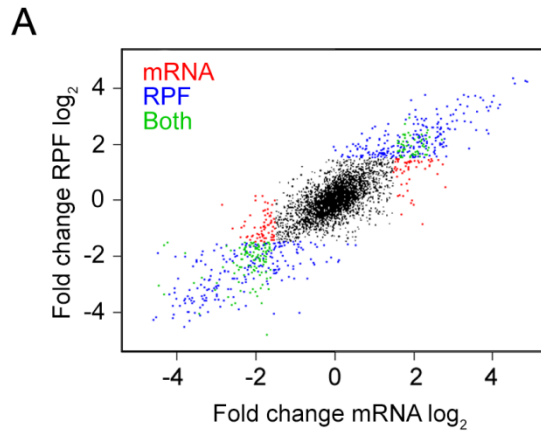


Figure 20. Fold change analysis on transcriptional and translational level in *B.licheniformis* under LB or MM growth.

(A) Correlation between the \log_2 -fold changes of the normalized RPF and mRNA read counts from bacteria grown in LB and MM media. The \log_2 -fold change at 95% for mRNA (red) and for RPF (blue) is equals to 1.5. \log_2 -fold change > 1.5 represent genes up-regulated in LB; \log_2 -fold change < 1.5 represent genes down-regulated in LB; in green are shown genes regulated both at the mRNA and RPF level. (B-F) Functional gene groups enrichment analysis using DAVID functional annotation tool for: mRNA uniquely up-regulated (B), RPF uniquely up-regulated (C), both up-regulated (D), uniquely mRNA down-regulated (E), both down-regulated (F).

2.3.5. Transcriptional and translational response induced in the stationary phase

When bacteria enter the stationary phase and cease the growth about 500 genes change. In particular, 223 and 176 genes were found to be up-regulated, at the translational (RPF) and transcriptional (mRNA) level respectively, in exponentially growing cells. Entering the stationary phase bacteria activate the expression of 227 (RPF) and 267 (mRNA) genes (Figure 21 A).

During exponential growth the 86% of genes up-regulated, at both level of expression, belong to the translational machinery assembly (Figure 21 B). Those groups comprise mainly ribosomal proteins (*rpl*, *rps* and *rpm* families). The genes up-regulated only at the mRNA level (Figure 21 C) are involved in the generation of precursor metabolites (implicated in energy production via the respiratory electron transport chain) such as cytochrome aa3 quinol oxidase (encoded by the *qox* operon) and energy (mainly genes of the *atp* family, glycolytic enzymes like enolase, phosphoglycerate kinase, the *ptsGHI* operon, encoding genes for glucose uptake and TCA cycle enzymes encoded by *pdhABCD*). Moreover, there is enrichment for purine biosynthesis (*pur*) and cellular amide metabolic processes, like NAD biosynthesis (*nad* operon) and biotin biosynthesis (*bio* operons). Genes responsible for building the translational apparatus are found to be also uniquely up-regulated on the translational level (i.e. higher RPFs in The Ribo-Seq data set) (Figure 21 D).

The entrance in the stationary phase induces changes connected to the carbohydrate metabolism. In particular, up-regulation, only at the transcriptional level, was detected for

genes encoding carbohydrate transporters (*manP* for mannose, *licB* for sorbitol) and genes involved in carbohydrate catabolism (*acoABC* operon) (Figure 21 E). Additionally, the translational up-regulated genes showed a unique enrichment under the term of glycogen metabolism process, containing genes of the *glg* operon (Figure 21 F).

Supporting our previous hypothesis we observed a GTP-dependent expression of genes, encoded by *ptsGHI* and *pdhABCD* operons which transcription initiator nucleotide was identified as a G (Tojo et al. 2010). Up-regulation of these was induced under exponential growth, where the availability of the GTP pool is higher (Krasny and Gourse 2004).

Taken together, the majority of changes in stationary growing bacteria, driven by nutrient depletions, interest their carbohydrate metabolism. Under glucose starvation cells new metabolic pathways are activated allowing degradation of specific components, like acetoin, and search for alternative nutrients, mediated by expression of new carbohydrate transporters. The synthesis of the translational machinery components also decreases ceasing the growth.

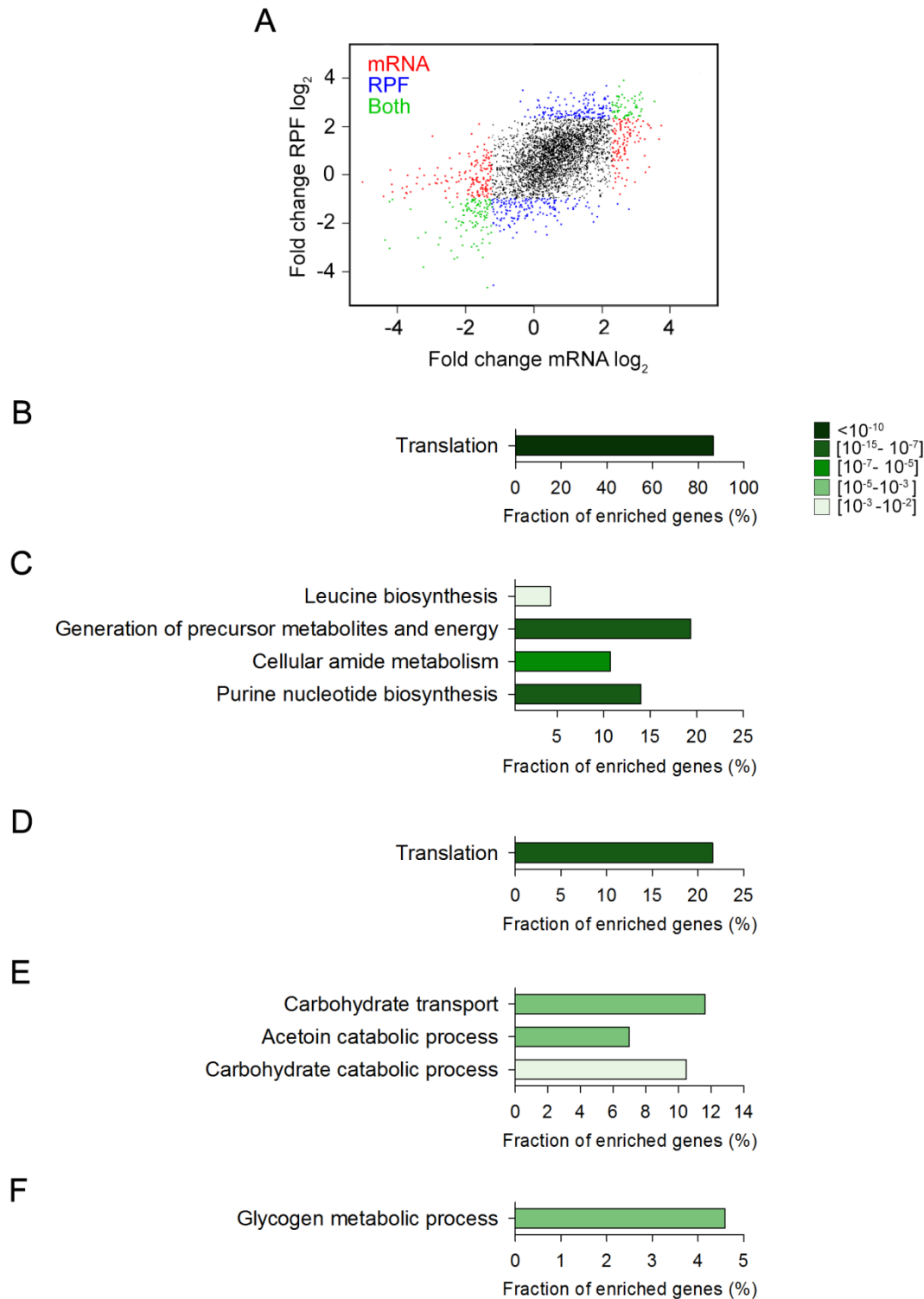


Figure 21. Fold change analysis on transcriptional and translational level in *B.licheniformis* exponentially or stationary growing in MM.

(A) Correlation between the log₂-fold changes of the normalized RPF and mRNA read counts from exponential and stationary phase of bacteria grown in MM. The log₂-fold change at 95% for mRNA (red) is equal to 1.5 and for RPF (blue) is equal to 1.6. Log₂-fold change in the upper right genes up-regulated in exponentially growing cells; Log₂-fold change in the lower left side represent genes down-regulated in exponentially growing cells; transcriptionally regulated genes are coloured in red, translationally changed in blue, genes

regulated both at the mRNA and RPF level are in green. (B-F) Functional gene groups enrichment analysis using DAVID functional annotation tool for: both up-regulated (B), mRNA uniquely up-regulated (C), RPF uniquely up-regulated (D), uniquely mRNA down-regulated (E), RPF uniquely down-regulated (F).

2.3.6. Keeping under control the concentration of toxic amino acid in the cell

Guided by our observation that the T-box regulated amino acids inhibit the growth of *B.licheniformis* while the non-T-box regulated had no effect (paragraph 2.2.4), we next investigated the expression of the genes from the catabolic pathway in LB and MM medium using our deep-sequencing data.

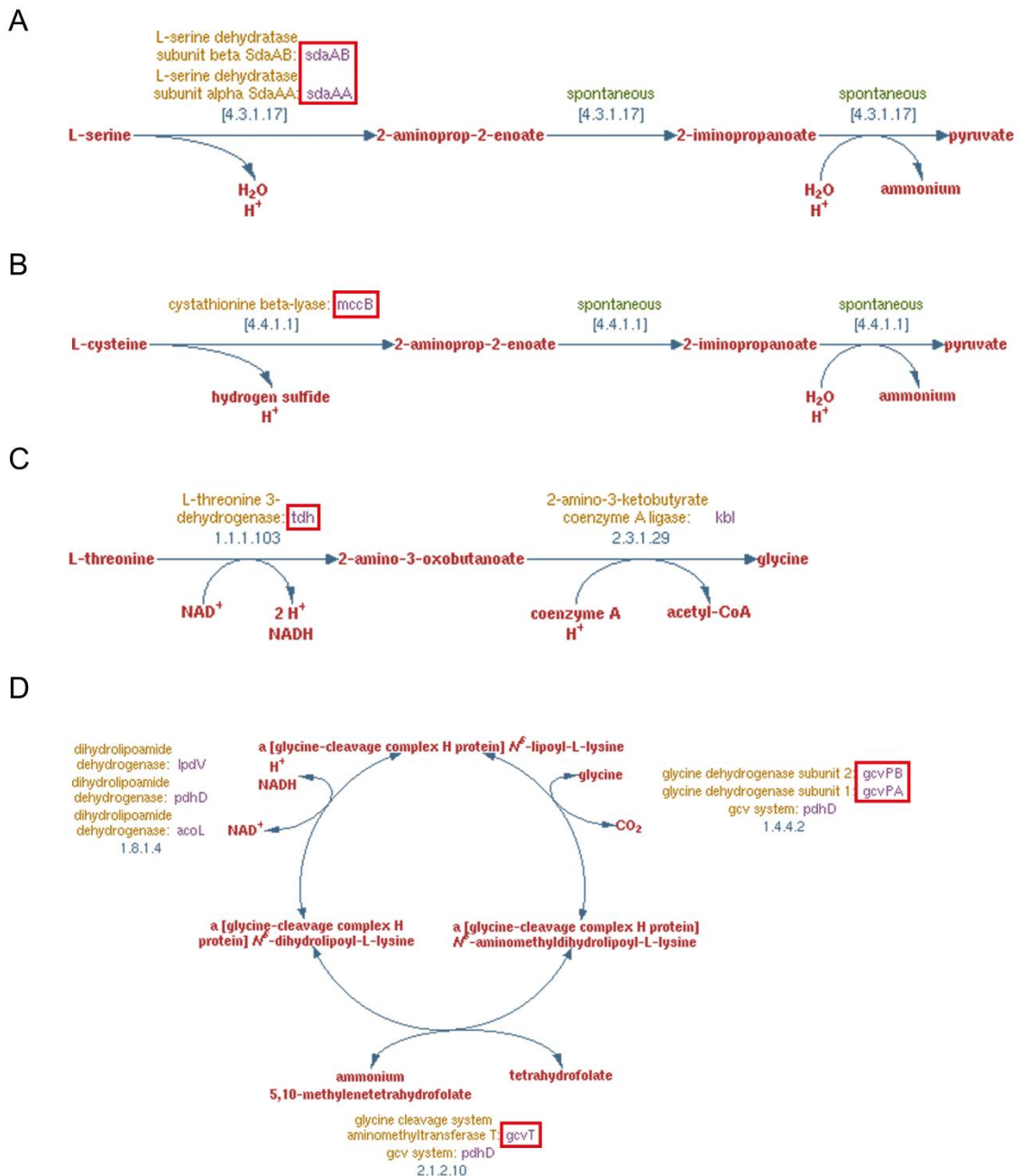


Figure 22. Catabolic pathway of T-box related amino acids

The catabolic pathways shown are adopted from the ByoCyc database collection. The genes examined in our analysis are squared in red.

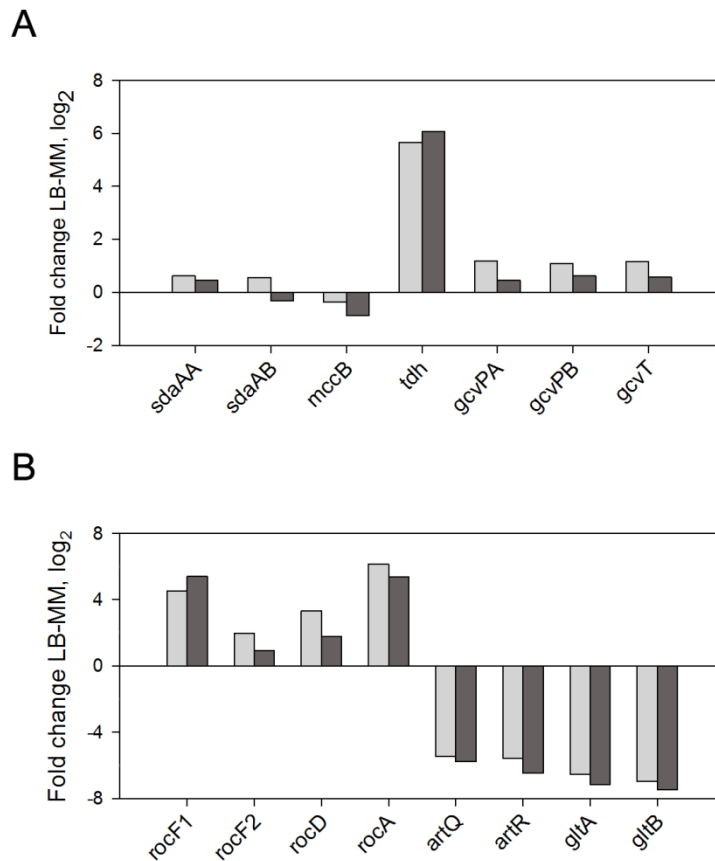


Figure 23. Fold-change analysis of genes from amino acid metabolic pathways.

Fold-change analysis of mRNA (light grey) and RPF (dark grey) level of genes involved in the catabolic pathway of T-box (A) and non (B) related amino acids. Fold changes ≥ 1.5 are considered as differential expressed. Positive values indicate increased level in LB growing cells compared to MM growing cells, while negative values indicate reduced level.

The enzymes involved in the catabolic pathway of the examined T-box related amino acids are shown in Figure 22. The most toxic amino acids, serine and cysteine, are metabolically interconnected being both precursor of pyruvate. The genes involved in their conversion to pyruvate (*sdaAA* and *sdaAB* (L-serine dehydratase subunit α and β) for serine and *mccB* (cystathionine beta-lyase) for cysteine) are not differentially expressed among the media (Figure 23 A and Figure 24). This suggests that they are not used as energy source. In contrast, *tdh* (L-threonine 3-dehydrogenase), gene for threonine catabolism, which

catalyses its conversion to glycine and acetaldehyde, results differentially up regulated in LB at both transcriptional and translational level. While glycine can be converted then to pyruvate, the latter is transformed into acetyl-coA. This may suggest the entry of threonine into the TCA cycle, which is active in LB growing cells. Any significant difference in the expression of the glycine cleavage system, involving the operon *gcv* (encoding the genes *gcvT*, (aminomethyltransferase T) *gcvPA* and *gcvPB*, (glycine dehydrogenase subunit 1 and II respectively)), was detected.

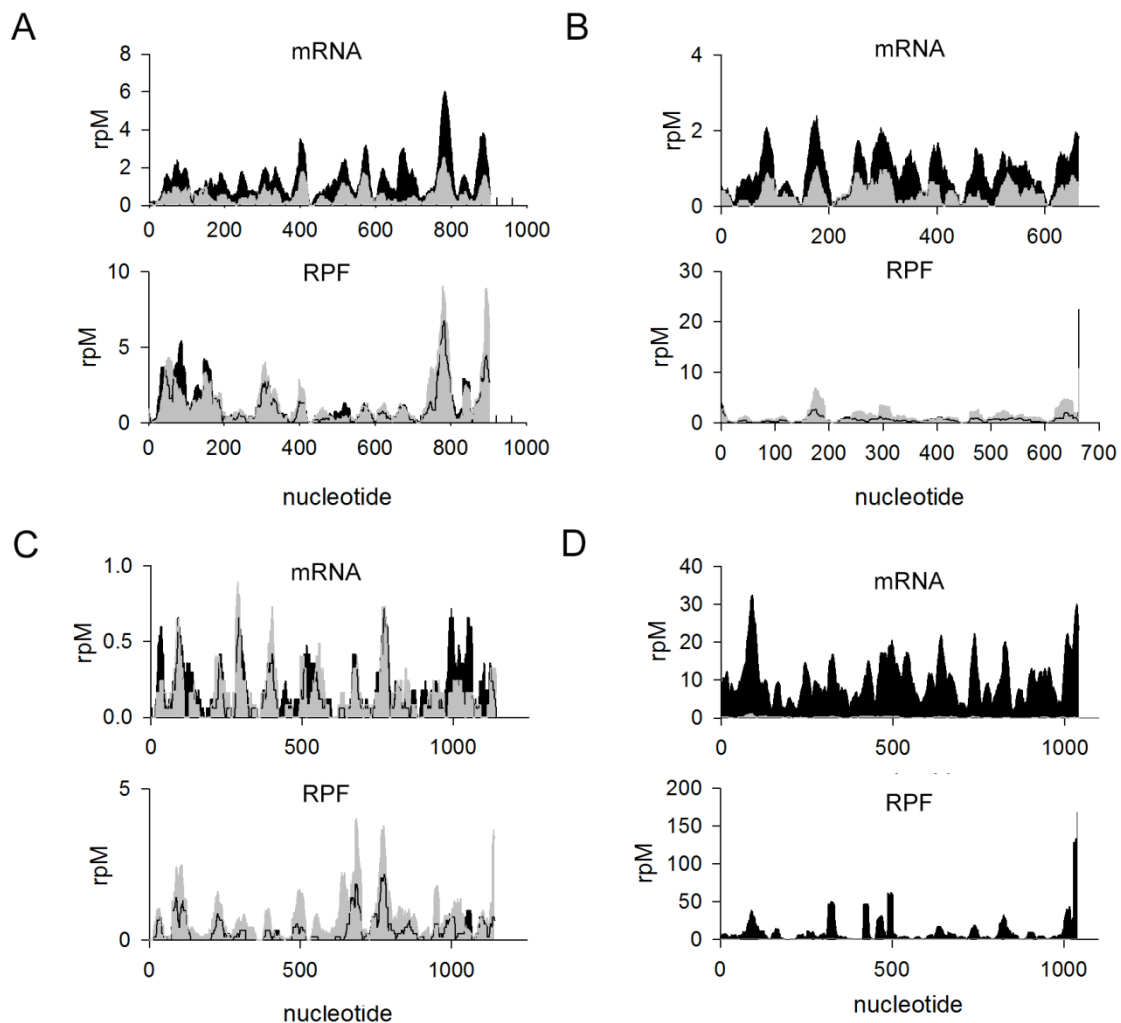


Figure 24. Expression levels of catabolic enzymes for T-box related amino acids.

The expression level, mRNA in the upper and RPF in the bottom part, for (A) *sdaAA*, (B) *sdaAB*, (C) *mccB* and (D) *tdh*. The expression level in LB is colour coded in black and compared with the MM (grey) level. The mRNA and RPF coverage along each gene is shown. Data are normalized to the total number of mapped reads (rpM) for each sample.

Genes involved in the catabolic pathways for the non T-box regulated amino acids (Figure 25) are all differentially expressed but with different behaviours (Figure 23 B). The arginine degradation pathway is up-regulated in LB. The genes engaged in this pathway, catabolising arginine into glutamate, are *rocF1* (arginase 1), *rocF2* (arginase 2), *rocD* (ornithine-oxo-acid transaminase) and *rocA* (1-pyrroline-5-carboxylate dehydrogenase). The only translationally up-regulated genes are *rocA* and *rocF1*. All of them are highly expressed on a transcriptional level (Figure 23 B and Figure 26). Interestingly, the arginine transporter system (*artR* and *artQ* genes, encoding for high affinity arginine ABC transporter ATP-binding protein and high affinity arginine ABC transporter permease respectively) is up regulated during MM growth (Figure 26) suggesting a specific regulation depending on the presence or absence of arginine in the cell. One more interesting example is represented by glutamine, the principal nitrogen source for *Bacillus*. The glutamate synthesis pathway, implying the *gltAB* operon expression (encoding the glutamate synthase), which is under glucose and glutamine control. Sufficient concentration of glutamate inhibits *gltAB* expression. This operon is more expressed in MM growing cells indicating a lack of glutamate and the use of glutamine for its synthesis.

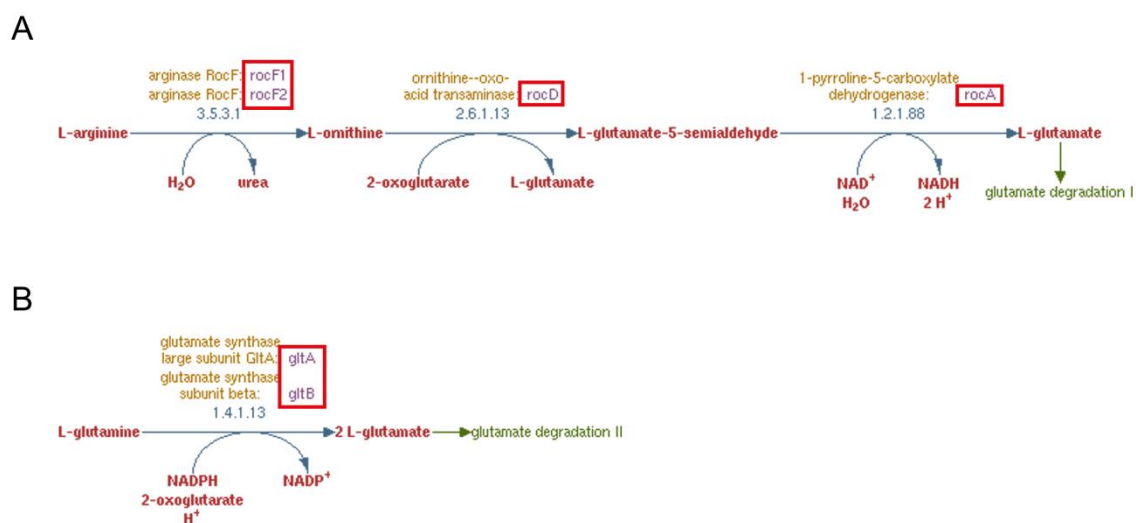


Figure 25. Catabolic pathway of non T-box related amino acids

The catabolic pathways shown are adopted from the ByoCyc database collection. The genes examined in our analysis are squared in red.

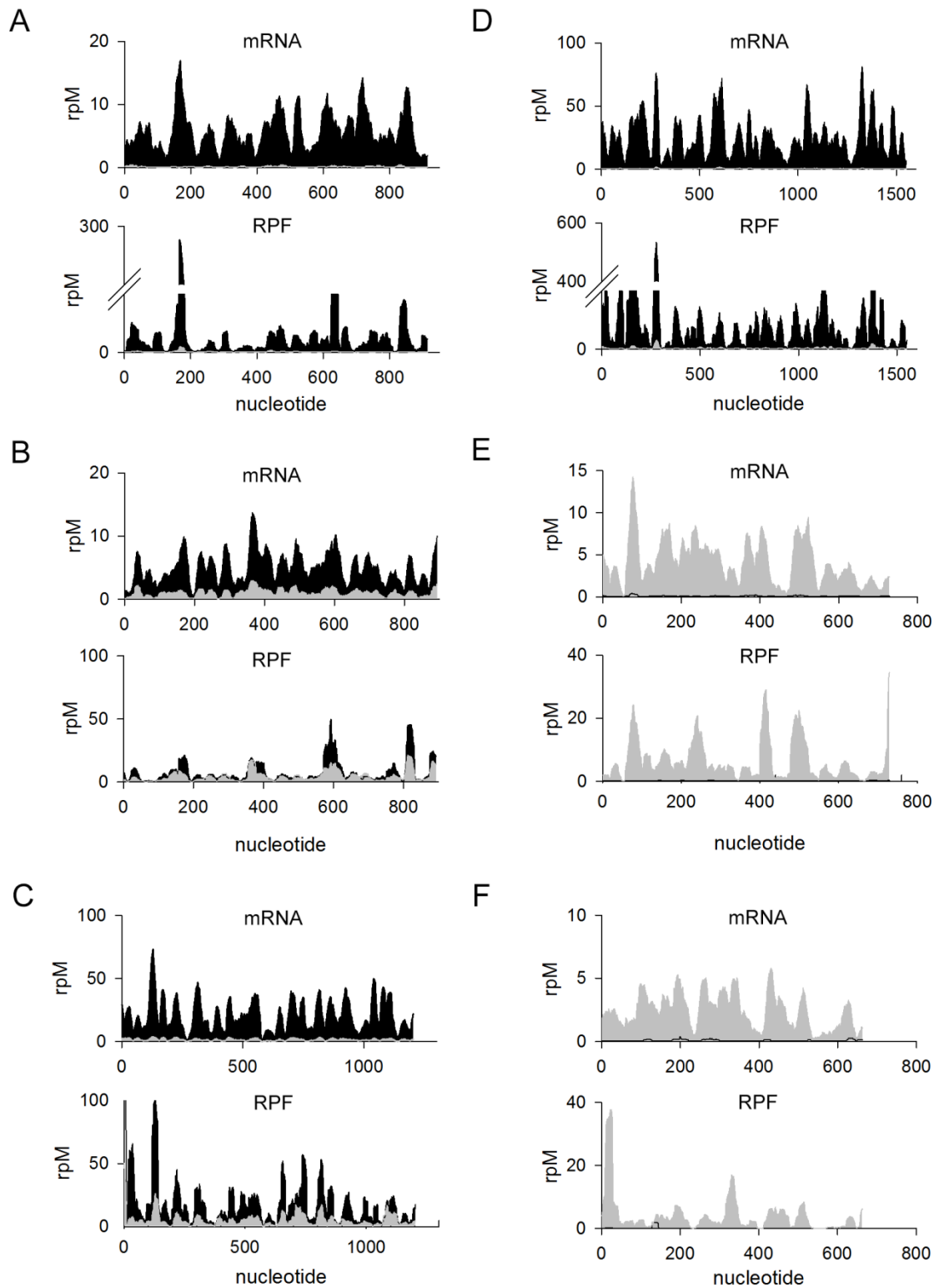


Figure 26. Expression levels of catabolic enzymes for non T-box related amino acid.

The expression level, mRNA in the upper and RPF in the bottom part, for (A) *rocF1*, (B) *rocF2*, (C) *rocD*, (D) *rocA*, (E) *artR*, (F) *artQ*. The expression level in LB is colour coded in black and compared with the MM (grey) level. The mRNA and RPF coverage along each

gene is shown. Data are normalized to the total number of mapped reads (rpM) for each sample.

In sum these data suggest that the expression of catabolic pathways is different for T-box and non T-box related amino acids. The first ones result to be unchanged among LB or MM growing cells, probably to immediately respond to increasing amino acid concentrations. Opposite, the non T-box associated ones can modulate the expression of catabolic enzyme according to their abundance and the cellular need.

3. Discussion and conclusion

Bacteria quickly respond to environmental changes by modulating their growth rate (μ) via changes in gene expression, which in turn influences their physiology and adjusts their proteome to adapt and maintain metabolic efficiency (Voigt et al. 2004). The growth is crucially dependent on protein synthesis, hence on the abundance of translational components, among which are tRNAs and more specifically the aminoacyl-tRNAs which shape the kinetics of translational elongation and influence protein production. Previous studies demonstrate that increase in tRNA concentrations correlates with high growth rates for the gram negative bacterium *E. coli* (Emilsson and Kurland 1990; Emilsson et al. 1993; Dong et al. 1996).

Here, we characterized the tRNAome of *Bacillus licheniformis* under various growth rate in different nutrient conditions and investigated the dynamics of transcription and translation dependent on the nutrient availability. We have firstly summarized and reviewed different approaches that are available for identification and quantification of tRNAs and their functional integrity.

The role of tRNAs in translation and their emerging role in adaptation, signalling and diseases (Kirchner and Ignatova 2015) highlights the importance to identify tRNAs and truly quantify their expression. Many of the classical techniques are limited by tRNA modifications which make tRNAs quantification and identification very difficult. Despite new advances in experimental technologies and specifically in high throughput sequencing methods still bear caveats in quantification as they are majorly based on cDNA synthesis. The latter is sensitive to modifications and thus not quantitative. Thus, tRNA biology clearly needs improvement in the resolution of high-throughput technologies for detection of all tRNA isodecoders.

On the basis of our review on the methods available for tRNA quantification, we have chosen tRNA microarray technology which allows comparison of tRNA abundance and tRNA charging level. However, despite its power, it is limited to distinguish only tRNAs with at least eight nucleotides difference in their sequences. For small tRNAomes (that is all tRNAs in one species) tRNA-based microarray is a good choice and enables a resolution down to a tRNA isoacceptor.

The aminoacyl-tRNAs level in different nutrient availability

Based on experimental evidence with few tRNAs, the fraction of aminoacylate tRNAs has been extrapolated to all tRNAs in *E. coli* and suggested to be around the 80% during exponential growth phase (Jakubowski and Goldman 1984; Varshney et al. 1991; McClain et al. 1999; Sorensen 2001). For *B. licheniformis* we detected near complete charging level (i.e. > than 80%) for only few tRNAs; for some tRNA isoacceptors families (tRNA^{His}, tRNA^{Thr}, tRNA^{Tyr} and tRNA^{Phe}) the charging was lower than 50%. Opposite to our expectations, the aminoacyl-tRNA fraction is not enhanced by an increase in nutrient availability, e.g. amino acids or constant nutrient supply in chemostat. Similarly, it was not influenced by growth in MM, where all amino acids are internally synthesized, or by changes of the growth temperature. These observations clearly indicate that tRNA aminoacylation level in *B. licheniformis* is independent and moreover non-controlled by the amino acid availability in the medium. Thereby, we realized another interesting fact: despite variations in the growth rate the charging level of all tRNA isoacceptors within some tRNA isoacceptor families remained nearly constant for all three conditions (i.e., LB, MM and MMaa) suggesting the presence of a regulatory mechanism to keep the aminoacylation level constant. Unlike *E. coli* in which the the tRNA aminoacylation level changes with growth rate and medium composition (Avcilar et al., submitted; Dittmar et al. 2005), the gram positive *B. licheniformis* obviously uses different strategy. Adaptation and growth rate regulation, may take place by controlling the tRNA pool rather than regulating the aminoacylation level.

T-box riboswitch regulates the charged fraction of tRNA in Bacillus

Bacillus, and many other gram positive bacteria, modulates the expression of amino acid-related genes accordingly to the aminoacylation level of the cognate tRNA (Gutierrez-Preciado et al. 2009). The uncharged tRNA interacts with specific regulatory RNA elements, T-box elements which are located in the 5'UTR region of the related genes, inducing structural changes which allow transcription of the downstream gene (Green et al. 2010). Strikingly our results indicate that the total tRNA varies, however, the percentage of aminoacylated-tRNA remains unchanged suggesting that the charging of these tRNA is under T-box control.

We clearly observed a change in the mRNA level of T-box regulated aminoacyl-tRNA-synthetases, *ThrRS*, *ValRS*, and the T-box regulated biosynthetic *ProI* gene, involved in proline biosynthesis. The aminoacylation of tRNA mirrors the expression pattern of these genes. In contrast, for the non T-box regulated gene *ArgS*, encoding arginyl-tRNA-synthetase, this correlation does not exist. Our results clearly demonstrate that the T-box regulation in *B. licheniformis* is a strategy to maintain constant level of aminoacylation, even when changes on the total tRNA abundance occur.

T-boxes monitor the amino acid levels in cells

Genes involved in the of amino acids metabolism are regulated by a wide range of mechanisms. In Gram-negative bacteria, the intracellular amino acid availability of triptophane is monitored measuring the rate of translation of the leader peptide (Merino and Yanofsky 2005). One way to control amino acid availability in *Bacillus* may involve the use of riboswitches. Addition of T-box related amino acids to the medium (e.g., Ser, Cys) resulted in growth inhibition or slowdown of the growth. Additionally, bacteria early plateaued into the stationary phase. We suggested that T-box related amino acid may be toxic for cells which may explain the evolutionarily pressure to select for tight regulatory system that controls the free amino acid levels in the cell. Supporting this hypothesis non T-box related amino acid, with the exception of lysine, had no toxic effects. Although lysine does not possess a T-box regulation, *Bacillus* possesses a specific lysine riboswitch system (LYS-elements, or L-boxes) (Grundy et al. 2003) responding to Lys concentration. Many amino acids are good energy substrates for bacteria, but some exhibit toxic effects (Rowley 1953). Overall, our results highlight the crucial role of T-box mechanism, and other riboswitches (e.g. lysine riboswitches glycine riboswitches regulating the glycine cleavage in *gcvT* operon) (Mandal et al. 2004) and S-boxes regulating methionine and cysteine genes in response to concentration of a methionine derivative, *S*-adenosylmethionine(Winkler et al. 2003)) in regulating and maintaining low level of free amino acid in cells to avoid toxic effects.

Regulation of the amino acid catabolic pathways

The expression of enzymes involved in amino acid catabolism is under the control of different regulatory mechanisms. Amino acids are divided into ketogenic, glucogenic and both keto- and glucogenic precursor. Degradation of ketogenic amino acids produces α -

keto acids that, directly or via additional reactions, enter major metabolic pathways. Glucogenic amino acids are catabolized to pyruvate or to one of the intermediates of TCA cycle that are precursors for gluconeogenesis (Berg 2002). The latter, under glucose starvation, can be used as carbon source. In contrast, ketogenic amino acids, which are degraded to acetyl-CoA or acetoacetate, enter the TCA cycle or are transformed to ketone bodies or fatty acids (Berg 2002). Among the T-box related amino acids serine, cysteine and glycine belong to the glucogenic class. *sdaAA* and *sdaAB*, L-serine dehydratase for serine and *mccB*, cystathionine beta-lyase, for cysteine are the enzymes catalysing the conversion to pyruvate. Glycine is firstly converted to serine by the glycine cleavage complex encoded by the genes *gcvT* (aminomethyltransferase T), *gcvPA* and *gcvPB* (glycine dehydrogenase subunit 1 and II). Interestingly, no change in the expression level, both transcriptional and translational, of all these genes was detected in LB or MM. This indicates that despite the low glucose level in LB, serine, cysteine and glycine are not allocated as energy source. Threonine, which is also a T-box related amino acid, can be both glucogenic and ketogenic precursor. Threonine is degraded into glycine and acetaldehyde by L-threonine 3-dehydrogenase (*tdh*). The first one can be converted then to pyruvate, while the latter is transformed into acetyl-coA. Analysing the expression of *tdh* gene we noticed a clear up-regulation in LB growing cells. In line with our previous observation, this suggests the entry of the threonine into the TCA cycle.

Among the non T-box related amino acids the metabolic pathway of arginine and glutamine seems to be diverse. Both amino acids belong to the glucogenic class and can be converted to α -ketoglutarate via glutamate. In agreement with previous results indicating that arginine can be a source of nitrogen but not of carbon for *Bacillus* (Maghnouj et al. 1998) we observed in LB high expression of *rocF1* (arginase 1), *rocF2* (arginase 2), *rocD* (ornithine-oxo-acid transaminase) and *rocA* (1-pyrroline-5-carboxylate dehydrogenase), involved in its conversion to glutamate. At the same time, the arginine transporter system, encoded by *artR* and *artQ* genes, is shut-down in LB. Taken together these data indicate that arginine availability regulates the expression of transporters and catabolic enzymes corroborating previous observations (Maghnouj et al. 1998).

In *Bacillus* glutamine represents the preferred nitrogen source. The expression of glutamine synthase, GS, is induced in absence of glutamine and inhibited when present (Gunka and Commichau 2012). The glutamine catabolism requires the expression of the

GOGAT, mediated by the operon *gltAB*, which can form two molecules of glutamate from glutamine and 2-oxoglutarate. The *gltAB* operon represents an important metabolic intersection, connecting carbon with nitrogen metabolism, thus responding to signals derived from both. *gltAB* operon expression is modulated positively by glutamine presence and inhibited by its absence (Belitsky et al. 2000). In the presence of glucose, a transcriptional activator *GltC*, induce *gltAB* expression to compensate for the increasing demand of glutamate thus, increasing the growth rate (Wacker et al. 2003). In agreement, our data indicate that the expression of this operon is higher in bacteria growing in MM where glucose is present.

The results indicate that the amino acid metabolism is governed by different and complex signals. Thus, we cannot clearly delineate a difference between the amino acid metabolism of T-box and non T-box regulated since even amino acids belonging to the same group showed different expression pattern which partially correlates with the carbon and nitrogen metabolism they are involved with.

Adjusting of the tRNA expression in response to growth rate and nutrient availability

The growth rate is strongly proportional to the rRNA and total tRNA concentration (Jin et al. 2012). Accordingly, increasing the growth rate, by growing the *B. licheniformis* at higher temperature of 45°C (i.e., its optimal growth temperature), the expression of the majority of tRNA increased compared to the growth at 37°C. Generally, elevation of a set of specific tRNA isoacceptors has been described to adequately adjust to the codon usage of highly expressed genes at each condition (Novoa et al. 2012). Strikingly, in *B. licheniformis* all tRNAs, with few exceptions, underwent changes. Similar changes we observed when comparing the tRNA expression under different nutrient growth conditions. In line with these observations, no changes in the effective codon usage were detected. Hence, the adaptation to nutrient variability and growth rate requires expression of genes with same codon frequency. Faster growth needs higher translation rates to maintain sufficient translational capacity (Valgepea et al. 2013) thereby increasing the abundance of tRNAs *Bacillus* most likely increases translation to support higher growth rate.

Thus, we conclude that in *B. licheniformis* the abundance of tRNA is nutrient dependent. Interestingly, there is a clear regulation on the expression levels of tRNA rather than affecting their aminoacylation level.

GTP-dependent expression of tRNAs

Considering that tRNA processing is a not specific step, such a regulation must occur at the level of transcription in a way that it is sensible to the nutrient stimuli, like cellular energy level. GTP and ATP are the two gauges of energy in the cell. It has been shown that in *B. subtilis* the GTP concentrations changes with growth phase and nutrient conditions; it is higher in rich medium, and lower under carbon, nitrogen, or phosphorus limitation (Fujita and Losick 2005). Also, GTP level positively correlates with steady-state growth rate and tunes growth in a dose-dependent manner, such that decreasing GTP level reduces the growth rate (Bittner et al. 2014).

In *E. coli* GTP represents a regulatory molecule which influences indirectly gene expression via the alarmone ppGpp (guanosine-tetraphosphate). Under starvation conditions, which cause ribosomal stalling, the GTP pyrophosphokinase RelA catalyses the synthesis of ppGpp from GTP (Dalebroux and Swanson 2012). ppGpp, causes a decrease in the GTP level, alters transcription on a global level by regulating RNAP and redirects it to stress-specific genes (Magnusson et al. 2005). In contrast, in *Bacillus*, GTP regulates RNAP directly with no intermediary acting entities (Bittner et al. 2014). Changes in the GTP concentration affect the rate of transcription initiation of certain genes, such *rrn* encoding ribosomal RNAs, depending on the purines at their transcription initiation site and changes in the promoter preferences of RNAP (Krasny and Gourse 2004). Transcription begins when the interaction between RNAP and the promoter forms an open complex which allows the incorporation of incoming NTPs. In the absence of nucleotide triphosphate this open complex is unstable (Tojo et al. 2010), thus transcription decrease. In *B. subtilis*, in the majority of the rRNA operons GTP is the initiating nucleotide, hence under nutrient limitation conditions, when GTP decreases and the growth need to be lowered, rRNA transcription is inhibited (Bittner et al. 2014).

We found that in *B. licheniformis* the rRNA transcription is also regulated in a GTP-dependent way being reduced of about 30% in MM as compared to LB. Additionally, upshift, e.g. shift from MM to MMaa medium, and down shift, e.g. shift from MMaa to MM, the rRNA expression increase and decrease, respectively. It is plausible to assume that a similar mechanism of transcriptional regulation exists for the rRNA-coregulated tRNA genes. The 72 tRNA genes of *B. licheniformis* are distributed in seven single genes and ten clusters, each containing from 2 to 20 tRNA genes. Five of the ten clustered genes

are associated with the rRNA operons and thus may follow the same GTP-dependent regulation of expression. Supportive for this hypothesis is our observation that tRNA^{Ser}TGA and tRNA^{Arg}CCT, whose iNTP has been previously identified as an A and C, respectively, (Wiegand et al. 2013a), did not show changes in LB and MM growth.

Overall, these findings suggest that in *Bacillus* the rRNA and tRNA promoters are most likely directly regulated by the concentration of their iNTP. Thus, tRNA genes expression mirrors nutrient availability to consequently control growth rate in a GTP-dependent manner.

Translational efficiency: interplay between codon usage tRNA availability

The global analysis we have done on the tRNAome revealed how *B. licheniformis* maximizes growth in varying environments and nutrients. Many studies, in unicellular organisms, demonstrate that the concentration of tRNAs greatly correlates with the frequency of the codons they pair to (Ikemura 1981; Percudani et al. 1997; Kanaya et al. 1999). In multicellular organisms this correlation is poor (Kanaya et al. 2001). The tRNA adaptation index (tAI) was adopted to account for tRNA wobble base pairing and gene copy numbers, from which tRNA abundance is generally estimated (dos Reis et al. 2004). Using tAI improves the correlation between codon usage and tRNA abundance in multicellular organism as well. Thus, this suggests that codon usage and tRNA abundances coevolved to maximize translational efficiency (Quax et al. 2015). Indisputable the initiation of translation is the major rate-limiting step (Kudla et al. 2009; Salis et al. 2009), but the aggregated elongation of each single codon also shapes the kinetics of protein synthesis (Zhang et al. 2009; Fedyunin et al. 2012). The major determinant of ribosomal speed at each codon is the availability of cognate aminoacyl-tRNA. Since the concentration of aminoacyl-tRNA is not uniform, the decoding time of codons recognized by tRNA species with lower intracellular concentrations tends to be longer and vice versa. Our Ribo-Seq data confirmed that translational speed greatly correlates with tRNA availability. High ribosomal dwelling time was detected for triplets encoded by tRNAs (e.g., tRNA^{Trp}CCA and tRNA^{Cys}GCA) which, despite their high charging level, were among the lowest abundant in all conditions. Thus, independently of the growth conditions those codons are obviously representing a bottleneck point in translation. Some codons (e.g. CCA) showed higher ribosome dwelling occupancy despite the fact their total and

charged tRNAs were plentiful. As previously reported (Ingolia et al. 2009; Pavlov et al. 2009; Tanner et al. 2009) a long dwelling occupancy can also be independent of tRNA availability but controlled by chemical properties of certain amino acids. For example, proline slows down ribosomal speed because of its lower reactivity during peptide bond formation (Wohlgemuth et al. 2008; Pavlov et al. 2009). Previous results described that depending on the tRNA copy number (i.e. lowly abundant tRNAs more influenced) the higher demand for certain tRNA genes induces changes in cell physiology (Bloom-Ackermann et al. 2014). Altering the tRNA demand-supply equilibrium in *B. licheniformis* by overexpression of heterologous gene (here *aprE*) led to global reduction of charging of all isoacceptors; the most affected were lowly abundant tRNAs. Thus, the level of aminoacyl-tRNA sensitively reacts on the demand whereby the effect on different tRNAs correlates with their abundance. Under persistent translational imbalance a genetic change in the tRNA pool may trigger changes in order to adapt (Yona et al. 2013). However overexpression is rather a transient burden for the cell. Altering translation demand affects cellular fitness inducing a global inefficient allocation of resources, such as ribosomes (Gorochowski et al. 2016). Therefore, it is crucial to maintain the optimal state of the cells, by shaping translational elongation rate using low-copy number plasmid or weaker ribosomal binding site. This will increase the productivity of heterologous proteins while minimizing their impact on endogenous cellular processes.

Metabolic changes induced by different nutrient availability

Many studies describe the physiological state of *B. licheniformis* growing in different conditions from the proteomic point of view (Voigt et al. 2004; Voigt et al. 2009). A growing interest for this bacterium has driven the focus on understanding bacterial metabolism and regulation, during different stages of a fermentation process. Several transcriptome analysis have provided an overview of the metabolic changes as well as stress responses and secretion capacities *B. licheniformis* during fermentation process (Wiegand et al. 2013a; Wiegand et al. 2013b; Guo et al. 2015). There is a clear metabolic differentiation of energy yielding bacteria, i.e. growing in LB, and energy consuming bacteria, i.e. growing in MM. In absence of glucose amino acids are valuable nutrient sources, as nitrogen, carbon or energy sources, for bacteria (Halvorson 1972). *E.coli* metabolism switches to using amino acids as a carbon source in LB when the concentration of sugars is low (Sezonov et al. 2007). Also, a positive correlation between consumption of

amino acids and chemotaxis have been also reported (Yang et al. 2015). In LB, we observe an increased expression of enzymes responsible for amino acid degradation. Moreover, many of the highly expressed genes in LB are involved in chemotaxis, motility and flagellar assembly. At the contrary, the majority of differentially expressed genes, in bacteria growing in MM are involved in biosynthetic pathways, mainly amino acids and nucleotides. Consequently, the major metabolic difference involves the carbon metabolism: bacteria grown in absence of glucose, i.e. in LB, express enzymes for the catabolism of alternative carbon sources. At the contrary, growth on glucose, i.e. in MM medium, induce the expression of enzymes involved in the glycolytic pathway in conjunction with repression of the TCA cycle. These observations imply that intermediate of the glycolytic pathway may serve, in MM growing cells, for de novo biosynthesis and for production of metabolites, like acetoin. These observations are in line with previous studies (Cruz Ramos et al. 2000; Ali et al. 2001) suggesting that several products, such as lactate, acetate, succinate, acetoin, butanediol, and ethanol are secreted during exponential growth phase and serve as a carbon storage that is used when glucose is exhausted. Indeed, we could detect a switch in the carbon metabolism when bacteria enter the stationary phase. Genes involved in the glycolysis pathway like ones encoding genes for glucose uptake and pyruvate dehydrogenase complex, were down-regulated. At the contrary, the operon encoding the acetoin dehydrogenase complex was up-regulated. The expression of this operon is under positive control of acetoin and can be repressed by glucose, via the catabolite control protein A (CcpA) (Fujita 2009), indicating that only bacteria encountering glucose starvation, present in stationary phase. Thus, in line with previously observed (Ali et al. 2001; Chubukov and Sauer 2014) *B. licheniformis* can fine-tune this carbon system by regulating both the synthesis and the degradation of secondary metabolites, such as acetate and acetoin. Taken together these results underline the ability of bacteria to switch their metabolic pathway for adaptation and /or survival to different nutrient conditions.

Conclusions

In conclusion, this study provides a detailed map of the general response of *Bacillus licheniformis* to adapt to different nutrient conditions. We have described the impact of

nutrient availability on translation machinery components demonstrating that the strategies adopted in response to changes are very different than *E. coli*.

The expression of the tRNA pool is tightly modulated via GTP-dependent mechanism, which allows sensing the nutrient concentration and consequently increase the tRNA abundance in order to achieve higher growth rate. We demonstrate that the total tRNA is rather adjusted than the aminoacyl-tRNA level. Indeed, for many tRNAs the level of aminoacylation is maintained constant, despite changes in the total tRNA abundance, via T-box mechanism which precisely monitors the ratio between charged and uncharged tRNAs. For the first time we suggested an evolutionary reason for selecting the T-box system which senses the amino acid concentration of only few tRNAs. Our results support the hypothesis that T-box related amino are toxic at high concentration, thus their intracellular concentration should be kept minimal and the genes regulating their metabolism is a powerful way to keep the intracellular concentration low.

Using coupled analysis based on RNA-Seq and Ribo-Seq approaches we detected precise position of translating ribosomes and estimated the dwelling occupancy of the ribosomal A-site which welcomes the aminoacyl-tRNAs. Furthermore, we describe the global changes occurring during different growth conditions, in LB and MM, both in exponential and stationary growth phase, and analyze the metabolic changes which allow bacterial adaptations to different nutrient availability.

4. Materials and Methods

4.1. Materials

4.1.1. Chemicals and reagents

All chemicals used in this work were purchased in the highest quality available. Chemicals used for RNA work were purchased with RNase-free quality and handled under RNase-free conditions.

Chloramphenicol	Roth
SUPERase•In™ RNase Inhibitor, 20U/μl	Life Technologies
Saccharose	Roth
RiboLock RNase Inhibitor, 40 U/μl	Fermentas
Isopropanol	Roth
Acid phenol-chloroform (5:1, ph 4.5)	Ambion
TRI Reagent	Sigma-Aldrich
Chloroform-IAA (24:1)	Sigma-Aldrich
Ethanol, 100%	Roth
PEG8000, 50%	New England Biolabs
SybrGold	Sigma-Aldrich
2x RNA Loading Dye	Thermo Scientific
Acid phenol-chloroform (5:1, pH 4.5)	Ambion
Glycogen (20 mg/ml)	Thermo Scientific
UltraPure™ Salmon Sperm DNA Solution	Life Technologies
PerfectHyb Plus	Sigma-Aldrich
polyA GE	Healthcare
DMSO	Sigma-Aldrich

4.1.2. Enzymes

All enzymes used for RNA work were purchased RNase-free quality and handled under RNase-free conditions. Unless differently specified in the methods, all the enzymatic reactions were performed according to manufacturer instructions.

Lysozyme	Roth
T4 DNA-Ligase	New England BioLabs
RevertAid H Minus Reverse Transcriptase	Thermo-Scientific
T7 RNA Polymerase	Thermo-Scientific
T4 PNK	NEB
T4 RNA Ligase 1	NEB
T4 RNA Ligase 2, truncated	NEB
<i>Pfu</i> DNA Polymerase	Thermo Scientific
DNase I (RNase-free)	Thermo Scientific
Micrococcal nuclease	Thermo Scientific
T7 RNA Polymerase	Thermo Scientific
SUPERase•In™ RNase Inhibitor (20 U/μl)	Life Technologies

4.1.3. Oligonucleotides

Table 4. Sequences of the tDNA probes used in the microarrays.

Degenerated based used (bold typed) are: *R* (A,G), *Y* (C,T) and *S* (C,G)

tRNA	Genomic copy number	Sequence (5' – 3')
tRNA ^{Ala} GGC	1	TGGAGCATAGCGGGCTCGAACCGCTGACCTCTACACTGCCA GTGTAGCGCTCTCCCAGCTGAGCTAATGCCCC
tRNA ^{Ala} TGC	3	TGGAGCCTAGCGGGATCGAACCGCTGACCTCTGCGTGCAA AGCAGGCGCTCTCCCAGCTGAGCTAAGGCCCC
tRNA ^{Arg} ACG	2	CGCGCCCGAGAGGAGTTCGAACCCCTAACCTTTTGATCCGTAG TCAAACGCTCTATCCAATTGAGCTACGGGCGC
tRNA ^{Arg} CCG	1	CGCGCTCGGAGGGATTTCGAACCCCGGCAGACGTGGTACCG GAAACCACCGCTCTATCCAGCTGAGCTACGAGCGC
tRNA ^{Arg} CCT	1	CGTCCCAGGAGAGATTTCGAACTCCCGACACACAGCTTAGGA GGCTGTTGCTCTATCCACCTGAGCTACTGGGAC
tRNA ^{Arg} TCT	1	TGACGTCCAGGAGAGATTTCGAACTCCCGACCGACGGCTTA GAAGGCCGTTGCTCTATCCAGCTGAGCTACTGGGAC
tRNA ^{Asn} GTT	4	CTCC R CAGGCAGGATTTCGAACTGCGACCGATCGGTAAACA GCCGATAGCTCTACCACTGAGCTACTGTGGA
tRNA ^{Asp} GTC	4	GTCCGGACGGGACTCGAACCCGCGACCTCTGCGTGACAGG CAGGCATTCTAACCAACTGAACTACCGGACC
tRNA ^{Cys} GCA	1	AGGCGACACCCGATTTCGAACCGGGGATAAAGGTTTTGCAG ACCTCTGCCTTACCACTTGGCTATGCCGCC
tRNA ^{Gln} TTG	4	CTGGGCTAGCTGGATTTCGAACCGCG R TGASGGAGTCAAA GTCCGTTGCCTTACCGCTTGGCTATAGCCCA
tRNA ^{Glu} TTC	6	TGACCCGTACGGGATTTCGAACCCGTGTACCGCCGTGAAAG GGCGGTGTCTTAACCACTTGACCAACGGGCC

tRNA ^{Gly} GCC	2	AGCGGAAGACGGGATTTCGAACCCGCGACCCCCACCTTGGCA AGGTGGTGTCTACCACTGAACTACTTCCGC
tRNA ^{Gly} TCC	3	AGCGGGTGTATRGAATCGAACYCACGACATCAGCTTGGAAAG GCTGAGGTTTTACCACTAAACTACACCCGC
tRNA ^{His} GTG	2	GGCGGTTGATGGGAATCGAACCCACGAATGAGAGCCACAAT CTGGTGCCTTAACCACTTCGCCACAACCCGC
tRNA ^{Ile} GAT	3	TGGGCCTGAGTGGACTCGAACCA ^Y CGACCTCACGCTTATCA GGCGTGCCTCTAACCACTGAGCTACAGGCCCG
tRNA ^{Leu} GAG	1	TGCGGCCGAGAGGACTTGAACCTCCACGGGTTATTCACCCAC TAGGCCCTCAACCTAGCGCGTCTGCCATTCCGCCACGACCCGC
tRNA ^{Leu} CAG	1	TGCGGATGAAGGGACTTGAACCCCACTGCTTTAAAAGACA CTAGAGCCTGATTCTAGCGCGTCTGCCAATTCCGCCACATCC GC
tRNA ^{Leu} TAG	1	TGCGGGTGAAGGGACTCGAACCCCACTGCGCGTAAAGACACT AGATCCTAAGTCTAGCGCGTCTGCCAATTCCGCCACACCCGC
tRNA ^{Leu} CAA	1	TGATACCGGTGGTTCGGGGTCGAACCGACACTCCCGAAGGAA CACGATTTTGAGTCGTGCGCGTCTGCCAATTCCGCCACACCCG GC
tRNA ^{Leu} TAA	1	TGCCGAGGGCCGGACTTGAACCGGCACGGTAGTCACCTACC GCAGGATTTAAGTCCTGTGTGTCTGCCAATTCCACCACCCCG GGC
tRNA ^{Lys} TTT	1	TGAGCCATGAAGGACTCGAACCTTCGACCTCTGATTAATA GTCAGATGCTCTACCAACTGAGCTAATGGCTC
tRNA ^{Met 1} CAT	1	TTGCGGGGGCAGGATTTGAACCTGCGACCTTCGGGTTATGAG CCCGACGAGCTACCGAACTGCTCCACCCCGCG
tRNA ^{Met 2} CAT	1	TAGCGCGGGAGGG ^R ATCGAACCCCGACCTCACGGGTATGA ACCGTACGCTCTAGCCAGCTGAGCTACACCCGC
tRNA ^{Met 3} CAT	1	TGGACCTTGTAGGACTCGAACCTACGACCCGACGGTTATGA GCCGTCTGCTCTAACCAACTGAGCTAAAGGTCC
tRNA ^{Phe} GAA	3	TGGCTCGGGACGGAATCGAACCGCCGACACACGGATTTTCA GTCCGTTGCTCTACCAACTGAGCTACCGAGCC
tRNA ^{Pro} TGG	1	TCGGGAAGACAGGATTCGAACCTGCGACCCCATGGTCCCAA ACCATGTGCTCTACCAAGCTGAGCTACTTCCCG
tRNA ^{Ser} GGA	1	CGGAGAGCAAGGGATTTCGAACCCCGCGGGCTTTGACACCC CTGTGCGTTTTCAAGACCGATCCCTTCAGCCAGACTTGGGTA TTCCTCC
tRNA ^{Ser} TGA	2	CGGAGAAGGAGGGATTTGAACCCCTCGCGCCGCTTACGCGAC CTACACCCTTAGCAGGGGCGCCTCTTCAGCCACTTGAGTACT TCTCC
tRNA ^{Ser} GCT	2	CGGAGAAGGAGGGATTTGAACCCCTCGCGCCGCTTACGCGAC CTACACCCTTAGCAGGGGCGCCTCTTCAGCCACTTGAGTACT TCTCC
tRNA ^{Thr} GGT	1	AGCTTCCAAGCGGGCTCGAACCGCTGACCTCTTCCTTACCAT GGAAGTGCTCTACCTGCTGAGCTATGGAAGC
tRNA ^{Thr} CGT	1	TGCCGGCAAGAGGACTTGAACCCCAACCTACTGATTACGA TTCAGTTGCTCTACCAATTGAGCTACACCCGC
tRNA ^{Thr} TGT	2	TGCCGGCCAGAGGACTTGAACCCCAACCTACTGATTACAA GTCAGTTGCTCTACCAATTGAGCTAGACCCGC
tRNA ^{Trp} CCA	1	CAGGGGCAGTAGGAATCGAACCCACACCCGAGGTTTTGGAG ACCTCTGTTCTACCGTTAAACTATGCCCT
tRNA ^{Tyr} GTA	2	TGGAGGGGGACGGATTTCGAACCGCCGACCCCTGAGGGAGCG GATTTACAGTCCGCGCGTTTAGCCACTTCGCTACCCCTCC
tRNA ^{al} GAC	1	TGATTCCGACTGGGCTCGAACCCAGCGACCTCTACCCTGTCAA GGTAGCGCTCTCCAGCTGAGCTACGGAATC
tRNA ^{Val} TAC	3	TGGAGGATGACGGGATCGAACCGCCGACCCCTCTGCTTGTA GGCAGATGCTCTCCAGCTGAGCTAATCCTCC

Table 5. Oligonucleotides used for qRT-PCR and library preparation

Name	Sequence (5' → 3')	Application	Comments
<i>ThrRS_Fw</i>	CACAGAGGTGTCGTATC	qRT-PCR	
<i>ThrRS_Rv</i>	ATGACCTGGAACCTGAAC		
<i>ValRS_Fw</i>	CGAAGGAAGTTGAACGG	qRT-PCR	
<i>ValRS_Rv</i>	TAATCGGCTTCTTTCCG		
<i>ProRS_Fw</i>	ATCCAATCGAAGTTCCG	qRT-PCR	
<i>ProRS_Rv</i>	TTCATCAAGGCTTTCCG		
<i>ArgS_Fw</i>	GTGCGTACTTCTTTGC	qRT-PCR	
<i>ArgS_Rv</i>	CTCAGAACCGATCTTCG		
<i>rpoB_Fw</i>	GTCATGGTCGGCTTTAT	qRT-PCR	
<i>rpoB_Rv</i>	GCCTCTGATTCGTATTCT		
<i>5SrRNA_Fw</i>	TAGCGAAGAGGTCACA	qRT-PCR	
<i>5SrRNA_Rv</i>	GGCGTCCTACTCTCA		
<i>16SrRNA_Fw</i>	GTAGAGATGTGGAGGAAC	qRT-PCR	
<i>16SrRNA_Rv</i>	GACTACCAGGGTATCTAATC		
3' adapter	rApp/TGGAATTCTCGGGTGCCAAGG/3ddC/	TruSeq library preparation	rApp indicates 5' adenylation /3ddC/ indicates 3' dideoxycyto sine (Guo et al. 2010)
5' adapter	GUUCAGAGUUCUACAGUCCGACGAUC		
RT primer	CCTTGGCACCCGAGAATTCCA		
PCR primer 1	AATGATACGGCGACCACCGACAGGTTTCAGAGTTCTACAGTCCGA		
PCR primer 2	CAAGCAGAAGACGGCATAACGAGATATTGGCGTGACTGGAGTTCCTTGGCACCCGA GAATTCCA		

4.1.4. Buffers and reagents

Cold sucrose buffer

0.5 M RNase-free sucrose, 50 mM KCl, 16 mM Tris-HCl pH 8.1
100 mM NaOAc, 100 mM NaCl pH 4.5

Acidic buffer RNA isolation 1

0.3 M NaOAc pH 4.5, 10 mM EDTA

Acidic buffer RNA isolation 2

0.01 M NaOAc pH 4.5, 1 mM EDTA

Crush and Soak Buffer

50 mM KOAc, 200 mM KCl pH = 7;

Polysome lysis buffer

10 mM Tris pH 7.8

50 mM NH₄Cl

10 mM MgCl₂

0.2% triton X-100

100 µg/ml chloramphenicol

20 mM CaCl₂

10 U/ml DNase I (RNase-free)

Polysome lysis buffer with pH 9.2

10 mM Tris pH 11

50 mM NH₄Cl

10 mM MgCl₂

0.2% triton X-100

100 µg/ml chloramphenicol

20 mM CaCl₂

70% (w/v) Sucrose

35 g sucrose were dissolved step by step in 20-30 ml DEPC-treated H₂O in a water bath (~70°C). DEPC-treated H₂O was added to a final volume of 50 ml.

Sucrose gradients

Gradients for ultracentrifugation contain sucrose to a final concentration of 15%, 23%, 31%, 40%, 50%. Each concentration was supplemented with 1X Polysome lysis buffer and 0.35 mg/ml chloramphenicol.

2× Alkaline fragmentation solution

0.5 Vol 0.5 M EDTA

15 Vol 100 mM Na₂CO₃

110 Vol 100 mM NaHCO₃

Solution was prepared freshly before using from stock solutions combined in the indicated ratios, resulting in an unadjusted pH of ~9.2.

Stop/Precipitation solution

60 µl 3 M NaACo (pH 5.5)

1.5 µl Glycogen

500 µl DEPC-H₂O

20× SSC buffer

3 M NaCl

0.3 M Na-citrate, pH 7.0

10× T4 RNA ligase 2 buffer

500 mM Tris/HCl (pH 7.5)

20 mM MgCl₂

10 mM DTT

The buffer was stored at -20 °C. SUPERase•InTM was added freshly prior to use.

10× T4 RNA ligase 1 buffer

500 mM Tris/HCl (pH 7.8)

100 mM MgCl₂

100 mM DTT

Buffer was stored at -20 °C. SUPERase•InTM was added freshly prior to use.

DNA elution buffer

10 mM Tris/HCl (pH 8.0)

300 mM NaCl

1 mM EDTA

4.1.5. Kits

illustra MicroSpin G-25 Columns

GE Healthcare Life Science

RevertAid H Minus First Strand cDNA Synthesis kit

Thermo

ERCC RNA Spike-In Control Mix

Ambion

TruSeq SBS Kit v3 – HS

Illumina

TruSeq SR Cluster Kit v3 cBot – HS

Illumina

Qubit dsDNA HS Assay

Life Technologies

RNA 6000 Nano kit	Agilent
DNA 1000 kit	Agilent
GeneJET™ RNA Purification Kit	Thermo Scientific
MICROBExpress™ Bacterial mRNA Enrichment Kit	Ambion
RNA Clean & Concentrator™ kit	Zymo Research
DNA1000 Chips	Agilent

4.1.6. Media

Luria-Bertani medium (LB) (for 1L)

Tryptone	10 g
NaCl	10 g
Yeast extract	5 g

Minimal medium (MM) (for 1L)

Na ₂ HPO ₄ x 7H ₂ O	12.8 g
KH ₂ PO ₄	3g
NaCl ₂	0.5 g
NH ₄ Cl	1g
1M MgSO ₄	1ml
0.1M CaCl ₂	1ml
20% glucose	20ml

Supplemented with 1ml of *trace elements solution* (FeCl₃*6H₂O, CaCl₂*2H₂O, MnCl₂*4H₂O, ZnSO₄*7H₂O, CoCl₂*6H₂O, CuCl₂, NiCl₂*6H₂O, Na₂MoO₄*2H₂O, Na₂SeO₃, H₃BO₃)

(MMaa)

Consisting of MM supplemented with all the amino acids listed in Table 6

Table 6. Amino acid concentration for MMaa

Amino Acid	mM
Ala	0.56
Arg	0.24
Asn	0.33
Asp	3.76
Cys	0.33
Gln	0.34
Glu	2.96
Gly	0.67
His	0.24
Ile	0.38
Leu	0.38
Lys	0.34
Met	0.34
Phe	0.30
Pro	0.43
Ser	0.48
Thr	0.42
Trp	0.10
Tyr	0.11
Val	0.43

4.2. Methods

4.2.1. Bacterial strains and growth conditions

The following strains, wild-type *B. licheniformis* ATCC 14580/DSM 13 (DSMZ, Germany, provided by BRAIN), *B. subtilis* 168, *B. licheniformis* HD0583 (naturally selected variant with enhanced protein secretion provided by BRAIN), *B. licheniformis* HD0583 aprE (transformed with pUBM72-aprE and overexpressing subtilisin encoded by *aprE* gene, provided by BRAIN), were grown in Luria-Bertani medium (LB, pH 7.0), MM and MM complemented with all 20 proteinogenic amino acids (each 50µg/ml, MMaa). *B. subtilis* 168 and *B. licheniformis* DSM13 were cultured at 37°C, while *B. licheniformis* HD0583 at 37°C or 45°C in both flasks or chemostat. In flasks all cultures were cultured in any of the three media and the chemostat experiments were performed only in MM. For toxicity assay bacterial cultures were performed in MM supplemented with single amino acid with a final concentration of 5mM, 10mM, 30mM, and 50mM. Growth was performed in 96 wells plate using Tecan Plate Reader at 37°C with 2 mm shaking amplitude for 24 hours. OD_{600nm} was recorded every 10 min.

4.2.2. RNA isolation, labelling and microarray detection

All RNA work was carried out under RNase-free conditions using RNase-free buffers and solutions. Bacterial cells were harvested in exponential or stationary phase by centrifugation for 5 min at 5000xg at 4°C. The cell pellet was dissolved in *cold sucrose buffer* and treated with freshly dissolved lysozyme (50 mg/ml) for 5 min on ice. Total RNA was isolated with Tri Reagent according to the manufacturer's protocol. Note that at this alkaline pH all tRNAs are deacylated and isolated in their non-aminoacylated form. The tRNAs were subsequently fluorescently labeled by ligating of Atto653- or Cy3-labeled RNA/DNA stem-loop oligonucleotide (Dittmar et al. 2004) that pairs to the common single-stranded 3' CCA ends of all tRNAs. To analyse aminoacyl-tRNAs, the total tRNAs were extracted from the cells with acidic phenol (pH 4.5) which preserves the aminoacyl group (Varshney et al. 1991). Thereafter the tRNA fraction was subjected to periodate treatment which oxidizes the 5' ends of the amino acid-free tRNAs (Dittmar et al. 2005) which were unable to ligate the fluorescent oligonucleotide. Aminoacyl-tRNAs remain intact upon periodate treatment (Dittmar et al. 2005) and were subsequently deacylated at

low pH and hybridized to Atto653-labeled RNA/DNA stem-loop oligonucleotide. Identical amounts of *in vitro* synthesized tRNA standards (two yeast tRNAs, tRNA^{Phe} tRNA^{Ala} and one human tRNA, tRNA^{HisGTG}) were added to each labeled tRNA batch prior to deacetylation and used for subsequent normalization. The ligation efficiency was determined on denaturing 10% PAGE by SYBR gold staining (the stem-loop ligated tRNAs migrated at much higher molecular weights than non-ligated tRNAs). Fluorescently labeled tRNAs were hybridized on microarrays for 16 h at 60°C, washed three times in 6x saline-sodium citrate buffer, at 35°C, once in 2x SSC and once in 0.2x SSC at 30°C, and recorded with a GenPIX 4200A scanner (Molecular Devices). Each microarray contained 12 identical blocks each with two replicates of the 36 tDNA probes covering all tRNAs of both *B. licheniformis* and *B. subtilis* tRNAs (Table 4) spotted. Each array contains two tRNA sets labeled with Atto653 and Cy3 and the Cy3-labeled tRNA set was always loaded as a reference for the Atto-labeled tRNA set (e.g., total uncharged Atto653-labeled tRNA sample 1 was compared to the total uncharged Cy3-labeled tRNA of a control sample; Atto653-labeled charged tRNA set was compared to its Cy3-labeled non-charged tRNA). Each array set contained a control array with Cy3- and Atto653-labeled total uncharged tRNA of the control sample to normalize for dye-labeling variations. For quantification each microarray was first normalized to the mean of the three tRNA standards using their Atto/Cy3 median averaged value and subsequently to the median of the control array. Welch's two-sample t-test was used as test to check significative differences among samples. To calculate the absolute concentration of *B. licheniformis* DSM 13, it was Atto653-labeled and compared on microarray to the *B. subtilis* tRNA whose absolute concentration was previously determined (Kanaya et al. 1999). The concentration of five tRNAs (tRNA^{Arg}CCG, tRNA^{Arg}CCU, tRNA^{His}GUG, tRNA^{Cys}GCA, tRNA^{Gln}UUG), which are absent in the quantitative set of *B. subtilis* tRNA (Kanaya et al. 1999), was linearly extrapolated using regression analysis of the tRNAs concentration and gene copy number.

4.2.3. Northern blot and qRT-PCR analysis

For Northern blotting, equal amounts of total RNA were separated by denaturing PAGE, in some cases stained with SybrGold for visualization, and subsequently transferred onto a HyBond-N⁺ membrane (GE Healthcare). The fraction of amino acid charged tRNA^{His}GUG, tRNA^{Asn}GUU and tRNA^{Ile}GAU was determined by Northern blot using ³³P-labeled tDNA probe and for tRNA^{Val}GAC, tRNA^{Val}UAC and tRNA^{Pro}UGG with Cy3-labeled tDNA

probe pairing to the full-length tRNA (Table 4). Blots were subsequently washed at 35 °C three times with 6× SSC (supplemented with 0.1% SDS), followed by one wash with 6× SSC, one wash with 2× SSC and a final wash with 0.2× SSC and imaged on the FujiFilm Las-4000 system. Intensities were normalized to 5S rRNA probed also with 5'-Cy3-labeled oligonucleotide.

For quantitative RT-PCR (qRT-PCR) one µg of the total mRNA (extracted using the total RNA isolation protocol) was treated with DNase I (Fermentas), cDNA was reverse transcribed using oligo-dT primer (Fermentas) and quantified on RT-PCR MX-3005-P machine (Stratagene). Amplification was performed in clear 96-well plates (Sarstedt) sealed with adhesive tape (Sarstedt) in a Mx3005P qPCR cycler (Agilent) using the QuantiFast SYBR Green PCR kit containing 6-carboxyl-Xrhodamin (ROX) as reference dye. PCR reaction conditions were as follows: initial denaturation for 5 min at 95 °C, followed by a three step amplification for 40 cycles at 95 °C for 10 s, 55 °C for 10 s and 72 °C for 30 s and a final melting curve analysis. Fluorescence was measured at the end of each elongation step. Relative expression levels were calculated using the $\Delta\Delta\text{CT}$ -method (Livak and Schmittgen 2001). Data analysis was performed using the MxPro QPCR (Agilent).

4.2.4. Ribosome profiling, RPF isolation

20 ml of bacterial culture is growth, filtered using a 0.45 µm nitrocellulose membrane and flash-frozen to isolate mRNA-bound ribosome complexes and extract the ribosome-protected fragments (RPF) following a previously described procedure (Oh et al. 2011).

Chloramphenicol (324 µg/ml) was present in all solutions after cell lysis. Cell pellet is pulverized using Retsch MM301 5 ml or 10 ml grinding jar together with a 10 mm or 12 mm grinding ball, respectively. 4 sets of grinding at 30 Hz for 2 min each were performed, with canisters pre-chilled in liquid nitrogen between each cycle. Pulverized cells were rapidly transferred in an Eppendorf tube and thawed at room temperature until the lysate completely thawed. The lysate was spun down at 10,000xg for 10 min at 4°C and the clarified supernatant was collected and transferred to a new tube. For the isolation of RPFs, an aliquot of 100 A260 units of ribosome-bound mRNA fraction was subjected to nucleolytic digestion with 10 units/µl micrococcal nuclease for 10 min at room temperature in buffer with pH 9.2. Equal amounts of supernatant (adjusted to the absorption at 260 nm) were applied onto a 15% to 50% (w/v) saccharose gradient. After

centrifugation for 1.5 h at 35,000 rpm (4 °C) in a SW55Ti Rotor (Beckman Coulter), gradients were analyzed from top to bottom by absorption measurement at 254 nm and the monosomal fraction of digested samples was collected. The RNA protected fragments were isolated from monosomes using the hot SDS/phenol extraction.

Total RNA was extracted using the previously described method followed by quality assessment (only total RNA with an RNA integrity index ≥ 8 was used). 2.5 μg DNase I treated total RNA was spiked with 5 μl External RNA Controls Consortium (ERCC) RNA Spike-In Control Mix. In order to enrich the mRNA fraction rRNA is depleted using GeneJet RNA purification kit (Fermentas).

4.2.5. Random mRNA fragmentation and size selection

Total RNA was mixed with equal volume of 2x *alkaline fragmentation solution* and incubated for 40 min at 95°C. The reaction was stopped by adding 560 μl of stop/precipitation solution, followed by isopropanol precipitation. RPFs and total RNA fragments were dephosphorylated using 0.5 U/ μl T4

PNK and 1 \times PNK buffer. For size selection, RPFs and RNA fragments were separated by denaturing PAGE on a 15% acrylamid gel, stained with SybrGold and fragments with a size of 20 – 30 nts were purified from the gel.

4.2.6. Library preparation

For library preparation, first, adenylated adapters ([Table 5](#)) were ligated to the 3'-end of fragments mRNA and RPFs. Ligation was done by combining samples with 1 μl of 3'-adapter (60 μM), incubating 2 min at 70 °C and adding 20 U/ μl T4 RNA ligase 2 truncated, 1x T4 RNA ligase 2 buffer and 10% PEG 8000 MW. Samples were incubated at 22 °C for 2.5 h. Ligated mRNA and RPF fragments were purified using Clean & ConcentratorTM-5 columns (Zymo Research, Freiburg, Germany). Next, the 5'-end of the 3'-adapter ligated fragments was phosphorylated using 0.4 U/ μl T4 PNK, 1 \times PNK buffer and 1 mM ATP to enable 5'-adapter ligation. After incubation at 37 °C for 30 min one step of purification was done again using Clean & ConcentratorTM-5 columns (Zymo Research). In order to ligate the 5'-adapter, 20 μM of RT primer ([Table 5](#)) was added to mRNA fragments as well as RPFs and samples were incubated for 5 min at 70 °C, followed by 30 min at 37 °C and 15 min at 25 °C to reduce the formation of adapter dimers. Then, 20 μM 5'-adapter (see [Table 5](#)) for each sample was pre-heated (2 min, 70 °C) and mixed with phosphorylated

mRNA and RPF samples. 1 U/ μ l T4 RNA ligase 1, 1xRNA ligase buffer and 0.24 mM ATP was added and samples were incubated at 22 °C for 18 h. 3'- and 5'-adapter ligated RPFs and mRNA fragments were purified using Clean & Concentrator™-5 columns (Zymo Research) and then reverse transcribed to generate a cDNA library. For reverse transcription, 0.85 μ M RT primer (Table 5), 1X RT buffer, 1 mM dNTPs and 10 U/ μ l RevertAid™ H Minus RT were added and samples were incubated at 44 °C for 1 h. The resulting RNA templates were denatured at 90 °C for 10 min with 145 mM NaOH subsequently neutralized by addition of 426 mM HEPES-NaOH (pH 7.0). First strand cDNA products were stored at -80 °C or directly processed for amplification. The generated library were amplified mixing the samples with 0.0625 U/ μ l *Pfu* DNA Polymerase, 1x *Pfu* buffer (+ MgSO₄), 0.375 mM dNTPs and 0.625 mM PCR primer 1 and PCR primer 2 (Table 5). Amplification was done in a thermal cycler (VWR Thermocycler; Biometra TProfessional Trio Thermocycler) using the following conditions: initial denaturation at 95 °C for 2 min, three step amplification cycle consisting of denaturation at 95 °C for 30 s, annealing at 60 °C for 30 s and elongation at 72 °C for 15 s, ending with a final elongation at 72 °C for 10 min. The optimal number of amplification cycles was determined for each sample individually by an initial test PCR and ranged from 8-16 cycles. After performing the final PCR, library products were mixed with 6xOrange Loading Dye (Thermo Scientific) and separated via a 10% TBE-PA gel (without urea) using O'GeneRuler™ Low Range Ladder (Thermo Scientific) as internal standard. After staining with SYBR® Gold, library products of 140 bp were excised from the gel, precipitated and resuspended in 8 μ l H₂O DEPC and stored at -80 °C. The library size was determined using DNA 1000 Kit and concentration was measured with the Qubit dsDNA HS Assay. Sequencing was performed on a HiSeq2000 sequencing machine (Illumina, Munich, Germany) using a TruSeq SBS Kit at the Sequencing Core Unit of the Max Delbrück Center for Molecular Medicine (Berlin, Germany).

4.2.7. Mapping of the sequencing reads

Sequenced reads were quality trimmed using fastx-toolkit (0.0.13.2; quality threshold: 20) and sequencing adapters were cut using cutadapt (1.2.1; minimal overlap: 1 nt). Processed reads were uniquely mapped to the *Bacillus licheniformis* DSM13 genome (Version: NC_006322.1, GI:52783855 download from NCBI) using Bowtie (0.12.9) allowing a maximum of two mismatches (parameter settings: -v 2 -m 1 --strata --best). The obtained

reads are calibrated assigning ribosome density to the 3' end which in prokaryotes contains precise and accurate information about the position of the ribosome (Woolstenhulme et al. 2015). The nucleotides corresponding to the A-site was determined and the calibration was validated using a known ribosomal stalling site of MifM (Sohmen et al. 2015) (Figure 17) The read counts were normalized in reads per kilobase per million mapped reads (RPKM) considering the length of a gene as well as the sequencing depth (equal to the total number of feature mapped reads) (Mortazavi *et al.*, 2008) as follows:

$$R_i = C_i / ((N/10^6) * (L_i/10^3))$$

where, C_i is the number of reads mapped to a feature i , N is the total number of feature mapped reads within the sample, and L_i is the length of the feature.

To calculate the ribosome density (RD) following formula was applied:

$$RD_i = RPF_i / mRNA_i$$

where, RPF_i represent the number of reads mapping to a feature i in the RPF dataset (expressed as RPKM) and $mRNA_i$ is the number of reads mapping to the same feature i in the rRNA depleted total RNA dataset (expressed as RPKM).

5. References

- Achsel T, Gross HJ. 1993. Identity determinants of human tRNA(Ser): sequence elements necessary for serylation and maturation of a tRNA with a long extra arm. *EMBO J* **12**: 3333-3338.
- Agris PF. 2008. Bringing order to translation: the contributions of transfer RNA anticodon-domain modifications. *EMBO Rep* **9**: 629-635.
- Agris PF, Vendeix FA, Graham WD. 2007. tRNA's wobble decoding of the genome: 40 years of modification. *J Mol Biol* **366**: 1-13.
- Akashi H, Gojobori T. 2002. Metabolic efficiency and amino acid composition in the proteomes of Escherichia coli and Bacillus subtilis. *Proc Natl Acad Sci U S A* **99**: 3695-3700.
- Albers S, Czech A. 2016. Exploiting tRNAs to Boost Virulence. *Life (Basel)* **6**.
- Ali NO, Bignon J, Rapoport G, Debarbouille M. 2001. Regulation of the acetoin catabolic pathway is controlled by sigma L in Bacillus subtilis. *J Bacteriol* **183**: 2497-2504.
- Altman S. 2011. Ribonuclease P. *Philos Trans R Soc Lond B Biol Sci* **366**: 2936-2941.
- Alwine JC, Kemp DJ, Stark GR. 1977. Method for detection of specific RNAs in agarose gels by transfer to diazobenzyloxymethyl-paper and hybridization with DNA probes. *Proc Natl Acad Sci U S A* **74**: 5350-5354.
- Anderson P, Ivanov P. 2014. tRNA fragments in human health and disease. *FEBS Lett* **588**: 4297-4304.
- Antoun A, Pavlov MY, Lovmar M, Ehrenberg M. 2006. How initiation factors maximize the accuracy of tRNA selection in initiation of bacterial protein synthesis. *Mol Cell* **23**: 183-193.
- Apirion D, Miczak A. 1993. RNA processing in prokaryotic cells. *Bioessays* **15**: 113-120.
- Bartholomaeus A, Del Campo C, Ignatova Z. 2016. Mapping the non-standardized biases of ribosome profiling. *Biol Chem* **397**: 23-35.
- Begley U, Dyavaiah M, Patil A, Rooney JP, DiRenzo D, Young CM, Conklin DS, Zitomer RS, Begley TJ. 2007. Trm9-catalyzed tRNA modifications link translation to the DNA damage response. *Mol Cell* **28**: 860-870.
- Belitsky BR, Wray LV, Jr., Fisher SH, Bohannon DE, Sonenshein AL. 2000. Role of TnrA in nitrogen source-dependent repression of Bacillus subtilis glutamate synthase gene expression. *J Bacteriol* **182**: 5939-5947.

- Bentele K, Saffert P, Rauscher R, Ignatova Z, Bluthgen N. 2013. Efficient translation initiation dictates codon usage at gene start. *Mol Syst Biol* **9**: 675.
- Berg JMT, John L.; Stryer, Lubert. 2002. *Biochemistry, Fifth Edition*.
- Berg OG, Kurland CG. 1997. Growth rate-optimised tRNA abundance and codon usage. *J Mol Biol* **270**: 544-550.
- Bittner AN, Kriel A, Wang JD. 2014. Lowering GTP level increases survival of amino acid starvation but slows growth rate for *Bacillus subtilis* cells lacking (p)ppGpp. *J Bacteriol* **196**: 2067-2076.
- Björk GR. 1996.
- Bjork GR, Hagervall TG. 2014. Transfer RNA Modification: Presence, Synthesis, and Function. *EcoSal Plus* **6**.
- Bloom-Ackermann Z, Navon S, Gingold H, Towers R, Pilpel Y, Dahan O. 2014. A comprehensive tRNA deletion library unravels the genetic architecture of the tRNA pool. *PLoS Genet* **10**: e1004084.
- Bremer H DP. 1996. Modulation of Chemical Composition and Other Parameters of the Cell by Growth Rate.
- Caron MP, Bastet L, Lussier A, Simoneau-Roy M, Masse E, Lafontaine DA. 2012. Dual-acting riboswitch control of translation initiation and mRNA decay. *Proc Natl Acad Sci U S A* **109**: E3444-3453.
- Chan CT, Deng W, Li F, DeMott MS, Babu IR, Begley TJ, Dedon PC. 2015. Highly Predictive Reprogramming of tRNA Modifications Is Linked to Selective Expression of Codon-Biased Genes. *Chem Res Toxicol* **28**: 978-988.
- Chan CT, Dyavaiah M, DeMott MS, Taghizadeh K, Dedon PC, Begley TJ. 2010. A quantitative systems approach reveals dynamic control of tRNA modifications during cellular stress. *PLoS Genet* **6**: e1001247.
- Chan PP, Lowe TM. 2009. GtRNADB: a database of transfer RNA genes detected in genomic sequence. *Nucleic Acids Res* **37**: D93-97.
- Chubukov V, Sauer U. 2014. Environmental dependence of stationary-phase metabolism in *Bacillus subtilis* and *Escherichia coli*. *Appl Environ Microbiol* **80**: 2901-2909.
- Ciryam P, Morimoto RI, Vendruscolo M, Dobson CM, O'Brien EP. 2013. In vivo translation rates can substantially delay the cotranslational folding of the *Escherichia coli* cytosolic proteome. *Proc Natl Acad Sci U S A* **110**: E132-140.
- Condon C. 2007. Maturation and degradation of RNA in bacteria. *Current opinion in microbiology* **10**: 271-278.
- Condon C, Grunberg-Manago M, Putzer H. 1996. Aminoacyl-tRNA synthetase gene regulation in *Bacillus subtilis*. *Biochimie* **78**: 381-389.
- Crick FH. 1966. Codon--anticodon pairing: the wobble hypothesis. *J Mol Biol* **19**: 548-555.

- Cruz Hernandez A, Millan ES, de Jesus Romero Gomez S, Antonio Cervantes Chavez J, Garcia Martinez R, Pastrana Martinez X, Gomez JL, Jones GH, Guillen JC. 2013. Exposure of *Bacillus subtilis* to mercury induces accumulation of shorter tRNA Cys species. *Metallomics : integrated biometal science* **5**: 398-403.
- Cruz Ramos H, Hoffmann T, Marino M, Nedjari H, Presecan-Siedel E, Dreesen O, Glaser P, Jahn D. 2000. Fermentative metabolism of *Bacillus subtilis*: physiology and regulation of gene expression. *J Bacteriol* **182**: 3072-3080.
- Czech A, Wende S, Morl M, Pan T, Ignatova Z. 2013. Reversible and rapid transfer-RNA deactivation as a mechanism of translational repression in stress. *PLoS Genet* **9**: e1003767.
- Czerwoniec A, Dunin-Horkawicz S, Purta E, Kaminska KH, Kasprzak JM, Bujnicki JM, Grosjean H, Rother K. 2009. MODOMICS: a database of RNA modification pathways. 2008 update. *Nucleic Acids Res* **37**: D118-121.
- Dalebroux ZD, Swanson MS. 2012. ppGpp: magic beyond RNA polymerase. *Nat Rev Microbiol* **10**: 203-212.
- Dare K, Ibba M. 2012. Roles of tRNA in cell wall biosynthesis. *Wiley Interdiscip Rev RNA* **3**: 247-264.
- de Vries MC, Siezen RJ, Wijman JG, Zhao Y, Kleerebezem M, de Vos WM, Vaughan EE. 2006. Comparative and functional analysis of the rRNA-operators and their tRNA gene complement in different lactic acid bacteria. *Syst Appl Microbiol* **29**: 358-367.
- Del Campo C, Bartholomaeus A, Fedyunin I, Ignatova Z. 2015. Secondary Structure across the Bacterial Transcriptome Reveals Versatile Roles in mRNA Regulation and Function. *PLoS Genet* **11**: e1005613.
- Deutscher MP. 2006. Degradation of RNA in bacteria: comparison of mRNA and stable RNA. *Nucleic Acids Res* **34**: 659-666.
- Dittmar KA, Goodenbour JM, Pan T. 2006. Tissue-specific differences in human transfer RNA expression. *PLoS Genet* **2**: e221.
- Dittmar KA, Mobley EM, Radek AJ, Pan T. 2004. Exploring the regulation of tRNA distribution on the genomic scale. *J Mol Biol* **337**: 31-47.
- Dittmar KA, Sorensen MA, Elf J, Ehrenberg M, Pan T. 2005. Selective charging of tRNA isoacceptors induced by amino-acid starvation. *EMBO Rep* **6**: 151-157.
- Dong H, Nilsson L, Kurland CG. 1996. Co-variation of tRNA abundance and codon usage in *Escherichia coli* at different growth rates. *J Mol Biol* **260**: 649-663.
- dos Reis M, Savva R, Wernisch L. 2004. Solving the riddle of codon usage preferences: a test for translational selection. *Nucleic Acids Res* **32**: 5036-5044.

- Durand S, Gilet L, Bessieres P, Nicolas P, Condon C. 2012. Three essential ribonucleases-RNase Y, J1, and III-control the abundance of a majority of *Bacillus subtilis* mRNAs. *PLoS Genet* **8**: e1002520.
- Dworkin J, Losick R. 2001. Linking nutritional status to gene activation and development. *Genes Dev* **15**: 1051-1054.
- Ebhardt HA, Tsang HH, Dai DC, Liu Y, Bostan B, Fahlman RP. 2009. Meta-analysis of small RNA-sequencing errors reveals ubiquitous post-transcriptional RNA modifications. *Nucleic Acids Res* **37**: 2461-2470.
- Ehrenberg M, Bremer H, Dennis PP. 2013. Medium-dependent control of the bacterial growth rate. *Biochimie* **95**: 643-658.
- Ehrenberg M, Kurland CG. 1984. Costs of accuracy determined by a maximal growth rate constraint. *Q Rev Biophys* **17**: 45-82.
- El Yacoubi B, Bailly M, de Crecy-Lagard V. 2012. Biosynthesis and function of posttranscriptional modifications of transfer RNAs. *Annual review of genetics* **46**: 69-95.
- Elf J, Nilsson D, Tenson T, Ehrenberg M. 2003. Selective charging of tRNA isoacceptors explains patterns of codon usage. *Science* **300**: 1718-1722.
- Emilsson V, Kurland CG. 1990. Growth rate dependence of transfer RNA abundance in *Escherichia coli*. *EMBO J* **9**: 4359-4366.
- Emilsson V, Naslund AK, Kurland CG. 1992. Thiolation of transfer RNA in *Escherichia coli* varies with growth rate. *Nucleic Acids Res* **20**: 4499-4505.
- . 1993. Growth-rate-dependent accumulation of twelve tRNA species in *Escherichia coli*. *J Mol Biol* **230**: 483-491.
- Emmrechts G, Barbe S, Herdewijn P, Anne J, Rozenski J. 2007. Post-transcriptional modification mapping in the *Clostridium acetobutylicum* 16S rRNA by mass spectrometry and reverse transcriptase assays. *Nucleic Acids Res* **35**: 3494-3503.
- Fedyunin I, Lehnhardt L, Bohmer N, Kaufmann P, Zhang G, Ignatova Z. 2012. tRNA concentration fine tunes protein solubility. *FEBS Lett* **586**: 3336-3340.
- Fluitt A, Pienaar E, Viljoen H. 2007. Ribosome kinetics and aa-tRNA competition determine rate and fidelity of peptide synthesis. *Comput Biol Chem* **31**: 335-346.
- Fluman N, Navon S, Bibi E, Pilpel Y. 2014. mRNA-programmed translation pauses in the targeting of *E. coli* membrane proteins. *Elife* **3**.
- Francklyn CS, Minajigi A. 2010. tRNA as an active chemical scaffold for diverse chemical transformations. *FEBS Lett* **584**: 366-375.
- Fraser HB, Hirsh AE, Wall DP, Eisen MB. 2004. Coevolution of gene expression among interacting proteins. *Proc Natl Acad Sci U S A* **101**: 9033-9038.
- Frenkel-Morgenstern M, Danon T, Christian T, Igarashi T, Cohen L, Hou YM, Jensen LJ. 2012. Genes adopt non-optimal codon usage to

- generate cell cycle-dependent oscillations in protein levels. *Mol Syst Biol* **8**: 572.
- Fu Y, Lee I, Lee YS, Bao X. 2015. Small Non-coding Transfer RNA-Derived RNA Fragments (tRFs): Their Biogenesis, Function and Implication in Human Diseases. *Genomics Inform* **13**: 94-101.
- Fujita M, Losick R. 2005. Evidence that entry into sporulation in *Bacillus subtilis* is governed by a gradual increase in the level and activity of the master regulator Spo0A. *Genes Dev* **19**: 2236-2244.
- Fujita Y. 2009. Carbon catabolite control of the metabolic network in *Bacillus subtilis*. *Biosci Biotechnol Biochem* **73**: 245-259.
- Giege R. 2008. Toward a more complete view of tRNA biology. *Nature structural & molecular biology* **15**: 1007-1014.
- Giege R, Sissler M, Florentz C. 1998. Universal rules and idiosyncratic features in tRNA identity. *Nucleic Acids Res* **26**: 5017-5035.
- Giege R, Springer M. 2012. Aminoacyl-tRNA Synthetases in the Bacterial World. *EcoSal Plus* **5**.
- Gingold H, Tehler D, Christoffersen NR, Nielsen MM, Asmar F, Kooistra SM, Christophersen NS, Christensen LL, Borre M, Sorensen KD et al. 2014. A dual program for translation regulation in cellular proliferation and differentiation. *Cell* **158**: 1281-1292.
- Goodenbour JM, Pan T. 2006. Diversity of tRNA genes in eukaryotes. *Nucleic Acids Res* **34**: 6137-6146.
- Gorochoowski TE, Avcilar-Kucukgoze I, Bovenberg RA, Roubos JA, Ignatova Z. 2016. A Minimal Model of Ribosome Allocation Dynamics Captures Trade-offs in Expression between Endogenous and Synthetic Genes. *ACS Synth Biol*.
- Gorochoowski TE, Ignatova Z, Bovenberg RA, Roubos JA. 2015. Trade-offs between tRNA abundance and mRNA secondary structure support smoothing of translation elongation rate. *Nucleic Acids Res* **43**: 3022-3032.
- Green NJ, Grundy FJ, Henkin TM. 2010. The T box mechanism: tRNA as a regulatory molecule. *FEBS Lett* **584**: 318-324.
- Grosjean H, de Crecy-Lagard V, Marck C. 2010. Deciphering synonymous codons in the three domains of life: co-evolution with specific tRNA modification enzymes. *FEBS Lett* **584**: 252-264.
- Grosjean H, Soll D, Crothers D. 1977. Studies of the complex between transfer RNA's with complementary anticodons : a direct approach to the "wobble" problem [proceedings]. *Arch Int Physiol Biochim* **85**: 414-415.
- Grunberg-Manago M, Hershey JB, Plumbridge JA, Sacerdot C, Springer M, Fayat G, Lestienne P, Mayaux JF, Blanquet S. 1985. Regulation of gene expression of translation components in *Escherichia coli*:

- initiation factors and aminoacyl tRNA synthetases. *Curr Top Cell Regul* **26**: 503-520.
- Grundy FJ, Henkin TM. 1993. tRNA as a positive regulator of transcription antitermination in *B. subtilis*. *Cell* **74**: 475-482.
- . 1994. Conservation of a transcription antitermination mechanism in aminoacyl-tRNA synthetase and amino acid biosynthesis genes in gram-positive bacteria. *J Mol Biol* **235**: 798-804.
- Grundy FJ, Lehman SC, Henkin TM. 2003. The L box regulon: lysine sensing by leader RNAs of bacterial lysine biosynthesis genes. *Proc Natl Acad Sci U S A* **100**: 12057-12062.
- Gualerzi CO, Pon CL. 2015. Initiation of mRNA translation in bacteria: structural and dynamic aspects. *Cell Mol Life Sci* **72**: 4341-4367.
- Gunka K, Commichau FM. 2012. Control of glutamate homeostasis in *Bacillus subtilis*: a complex interplay between ammonium assimilation, glutamate biosynthesis and degradation. *Mol Microbiol* **85**: 213-224.
- Guo H, Ingolia NT, Weissman JS, Bartel DP. 2010. Mammalian microRNAs predominantly act to decrease target mRNA levels. *Nature* **466**: 835-840.
- Guo J, Cheng G, Gou XY, Xing F, Li S, Han YC, Wang L, Song JM, Shu CC, Chen SW et al. 2015. Comprehensive transcriptome and improved genome annotation of *Bacillus licheniformis* WX-02. *FEBS Lett* **589**: 2372-2381.
- Gustilo EM, Vendeix FA, Agris PF. 2008. tRNA's modifications bring order to gene expression. *Current opinion in microbiology* **11**: 134-140.
- Gutierrez-Preciado A, Henkin TM, Grundy FJ, Yanofsky C, Merino E. 2009. Biochemical features and functional implications of the RNA-based T-box regulatory mechanism. *Microbiol Mol Biol Rev* **73**: 36-61.
- Halvorson H. 1972. Utilization of single L-amino acids as sole source of carbon and nitrogen by bacteria. *Can J Microbiol* **18**: 1647-1650.
- Hartmann RK, Gossringer M, Spath B, Fischer S, Marchfelder A. 2009. The making of tRNAs and more - RNase P and tRNase Z. *Prog Mol Biol Transl Sci* **85**: 319-368.
- Henkin TM. 2008. Riboswitch RNAs: using RNA to sense cellular metabolism. *Genes Dev* **22**: 3383-3390.
- Henkin TM, Grundy FJ. 2006. Sensing metabolic signals with nascent RNA transcripts: the T box and S box riboswitches as paradigms. *Cold Spring Harb Symp Quant Biol* **71**: 231-237.
- Hoagland MB, Stephenson ML, Scott JF, Hecht LI, Zamecnik PC. 1958. A soluble ribonucleic acid intermediate in protein synthesis. *J Biol Chem* **231**: 241-257.
- Honda S, Shigematsu M, Morichika K, Telonis AG, Kirino Y. 2015. Four-leaf clover qRT-PCR: A convenient method for selective quantification of mature tRNA. *RNA Biol* **12**: 501-508.

- Hossain M, Limbach PA. 2007. Mass spectrometry-based detection of transfer RNAs by their signature endonuclease digestion products. *RNA* **13**: 295-303.
- Hou YM, Schimmel P. 1988. A simple structural feature is a major determinant of the identity of a transfer RNA. *Nature* **333**: 140-145.
- Huang da W, Sherman BT, Lempicki RA. 2009a. Bioinformatics enrichment tools: paths toward the comprehensive functional analysis of large gene lists. *Nucleic Acids Res* **37**: 1-13.
- . 2009b. Systematic and integrative analysis of large gene lists using DAVID bioinformatics resources. *Nat Protoc* **4**: 44-57.
- Hussmann JA, Patchett S, Johnson A, Sawyer S, Press WH. 2015. Understanding Biases in Ribosome Profiling Experiments Reveals Signatures of Translation Dynamics in Yeast. *PLoS Genet* **11**: e1005732.
- Ibba M, Soll D. 1999. Quality control mechanisms during translation. *Science* **286**: 1893-1897.
- . 2004. Aminoacyl-tRNAs: setting the limits of the genetic code. *Genes Dev* **18**: 731-738.
- Ikemura T. 1981. Correlation between the abundance of Escherichia coli transfer RNAs and the occurrence of the respective codons in its protein genes: a proposal for a synonymous codon choice that is optimal for the E. coli translational system. *J Mol Biol* **151**: 389-409.
- . 1985. Codon usage and tRNA content in unicellular and multicellular organisms. *Mol Biol Evol* **2**: 13-34.
- Ingolia NT. 2014. Ribosome profiling: new views of translation, from single codons to genome scale. *Nat Rev Genet* **15**: 205-213.
- Ingolia NT, Ghaemmaghami S, Newman JR, Weissman JS. 2009. Genome-wide analysis in vivo of translation with nucleotide resolution using ribosome profiling. *Science* **324**: 218-223.
- Ishimura R, Nagy G, Dotu I, Zhou H, Yang XL, Schimmel P, Senju S, Nishimura Y, Chuang JH, Ackerman SL. 2014. RNA function. Ribosome stalling induced by mutation of a CNS-specific tRNA causes neurodegeneration. *Science* **345**: 455-459.
- Ivanov P, Emara MM, Villen J, Gygi SP, Anderson P. 2011. Angiogenin-induced tRNA fragments inhibit translation initiation. *Mol Cell* **43**: 613-623.
- Jakubowski H, Goldman E. 1984. Quantities of individual aminoacyl-tRNA families and their turnover in Escherichia coli. *J Bacteriol* **158**: 769-776.
- Jin DJ, Cagliero C, Zhou YN. 2012. Growth rate regulation in Escherichia coli. *FEMS Microbiol Rev* **36**: 269-287.

- Johansson MJ, Byström AS. 2005. Transfer RNA modifications and modifying enzymes in *S. cerevisiae*. In *Topics in Current Genetics*, Vol 12 (ed. H Grosjean), pp. 87-120. Springer Verlag, Berlin.
- Kanaya S, Yamada Y, Kinouchi M, Kudo Y, Ikemura T. 2001. Codon usage and tRNA genes in eukaryotes: correlation of codon usage diversity with translation efficiency and with CG-dinucleotide usage as assessed by multivariate analysis. *J Mol Evol* **53**: 290-298.
- Kanaya S, Yamada Y, Kudo Y, Ikemura T. 1999. Studies of codon usage and tRNA genes of 18 unicellular organisms and quantification of *Bacillus subtilis* tRNAs: gene expression level and species-specific diversity of codon usage based on multivariate analysis. *Gene* **238**: 143-155.
- Kanduc D. 1997. Changes of tRNA population during compensatory cell proliferation: differential expression of methionine-tRNA species. *Arch Biochem Biophys* **342**: 1-5.
- Kang Z, Zhang C, Zhang J, Jin P, Zhang J, Du G, Chen J. 2014. Small RNA regulators in bacteria: powerful tools for metabolic engineering and synthetic biology. *Appl Microbiol Biotechnol* **98**: 3413-3424.
- Katibah GE, Qin Y, Sidote DJ, Yao J, Lambowitz AM, Collins K. 2014. Broad and adaptable RNA structure recognition by the human interferon-induced tetratricopeptide repeat protein IFIT5. *Proc Natl Acad Sci U S A* **111**: 12025-12030.
- Kim SH, Quigley GJ, Suddath FL, McPherson A, Sneden D, Kim JJ, Weinzierl J, Rich A. 1973. Three-dimensional structure of yeast phenylalanine transfer RNA: folding of the polynucleotide chain. *Science* **179**: 285-288.
- Kirchner S, Ignatova Z. 2015. Emerging roles of tRNA in adaptive translation, signalling dynamics and disease. *Nat Rev Genet* **16**: 98-112.
- Korkmaz G, Holm M, Wiens T, Sanyal S. 2014. Comprehensive analysis of stop codon usage in bacteria and its correlation with release factor abundance. *J Biol Chem* **289**: 30334-30342.
- Krasny L, Gourse RL. 2004. An alternative strategy for bacterial ribosome synthesis: *Bacillus subtilis* rRNA transcription regulation. *EMBO J* **23**: 4473-4483.
- Krasny L, Tiserova H, Jonak J, Rejman D, Sanderova H. 2008. The identity of the transcription +1 position is crucial for changes in gene expression in response to amino acid starvation in *Bacillus subtilis*. *Mol Microbiol* **69**: 42-54.
- Kudla G, Murray AW, Tollervey D, Plotkin JB. 2009. Coding-sequence determinants of gene expression in *Escherichia coli*. *Science* **324**: 255-258.
- Kutter C, Brown GD, Goncalves A, Wilson MD, Watt S, Brazma A, White RJ, Odom DT. 2011. Pol III binding in six mammals shows

- conservation among amino acid isotypes despite divergence among tRNA genes. *Nature genetics* **43**: 948-955.
- Lavner Y, Kotlar D. 2005. Codon bias as a factor in regulating expression via translation rate in the human genome. *Gene* **345**: 127-138.
- Ling J, Reynolds N, Ibba M. 2009. Aminoacyl-tRNA synthesis and translational quality control. *Annu Rev Microbiol* **63**: 61-78.
- Livak KJ, Schmittgen TD. 2001. Analysis of relative gene expression data using real-time quantitative PCR and the 2(-Delta Delta C(T)) Method. *Methods* **25**: 402-408.
- Maghnouj A, de Sousa Cabral TF, Stalon V, Vander Wauven C. 1998. The arcABDC gene cluster, encoding the arginine deiminase pathway of *Bacillus licheniformis*, and its activation by the arginine repressor argR. *J Bacteriol* **180**: 6468-6475.
- Magnusson LU, Farewell A, Nystrom T. 2005. ppGpp: a global regulator in *Escherichia coli*. *Trends Microbiol* **13**: 236-242.
- Makhoul CH, Trifonov EN. 2002. Distribution of rare triplets along mRNA and their relation to protein folding. *J Biomol Struct Dyn* **20**: 413-420.
- Mandal M, Boese B, Barrick JE, Winkler WC, Breaker RR. 2003. Riboswitches control fundamental biochemical pathways in *Bacillus subtilis* and other bacteria. *Cell* **113**: 577-586.
- Mandal M, Lee M, Barrick JE, Weinberg Z, Emilsson GM, Ruzzo WL, Breaker RR. 2004. A glycine-dependent riboswitch that uses cooperative binding to control gene expression. *Science* **306**: 275-279.
- McClain WH, Jou YY, Bhattacharya S, Gabriel K, Schneider J. 1999. The reliability of in vivo structure-function analysis of tRNA aminoacylation. *J Mol Biol* **290**: 391-409.
- Melnikov S, Ben-Shem A, Garreau de Loubresse N, Jenner L, Yusupova G, Yusupov M. 2012. One core, two shells: bacterial and eukaryotic ribosomes. *Nature structural & molecular biology* **19**: 560-567.
- Merino E, Yanofsky C. 2005. Transcription attenuation: a highly conserved regulatory strategy used by bacteria. *Trends Genet* **21**: 260-264.
- Mohr S, Ghanem E, Smith W, Sheeter D, Qin Y, King O, Polioudakis D, Iyer VR, Hunicke-Smith S, Swamy S et al. 2013. Thermostable group II intron reverse transcriptase fusion proteins and their use in cDNA synthesis and next-generation RNA sequencing. *RNA* **19**: 958-970.
- Morl M, Marchfelder A. 2001. The final cut. The importance of tRNA 3'-processing. *EMBO Rep* **2**: 17-20.
- Murphy FVt, Ramakrishnan V, Malkiewicz A, Agris PF. 2004. The role of modifications in codon discrimination by tRNA(Lys)UUU. *Nature structural & molecular biology* **11**: 1186-1191.
- Noon KR, Guymon R, Crain PF, McCloskey JA, Thomm M, Lim J, Cavicchioli R. 2003. Influence of temperature on tRNA modification in archaea: *Methanococcus burtonii* (optimum growth temperature

- [Topt], 23 degrees C) and *Stetteria hydrogenophila* (Topt, 95 degrees C). *J Bacteriol* **185**: 5483-5490.
- Novichkov PS, Kazakov AE, Ravcheev DA, Leyn SA, Kovaleva GY, Sutormin RA, Kazanov MD, Riehl W, Arkin AP, Dubchak I et al. 2013. RegPrecise 3.0--a resource for genome-scale exploration of transcriptional regulation in bacteria. *BMC Genomics* **14**: 745.
- Novoa EM, Pavon-Eternod M, Pan T, Ribas de Pouplana L. 2012. A role for tRNA modifications in genome structure and codon usage. *Cell* **149**: 202-213.
- Oh E, Becker AH, Sandikci A, Huber D, Chaba R, Gloge F, Nichols RJ, Typas A, Gross CA, Kramer G et al. 2011. Selective ribosome profiling reveals the cotranslational chaperone action of trigger factor in vivo. *Cell* **147**: 1295-1308.
- Ohnishi M, Murata T, Nakayama K, Kuhara S, Hattori M, Kurokawa K, Yasunaga T, Yokoyama K, Makino K, Shinagawa H et al. 2000. Comparative analysis of the whole set of rRNA operons between an enterohemorrhagic *Escherichia coli* O157:H7 Sakai strain and an *Escherichia coli* K-12 strain MG1655. *Syst Appl Microbiol* **23**: 315-324.
- Pang YL, Abo R, Levine SS, Dedon PC. 2014a. Diverse cell stresses induce unique patterns of tRNA up- and down-regulation: tRNA-seq for quantifying changes in tRNA copy number. *Nucleic Acids Res* **42**: e170.
- Pang YL, Poruri K, Martinis SA. 2014b. tRNA synthetase: tRNA aminoacylation and beyond. *Wiley Interdiscip Rev RNA* **5**: 461-480.
- Pavlov MY, Watts RE, Tan Z, Cornish VW, Ehrenberg M, Forster AC. 2009. Slow peptide bond formation by proline and other N-alkylamino acids in translation. *Proc Natl Acad Sci U S A* **106**: 50-54.
- Pechmann S, Chartron JW, Frydman J. 2014. Local slowdown of translation by nonoptimal codons promotes nascent-chain recognition by SRP in vivo. *Nature structural & molecular biology* **21**: 1100-1105.
- Pelchat M, Lapointe J. 1999. Aminoacyl-tRNA synthetase genes of *Bacillus subtilis*: organization and regulation. *Biochem Cell Biol* **77**: 343-347.
- Percudani R, Pavesi A, Ottonello S. 1997. Transfer RNA gene redundancy and translational selection in *Saccharomyces cerevisiae*. *J Mol Biol* **268**: 322-330.
- Petry S, Weixlbaumer A, Ramakrishnan V. 2008. The termination of translation. *Curr Opin Struct Biol* **18**: 70-77.
- Phizicky EM, Alfonzo JD. 2010. Do all modifications benefit all tRNAs? *FEBS Lett* **584**: 265-271.
- Picard F, Milhem H, Loubiere P, Laurent B, Coccagn-Bousquet M, Girbal L. 2012. Bacterial translational regulations: high diversity between all mRNAs and major role in gene expression. *BMC Genomics* **13**: 528.

- Proshkin S, Rahmouni AR, Mironov A, Nudler E. 2010. Cooperation between translating ribosomes and RNA polymerase in transcription elongation. *Science* **328**: 504-508.
- Puri P, Wetzel C, Saffert P, Gaston KW, Russell SP, Cordero Varela JA, van der Vlies P, Zhang G, Limbach PA, Ignatova Z et al. 2014. Systematic identification of tRNAome and its dynamics in *Lactococcus lactis*. *Mol Microbiol* **93**: 944-956.
- Putzer H, Laalami S, Brakhage AA, Condon C, Grunberg-Manago M. 1995. Aminoacyl-tRNA synthetase gene regulation in *Bacillus subtilis*: induction, repression and growth-rate regulation. *Mol Microbiol* **16**: 709-718.
- Quax TE, Claassens NJ, Soll D, van der Oost J. 2015. Codon Bias as a Means to Fine-Tune Gene Expression. *Mol Cell* **59**: 149-161.
- Ray BK, Apirion D. 1981. RNAase P is dependent on RNAase E action in processing monomeric RNA precursors that accumulate in an RNAase E- mutant of *Escherichia coli*. *J Mol Biol* **149**: 599-617.
- Redko Y, Li de la Sierra-Gallay I, Condon C. 2007. When all's zed and done: the structure and function of RNase Z in prokaryotes. *Nat Rev Microbiol* **5**: 278-286.
- Reiter NJ, Osterman A, Torres-Larios A, Swinger KK, Pan T, Mondragon A. 2010. Structure of a bacterial ribonuclease P holoenzyme in complex with tRNA. *Nature* **468**: 784-789.
- Rodnina MV, Savelsbergh A, Wintermeyer W. 1999. Dynamics of translation on the ribosome: molecular mechanics of translocation. *FEMS Microbiol Rev* **23**: 317-333.
- Rodnina MV, Wintermeyer W. 2011. The ribosome as a molecular machine: the mechanism of tRNA-mRNA movement in translocation. *Biochem Soc Trans* **39**: 658-662.
- Rowley D. 1953. Interrelationships between amino-acids in the growth of coliform organisms. *J Gen Microbiol* **9**: 37-43.
- Salis HM, Mirsky EA, Voigt CA. 2009. Automated design of synthetic ribosome binding sites to control protein expression. *Nat Biotechnol* **27**: 946-950.
- Sezonov G, Joseleau-Petit D, D'Ari R. 2007. *Escherichia coli* physiology in Luria-Bertani broth. *J Bacteriol* **189**: 8746-8749.
- Sharp PM, Li WH. 1986. An evolutionary perspective on synonymous codon usage in unicellular organisms. *J Mol Evol* **24**: 28-38.
- Shen PS, Park J, Qin Y, Li X, Parsawar K, Larson MH, Cox J, Cheng Y, Lambowitz AM, Weissman JS et al. 2015. Protein synthesis. Rqc2p and 60S ribosomal subunits mediate mRNA-independent elongation of nascent chains. *Science* **347**: 75-78.

- Shepherd J, Ibba M. 2013. Direction of aminoacylated transfer RNAs into antibiotic synthesis and peptidoglycan-mediated antibiotic resistance. *FEBS Lett* **587**: 2895-2904.
- Shine J, Dalgarno L. 1975. Determinant of cistron specificity in bacterial ribosomes. *Nature* **254**: 34-38.
- Sohmen D, Chiba S, Shimokawa-Chiba N, Innis CA, Berninghausen O, Beckmann R, Ito K, Wilson DN. 2015. Structure of the *Bacillus subtilis* 70S ribosome reveals the basis for species-specific stalling. *Nat Commun* **6**: 6941.
- Soll D, Jones DS, Ohtsuka E, Faulkner RD, Lohrmann R, Hayatsu H, Khorana HG. 1966. Specificity of sRNA for recognition of codons as studied by the ribosomal binding technique. *J Mol Biol* **19**: 556-573.
- Soma A, Ikeuchi Y, Kanemasa S, Kobayashi K, Ogasawara N, Ote T, Kato J, Watanabe K, Sekine Y, Suzuki T. 2003. An RNA-modifying enzyme that governs both the codon and amino acid specificities of isoleucine tRNA. *Mol Cell* **12**: 689-698.
- Sorensen MA. 2001. Charging levels of four tRNA species in *Escherichia coli* Rel(+) and Rel(-) strains during amino acid starvation: a simple model for the effect of ppGpp on translational accuracy. *J Mol Biol* **307**: 785-798.
- Sorensen MA, Kurland CG, Pedersen S. 1989. Codon usage determines translation rate in *Escherichia coli*. *J Mol Biol* **207**: 365-377.
- Springer M, Mayaux JF, Fayat G, Plumbridge JA, Graffe M, Blanquet S, Grunberg-Manago M. 1985. Attenuation control of the *Escherichia coli* phenylalanyl-tRNA synthetase operon. *J Mol Biol* **181**: 467-478.
- Sprinzl M, Vassilenko KS. 2005. Compilation of tRNA sequences and sequences of tRNA genes. *Nucleic Acids Res* **33**: D139-140.
- Suess B, Weigand JE. 2008. Engineered riboswitches: overview, problems and trends. *RNA Biol* **5**: 24-29.
- Tanner DR, Cariello DA, Woolstenhulme CJ, Broadbent MA, Buskirk AR. 2009. Genetic identification of nascent peptides that induce ribosome stalling. *J Biol Chem* **284**: 34809-34818.
- Tojo S, Kumamoto K, Hirooka K, Fujita Y. 2010. Heavy involvement of stringent transcription control depending on the adenine or guanine species of the transcription initiation site in glucose and pyruvate metabolism in *Bacillus subtilis*. *J Bacteriol* **192**: 1573-1585.
- Tomita K, Yamashita S. 2014. Molecular mechanisms of template-independent RNA polymerization by tRNA nucleotidyltransferases. *Front Genet* **5**: 36.
- Torres AG, Batlle E, Ribas de Pouplana L. 2014. Role of tRNA modifications in human diseases. *Trends in molecular medicine* **20**: 306-314.

- Valgepea K, Adamberg K, Seiman A, Vilu R. 2013. Escherichia coli achieves faster growth by increasing catalytic and translation rates of proteins. *Mol Biosyst* **9**: 2344-2358.
- van Dijk EL, Jaszczyszyn Y, Thermes C. 2014. Library preparation methods for next-generation sequencing: tone down the bias. *Experimental cell research* **322**: 12-20.
- Varenne S, Buc J, Lloubes R, Lazdunski C. 1984. Translation is a non-uniform process. Effect of tRNA availability on the rate of elongation of nascent polypeptide chains. *J Mol Biol* **180**: 549-576.
- Varshney U, Lee CP, RajBhandary UL. 1991. Direct analysis of aminoacylation levels of tRNAs in vivo. Application to studying recognition of Escherichia coli initiator tRNA mutants by glutaminyl-tRNA synthetase. *J Biol Chem* **266**: 24712-24718.
- Vitreschak AG, Mironov AA, Lyubetsky VA, Gelfand MS. 2008. Comparative genomic analysis of T-box regulatory systems in bacteria. *RNA* **14**: 717-735.
- Voigt B, Antelmann H, Albrecht D, Ehrenreich A, Maurer KH, Evers S, Gottschalk G, van Dijk JM, Schweder T, Hecker M. 2009. Cell physiology and protein secretion of Bacillus licheniformis compared to Bacillus subtilis. *J Mol Microbiol Biotechnol* **16**: 53-68.
- Voigt B, Schweder T, Becher D, Ehrenreich A, Gottschalk G, Feesche J, Maurer KH, Hecker M. 2004. A proteomic view of cell physiology of Bacillus licheniformis. *Proteomics* **4**: 1465-1490.
- Wachsmuth M, Domin G, Lorenz R, Serfling R, Findeiss S, Stadler PF, Morl M. 2015. Design criteria for synthetic riboswitches acting on transcription. *RNA Biol* **12**: 221-231.
- Wacker I, Ludwig H, Reif I, Blencke HM, Detsch C, Stulke J. 2003. The regulatory link between carbon and nitrogen metabolism in Bacillus subtilis: regulation of the gltAB operon by the catabolite control protein CcpA. *Microbiology* **149**: 3001-3009.
- Wen T, Oussenko IA, Pellegrini O, Bechhofer DH, Condon C. 2005. Ribonuclease PH plays a major role in the exonucleolytic maturation of CCA-containing tRNA precursors in Bacillus subtilis. *Nucleic Acids Res* **33**: 3636-3643.
- Wetzel C, Limbach PA. 2013. The global identification of tRNA isoacceptors by targeted tandem mass spectrometry. *The Analyst* **138**: 6063-6072.
- Wiegand S, Dietrich S, Hertel R, Bongaerts J, Evers S, Volland S, Daniel R, Liesegang H. 2013a. RNA-Seq of Bacillus licheniformis: active regulatory RNA features expressed within a productive fermentation. *BMC Genomics* **14**: 667.
- Wiegand S, Voigt B, Albrecht D, Bongaerts J, Evers S, Hecker M, Daniel R, Liesegang H. 2013b. Fermentation stage-dependent adaptations of

- Bacillus licheniformis during enzyme production. *Microb Cell Fact* **12**: 120.
- Wilusz JE. 2015. Controlling translation via modulation of tRNA levels. *Wiley Interdiscip Rev RNA* **6**: 453-470.
- Winkler WC, Breaker RR. 2005. Regulation of bacterial gene expression by riboswitches. *Annu Rev Microbiol* **59**: 487-517.
- Winkler WC, Nahvi A, Sudarsan N, Barrick JE, Breaker RR. 2003. An mRNA structure that controls gene expression by binding S-adenosylmethionine. *Nat Struct Biol* **10**: 701-707.
- Wohlgemuth I, Brenner S, Beringer M, Rodnina MV. 2008. Modulation of the rate of peptidyl transfer on the ribosome by the nature of substrates. *J Biol Chem* **283**: 32229-32235.
- Woolhead CA, Johnson AE, Bernstein HD. 2006. Translation arrest requires two-way communication between a nascent polypeptide and the ribosome. *Mol Cell* **22**: 587-598.
- Woolstenhulme CJ, Guydosh NR, Green R, Buskirk AR. 2015. High-precision analysis of translational pausing by ribosome profiling in bacteria lacking EFP. *Cell Rep* **11**: 13-21.
- Yang Y, A MP, Hofler C, Poschet G, Wirtz M, Hell R, Sourjik V. 2015. Relation between chemotaxis and consumption of amino acids in bacteria. *Mol Microbiol* **96**: 1272-1282.
- Yona AH, Bloom-Ackermann Z, Frumkin I, Hanson-Smith V, Charpak-Amikam Y, Feng Q, Boeke JD, Dahan O, Pilpel Y. 2013. tRNA genes rapidly change in evolution to meet novel translational demands. *Elife* **2**: e01339.
- Yu CH, Dang Y, Zhou Z, Wu C, Zhao F, Sachs MS, Liu Y. 2015. Codon Usage Influences the Local Rate of Translation Elongation to Regulate Co-translational Protein Folding. *Mol Cell* **59**: 744-754.
- Zhang G, Fedyunin I, Miekley O, Valleriani A, Moura A, Ignatova Z. 2010. Global and local depletion of ternary complex limits translational elongation. *Nucleic Acids Res* **38**: 4778-4787.
- Zhang G, Hubalewska M, Ignatova Z. 2009. Transient ribosomal attenuation coordinates protein synthesis and co-translational folding. *Nature structural & molecular biology* **16**: 274-280.
- Zhang G, Ignatova Z. 2011. Folding at the birth of the nascent chain: coordinating translation with co-translational folding. *Curr Opin Struct Biol* **21**: 25-31.
- Zhang J, Ferre-D'Amare AR. 2015. Structure and mechanism of the T-box riboswitches. *Wiley Interdiscip Rev RNA* **6**: 419-433.
- Zhong J, Xiao C, Gu W, Du G, Sun X, He QY, Zhang G. 2015. Transfer RNAs Mediate the Rapid Adaptation of Escherichia coli to Oxidative Stress. *PLoS Genet* **11**: e1005302.

Zhou X, Wang E. 2013. Transfer RNA: a dancer between charging and mis-charging for protein biosynthesis. *Sci China Life Sci* **56**: 921-932.

6. Appendix

6.1. Hazard statements (H statements)

H225 – Highly flammable liquid and vapour.

H226 – Flammable liquid and vapour.

H227 – Combustible liquid

H228 – Flammable solid.

H290 – May be corrosive to metals.

H301 – Toxic if swallowed.

H302 – Harmful if swallowed.

H311 – Toxic in contact with skin.

H312 – Harmful in contact with skin.

H314 – Causes severe skin burns and eye damage.

H315 – Causes skin irritation.

H317 – May cause an allergic skin reaction.

H318 – Causes serious eye damage.

H319 – Causes serious eye irritation.

H331 – Toxic if inhaled.

H332 – Harmful if inhaled.

H335 – May cause respiratory irritation.

H336 – May cause drowsiness or dizziness.

H340 – May cause genetic defects.

H341 – Suspected of causing genetic defects.

H350 – May cause cancer.

H351 – Suspected of causing cancer.

H361 – Suspected of damaging fertility or the unborn child.

H370 – Causes damage to organs.

H372 – Causes damage to organs through prolonged or repeated exposure.

H373 – May cause damage to organs through prolonged or repeated exposure.

H412 – Harmful to aquatic life with long lasting effects.

6.2. Precautionary statements (P statements)

P210 – Keep away from heat/sparks/open flames/hot surfaces. — No smoking.

P233 – Keep container tightly closed.

P261 – Avoid breathing dust/fume/gas/mist/vapours/spray.

P280 – Wear protective gloves/protective clothing/eye protection/face protection.

P281 – Use personal protective equipment as required.

P310 – Immediately call a POISON CENTER or doctor/physician.

P314 – Get medical advice/attention if you feel unwell.

P301 + P310 – IF SWALLOWED: Immediately call a POISON CENTER or doctor/physician.

P301 + P312 – IF SWALLOWED: Call a POISON CENTER or doctor/physician if you feel unwell.

P301 + P330 + P331 – IF SWALLOWED: rinse mouth. Do NOT induce vomiting.

P302 + P352 – IF ON SKIN: Wash with plenty of soap and water.

P303 + P361 + P353 – IF ON SKIN (or hair): Remove/Take off immediately all contaminated clothing. Rinse skin with water/shower.

P304 + P340 – IF INHALED: Remove victim to fresh air and keep at rest in a position comfortable for breathing.

P304 + P341 – IF INHALED: If breathing is difficult, remove victim to fresh air and keep at rest in a position comfortable for breathing.

P305 + P351 + P338 – IF IN EYES: Rinse cautiously with water for several minutes. Remove contact lenses, if present and easy to do. Continue rinsing.

P308 + P310 – IF exposed or concerned: Immediately call a POISON CENTER or doctor/physician.

P308 + P313 – IF exposed or concerned: Get medical advice/attention.

P309 + P310 – IF exposed or if you feel unwell: Immediately call a POISON CENTER or doctor/physician.

P370 + P378 – In case of fire: Use ... for extinction.

P406 – Store in corrosive resistant/... container with a resistant inner liner.

6.3. List of hazardous substances used in the study

Chemical	Pictogram	H statement	P statement
Acrylamide		H301-H312- H315-H317- H319-H332- H340-H350- H361f-H372	P280-P302+P352- P305+P351+P338
Acetic Acid		H226-H314	P280- P301+P330+P331- P305+P351+P338
Bisacrylamide		H302	
Chloroform		H302, H315, H31 9, H332, H336, H3 51, H361, H373	P261, P281, P305+351 +338
Dithiothreitol		H302-H315- H319-H335	P261-P280- P301+P312- P304+P340
Ethanol		H225	P210-P233
Ethidium bromide		H332-H341	P281-P308+P313
Ethylenediamin etetraacetic acid		H319	P305+351+338
Formaldehyde		H301-H311- H314-H317- H331-H351- H370-H335	P281--P308+ P310- P303+P361+P353- P304+P340- P305+P351+P338
Hydrochloric acid		H290-H314-H335	P280- P301+P330+P331- P305+P351+P338
Isopropanol		H225-H319-H336	P210-P233- P305+P351+P338
Phenol		H301, H311, H31 4, H331, H341, H3 73	P261, P280, P301+310 , P305+351+338, P310

Chemical	Pictogram	H statement	P statement
Sodium carbonate		H319	P305+351+338
Sodium dodecyl sulfate		H228- H302+H332- H315-H318- H335-H412	P210-P280- P302+P352- P304+P340- P305+P351+P338- P314
Sodium hydroxide		H290-H314	P280- P303+P361+P353- P301+P330+P331- P305+P351+P338- P309+P310-P406
Syber gold		H227	P210, P280, P370 + P378
Tetramethyl-ethylendiamin			P210-P233-P280- P301+P330+P331- P305+P351+P338
Tris		H225-H302- H314-H332	P261-P280- P302+P352- P305+P351+P338- P304+P340
Xylen cyanol		H350	

7. Acknowledgments

Reaching the end always means thinking about the beginning. My beginning was not really easy, especially because it was in January, which says a lot. I had to measure up with being 2000km away from my family, my little beautiful niece Aurora and all my loves in a new, unknown, and super-cold (at least for me) country. As everybody knows my adaptation abilities are far away the one of my *Bacillus*. It didn't take so long for me to decide to quit. But, against all (my) expectations I made it. If now I'm here I mainly have to thanks Zoya and my extraordinary friends who didn't allow this to happen.

All my gratitude goes to Zoya, to the nice person who kept me here, and to the supervisor, who supported and encouraged me during these years, being a source of inspiration. Thanks for this great opportunity to grow, as a scientist but also as a person.

I would like to acknowledge the financial support by B.R.A.I.N. Biotechnology Research and Information Network.

Pinza, thanks for being there every moment, for enduring all my outbursts, for always cheering me up. It's partially also because of you I am here now.

I would have never done all this without my two towers of strength Silviò and Pollon. Thanks for making me reconsider any rash decisions, for the "good morning" and "good night" messages, thank you for being part of my life and having a positive word every time. "CPF" always! Additionally, a special thanks goes to the "Slais" group, you guys, directly and indirectly, have done a lot to support me during this time.

Despite the cold weather I was lucky to find great colleagues who created a friendly and pleasant working environment (and not only) to spend most of my day in.

I'm deeply grateful to Paul, even arguing a lot we had nice time and I could learn almost everything from you, especially to stay away from balconies; I would like to thank you Andreas, I will always look at you as the Wiseman of our lab; also a special thanks for you my dear friend/flatmate Cristian, especially for your patience (I know sometimes it was not easy!) and for the nice experience outside of work, it was great to share all this with you. Frauke thanks for your help and support, in the lab and outside, you are a really lovely person. Thanks Robert for cheering me up and "forcing" me to do extra-work activities.

Thanks Alex for the bioinformatics support, the patience to answer the everyday questions I had.

I will never forget how much fun I had and how noisy was (yes I'm talking about you Marina and also Max) to work with you all "AG biochemie" guys, the old and the new ones. It was amazing, really.

Thanks to my love, Frank, for taking care of me, especially during the writing time, I know it's not easy to deal with me every day but you manage pretty well!

All this would not have been possible without the support of my family. Thanks to be always having my back. I did and I will still do my best to make you proud of me.

This work is dedicated to my grandparents and to my beautiful niece Aurora.

9. Declaration on oath

Hiermit erkläre ich, Iolanda Ferro, an Eides statt, dass ich die vorliegende Dissertationsschrift selbst verfasst und keine anderen als die angegebenen Quellen und Hilfsmittel benutzt habe.

Hamburg, den 03.06.2016

I, Iolanda Ferro, hereby declare on oath, that I have written the present dissertation by my own and have not used other than the acknowledged resources and aids. I hereby declare that I have not previously applied or pursued for a doctorate (Ph.D. studies).

Hamburg, 03.06.2016

Iolanda Ferro